SUBGROUP MEETINGS

**SU-SUB-B1** ELECTROPHORESIS AND DIFFUSION IN THE PLANE OF CELL MEMBRANE. M. Poo, Univ. of Calif., Irvine, CA

The electrophoresis and diffusion of three types of surface receptors has been studied in the membrane of embryonic Xenopus muscle cells; a heterogeneous group of concanavalin A receptors, a specific glycolipid -ganglioside $G_{M1}$, and a defined protein-acetylcholine (ACh) receptor. A uniform electric field on the order of 10 mV across a cell rapidly accumulates cell surface receptors toward one side of the cell surface, as indicated by the post-field specific fluorescent ligand binding or ionophoretic mapping. The redistribution of the receptors is reversible and independent of cell metabolism. The asymmetric accumulation of the receptors by the field and the relaxation of asymmetry after removal of the field provides estimates of electrophoretic mobility and diffusion coefficient in the receptors in the plane of cell membrane. This in situ electrophoresis technique provides a means of manipulating the topological distribution of cell surface receptors in the study of interactions between membrane components in the plane of cell membrane. In the case of ACh receptors, long-term ($\gtrsim$ 3h) accumulation of the receptors by the electric field results in the formation of immobile aggregates of the receptors.

**SU-SUB-B2** IDENTIFICATION OF THE PROTEIN CONTRIBUTION TO X-RAY SCATTERING FROM MEMBRANES. G. Brady, New York Dept. of Public Health.

The scattering from the model membrane system: Egg Lecithin + Myelin Protein (N-2) has been analyzed by liquid diffraction methods. It is found that by manipulating the protein-lipid ratio the scattering domains of the protein and lipid can be identified. The multilayer contribution can also be identified by its position and concentration behavior in both the intensity pattern and its Fourier transform. When the multilayer and protein components are subtracted, there is left the phospholipid scattering and and interaction term; these two can be resolved by a reasonable assessment of their relative magnitude in the boudary region where they overlap. The interaction term can then be used to determine the most probable position of the protein in the membrane. The deconvoluted protein and lipid transforms can then be combined in the proper way to obtain the electron density profiles. The resolution of the interaction term is not yet complete, but a method for accomplishing this is discussed.

**SU-SUB-B3** ON THE ASSEMBLY OF CHOLESTEROL IN THE PHOSPHOLIPID BILAYER. C. Huang, Dept. of Biochemistry, University of Virginia School of Medicine, Charlottesville, VA 22901

Cholesterols are well-known to alter the molecular motions of natural phospholipids in bilayer membranes. The lateral diffusion rate of egg phosphatidylcholines for example, is decreased in the liquid crystalline state upon addition of cholesterol. Additionally, cholesterol selectively interacts with the hydrophobic portion of the egg phosphatidylcholine in bilayers, while the mobility of the polar $-N^{+}(CH_3)_3$ group of the phospholipid is not effected by cholesterol. Reference to the structural and motional properties of the cholesterol and natural occurring phosphatidylcholine with olefinic moieties, the cholesterol in the plane of the membrane may be viewed in terms of maximizing van der Waals interaction through complementary packing of cholesterol and natural phospholipid. A structural model (Huang, C., Chem. Phys. Lipids 19 (1977) 150; Lipids 12 (1977) 348) which illustrates a plausible complementary packing will be discussed.

**SU-SUB-B4** A BILAYER IS A BILAYER IS A BILAYER. S. Simon, Duke Univ. Med. Ctr., Durham, NC 27710

A description of lipid bilayers with particular emphasis on their solvent and mechanical properties will be presented. These properties of bilayers will be compared to isotropic materials. For example: in bilayers the interaction of molecules that are not anchored to the interface (e.g. alkanes) are very different than they are in isotropic liquids. These differences become more pronounced as the chain length of the alkane approaches or becomes larger than the length of the acyl chain of a phospholipid molecule. In the latter case it will be shown that it is possible to have a molecule with essentially an infinite oil-water partition coefficient that will be totally immiscible with bilayers! For molecules confined to the interface (e.g. fatty acids) a different behavior is observed in that the interactions are maximal when the chain lengths between the two molecules are identical. In contrast to isotropic liquids where a single modulus (Bulk modulus $K_B$) is sufficient to mechanically specify the system, lipid bilayers require a minimum of three moduli. They are the bulk modulus, $K_B$, a two dimensional compressibility modulus $K_A$ and a bending modulus B. Differences between bilayers with fixed and free boundaries will be discussed.

**SU-SUB-B5** PHYSICAL STATES AND PHASE TRANSITIONS IN LIPID FILMS. N. L. Gershfeld, Laboratory of Physical Biology, NIAMDD, NIH, Bethesda, Maryland 20014

Lipid films on water are analyzed under conditions in which the film is in equilibrium with bulk lipid (i.e. saturated lipid solutions). Phase transitions in the equilibrium films are treated by standard thermodynamic methods. The liquid-condensed/liquid-expanded film transition observed with various lipids had previously been thought to exhibit a critical temperature ($T_c$) and surface pressure ($\pi_c$); when $T < T_c$, the two surface phases were assumed to coexist over a range of temperatures. However, under equilibrium conditions the transition is shown to be similar to melting with a single transition temperature which is characteristic of the lipid. Lecithin films do not form the liquid-condensed state but form only the liquid-expanded state under equilibrium conditions. Unlike the other lipids, lecithin also forms a surface state in which the surface concentration exceeds that for a monomolecular film. This state exhibits an upper and lower critical temperature of formation. The implications of these phenomena for the properties of membrane lipids will be discussed.

**SU-SUB-C1** NUCLEAR OVERHAUSER EFFECT AND SPIN DIFFUSION IN BIOPOLYMERS, A. A. Bothner-By* and P. E. Johner*, (Intr. by D. W. Urry), Pittsburgh, Pennsylvania 15213

In low molecular weight biomolecules with short rotational correlation times, homonuclear Overhauser effects tend to be little perturbed by multinuclear interactions, and to give relatively specific information about nearest neighbors. The magnitudes of the observed effects in these cases is generally controlled by a compromise between magnetic dipolar interaction with the irradiated nucleus and all other sources of relaxation of the observed nucleus. In biomacromolecules, on the other hand, cross-relaxation can become very efficient and multinuclear effects can lessen the specificity of the observed effects. Theoretically expected behavior is given for some idealized model systems, and compared with effects observed for Gramicidin S dissolved in deuterated ethylene glycol. This viscous solvent lengthens the rotational correlation time so that Gramicidin S mimics the behavior of a protein of molecular weight 10,000-20,000.

**SU-SUB-C2** NOE AND TRANSFER OF SATURATION STUDIES OF PEPTIDE CONFORMATION. N. Rama Krishna,* David G. Agresti,* Roderich Walter, and Jerry D. Glickson,* University of Alabama in Birmingham, Birmingham, Alabama 35294 (N.R.K., D.G.A. and J.D.G.) and the University of Illinois Medical Center, Chicago, Illinois 60680 (R.W.).

In order to illustrate how intramolecular nuclear Overhauser effect (NOE) data can be employed to evaluate specific models of peptide conformations, we have analyzed data for valinomycin and gramicidin S employing a theoretical formalism applicable to peptides which do not satisfy the "extreme narrowing" limit. The extent of solvent exposure of NH and CH hydrogens is reflected in changes in the intensities of their corresponding resonances when the solvent is saturated. Quantitation of these effects can be accomplished by combining transfer of saturation measurements (for NH protons) and intermolecular NOE measurements (for CH hydrogens) with appropriate $T_1$ experiments. To illustrate the procedure we have compared the rates of NH proton exchange of oxytocin and 8-lysine vasopressin in $H_2O$ solution and the intermolecular dipolar relaxation rates of aromatic side chain hydrogens of cyclo(Gly-Tyr) and cyclo(Gly-Phe) in dimethyl sulfoxide solution.

**SU-SUB-C3** THROUGH SPACE AND THROUGH BOND INTERACTIONS IN PEPTIDES: THEIR ESCLATION BY DIFFERENCE RELAXATION AND DIFFERENCE DIPOLES SPECTROSCOPY, W. A. Gibbons, University of Wisconsin, Madison, Wisconsin

**SU-SUB-C4** QUANTITATIVE CONFORMATIONAL ANALYSIS OF MONO- AND DINUCLEOTIDES BY THE PHOSPHORUS-PROTON NUCLEAR OVERHAUSER EFFECT. Phillip A. Hart,* School of Pharmacy, University of Wisconsin, Madison, Wisconsin 53706

The phosphorus-proton nuclear Overhauser effect (NOE) was used to investigate the quantitative distribution of rotamers about the C3'-O3' bond ($\phi'$) of 3'-AMP and the C4'-C5',C5'-O5' bonds ($\psi$,$\phi$) of 5'-AMP. In the 5'-AMP case, there is general agreement based on coupling constant analyses, that the major contributor to the $\psi$ conformation is the 60° rotamer (gg) and that the major contributor to the $\phi$ conformation is the 180° rotamer (g'g'). Using the largest reported proportions of each of these angles, the joint probability of these major rotamers is 0.65. The NOE method, which gives the joint probability directly, yields similar results. In the 3'-AMP case, conformational analyses based on $^3J_{P,H}$ and $^3J_{^{13}C,H}$ give different results. The NOE method gives a $\phi'$ distribution of 0.85:0.15, 180°:60° ($g^-$:t) in agreement with recent analyses based on $^3J_{P,H}$. Details of the method will be given and it will be shown how the phosphorus-proton NOE can be applied to the conformational analysis of the backbone of dinucleoside monophosphates and dinucleotides.

S Y M P O S I U M

MOLECULAR STRUCTURE OF MACROMOLECULAR ASSEMBLIES

M-AM-1S STRUCTURE AND ASSEMBLY OF TOBACCO MOSAIC VIRUS. Aaron Klug, Laboratory of Molecular Biology, Cambridge, CB2 2QH, United Kingdom

M-AM-2S ON NEUTRON SCATTERING BY MACROMOLECULAR STRUCTURES. B. Schoenborn, Brookhaven National Laboratory, Upton, N.Y. 11973

**M-AM-3S** ASSEMBLIES OF GLUTAMINE SYNTHETASE. D. Eisenberg, E.G. Heidner*, U. Aebi*, R. Fenna*, Z. Burton*, M. Lei*, R. Weiss*, and J. Held*. Molecular Biology Institute, U.C.L.A., Los Angeles, CA 90024

The enzyme glutamine synthetase (GS) serves in E. coli as the central element in the regulation of nitrogen metabolism. It has been established by others that this regulation operates at both the levels of enzymatic and transcriptional controls: numerous end products of glutamine metabolism participate in feedback inhibition of GS, and GS controls the transcription of operons coding for enzymes whose substrates contain nitrogen. Both these levels of regulation are profoundly affected by the covalent addition of an AMP group to a tyrosyl residue of GS.

The molecular assemblies of GS display a complexity that equals that of regulation of the enzyme. In physiological solution, the GS molecule is a dodecamer of polypeptide chains, each of MW 50,000. As 10 mM concentrations of some divalent cations are added, the molecules polymerize into strands and the strands twist into cables. Some cables are formed from three strands, and others from seven. Electron micrographs of the seven stranded cables have been analyzed by optical diffraction and by computer reconstruction and refinement. Some principles of their assembly have been deduced.

Six crystal forms of GS have been grown, and all are consistent with symmetry 622 for the GS molecule. One of the six contains GS molecules lacking covalently bound AMP. It is isomorphous with another form, grown from molecules with nearly their full complement of AMP. This demonstrates that the addition of AMP groups does not cause a quaternary structural change in the GS molecule.

Solution studies of the interaction of GS with DNA and ligands will also be described.

This work has been supported by USPHS Grant GM 16925 and NSF Grant BMS PCM 75-02889.

**M-AM-4S** MECHANISMS IN THE ASSEMBLY OF BACTERIAL VIRUSES. J. King, W. Earnshaw, and P. Berget. Department of Biology, M.I.T., Cambridge, MA 02139

Two central problem areas in virus assembly are the assembly of closed shells, and the condensation of nucleic acids within the shells. The extensive genetic characterization of bacteriophages with double stranded DNA has led to a detailed analysis of the steps in these processes. In all of the phages that have been well studied -T4, lambda, P22, T7, T3, P2, and 29 - a precursor shell empty of DNA is formed first. This shell plays an active role in the condensation and encapsidation of a headful of viral DNA, a complex process involving specific enzymatic apparatus, and shell reorganization. The accurate assembly of the coat protein subunits into the precursor shell requires in all cases additional proteins which play a scaffolding or assembly core function. These copolymerize with the coat subunits yielding a double shell structure with the scaffolding proteins on the inside. After completion of the precursor shell, the 100-200 scaffolding protein molecules must be removed prior to the DNA packaging process. In phage P22 the scaffolding proteins exit intact through the coat lattice, and then recycle. In T4, the assembly core proteins are proteolytically cleaved within the shell to small peptides. These reactions are coupled to the expansion and rearrangement of the outer shell lattice. Though the enzymatic mechanisms for moving DNA into the precursor shell are still obscure, the organization of the condensed DNA has been clarified by electron microscopic and small angle X-ray scattering studies. The DNA is coiled in concentric shells, around a unique winding axis. Though the proteins involved in particle assembly are synthesized simultaneously, they assemble in a strictly ordered sequence. The mechanisms controlling this have emerged from the study of phage tail assembly which involves the sequential interaction of twenty-two protein species - the proteins are synthesized in an unreactive conformation; incorporation into a substrate structure results in conformational alteration of the subunit, or the whole complex, generating a new site, which is now reactive for the next protein in the sequence. Thus the reactive sites for morphogenesis are generated in the course of the assembly process itself.

M I N I S Y M P O S I U M

FUNDAMENTAL INTERACTIONS OF ENVIRONMENTAL INTOXICANTS

**M-AM-1M** THE BIOCHEMISTRY OF TOXIC ELEMENTS. J. M. Wood. Dept. of Biochemistry; Director, Freshwater Biological Institute; University of Minnesota; P.O. Box 100, Navarre, MN 55392.

Since the Industrial Revolution the movement of toxic elements in the biosphere has been greatly accelerated as a result of man's activities. For example there is evidence that the movements of mercury, lead, copper, nickel, arsenic and tin vastly exceed their global geological flux. As a result of this activity, living organisms in advanced industrial societies have had to adapt to environments which contain elevated levels of toxic inorganic complexes. In recent years we have shown that biological cycles exist for toxic elements, just as they do for essential elements, and furthermore we have shown that critical steps in these cycles are determined by oxidation-reduction chemistry. Molecular oxygen plays a very important role in determining the conditions for biomethylation of inorganic complexes to give their organometallic counterparts. We have examined the relationship between standard reduction potential ($E^\circ$) for different metal or metalloid couples, together with the vitamin $B_{12}$-dependent biomethylation of 12 toxic elements. These metals which have a standard reduction potential above that for molecular oxygen react by a different mechanism than those with a standard reduction potential below that for oxygen. Of even greater interest are those metals with standard reduction potentials close to molecular oxygen such as platinum and gold. These metals react by a mechanism called "redox-switch" because both oxidation states of the metal are required for biomethylation to occur. This reaction is especially interesting because it provides us with the key to understanding $B_{12}$-enzyme catalyzed rearrangement reactions.

**M-AM-2M** ENVIRONMENTAL LEAD DISEASE — RECENT BIOPHYSICAL AND EPIDEMIOLOGICAL STUDIES. Josef Eisinger *Bell Laboratories, Murray Hill, N.J. 07974.*

Lead is the oldest environmental pollutant and through the centuries has probably claimed more victims than any other. The long history of man's involvement with it shows lead to be a prototype for many modern environmental poisons. Although fatal lead disease is rare today, ever larger populations are being exposed to low levels of lead and cause serious concern, particularly for young children whose central nervous system is especially susceptible. The interference of lead with hematopoiesis, on the other hand, is rarely serious, but its elucidation has led to the emergence of an effective biological indicator of lead disease: In the presence of lead ions at the site of erythropoiesis, a small fraction of the globin incorporates zinc protoporphyrin (ZPP) instead of the heme, probably due to a malfunctioning of the ferrochelatase system. Red blood cells retain this abnormal hemoglobin for their lifespan (~120 days) and since ZPP, unlike heme, fluoresces when excited with blue light, the ZPP level in a person's blood can be measured fluorometrically. This provides the basis of a dedicated front face fluorometer (hematofluorometer), a field instrument requiring a drop of unprocessed blood, generally obtained by finger puncture (1). Recent epidemiological studies show the ZPP level to be a better indicator of the severity of chronic lead poisoning than is the level of lead in blood, a finding which is consistent with kinetic models. The significance of the correlation between the occurrence of anemia among lead smelter workers and their ZPP levels, for instance, is about 40 times greater than for the correlation between anemia and their lead-in-blood levels. Surveys of lead exposed populations making use of ZPP hematofluorometers are producing better understanding of lead disease, including significant correlations between central nervous system dysfunction and the ZPP levels in a cohort of lead-exposed workers.

(1) W. E. Blumberg, J. Eisinger, A. A. Lamola, and D. M. Zuckerman. *J. Lab. Clin. Med.* **89**, 712–723 (1977).

M-AM-3M CRYSTAL FACES AND CLEAVAGE PLANES IN QUARTZ AS TEMPLATES IN BIOLOGICAL PROCESSES. A. Langer and G. Oster, Mount Sinai School of Medicine of the City University of New York, New York New York 10029.

When inhaled, the mineral quartz causes nodular fibrosis of the lung parenchyma and hilar nodes. Occasionally, silicotic nodules occur in the liver and spleen, and is associated in rare instances with Caplan's syndrome and scleroderma. Tuberculosis is a frequent complication of the disease. It has been observed that the incidence and severity of silicosis, differs among the mining localities and industries in which it is used. Size of respirable quartz is considered one of the major factors influencing the patterns of silicosis: fine quartz(0.5–0.1μm) is more fibrogenic than coarse quartz(5.0–0.5μm) particles. This observation has been substantiated in experimental animal studies. What is frequently unrecognized is that size reduction is accompanied by the production of rare cleavage and parting planes otherwise not available for interaction.

On the basis of calculations of the template fraction energy for the development of expressed crystallographic planes in quartz, the three most common crystal faces (least, template fraction energy, therefore most likely to survive crystallization) are the hexagonal prism, m(10$\bar{1}$0), the positive rhombohedron, r(10$\bar{1}$1) and the negative rhombohedron, z(01$\bar{1}$1). These forms are frequently encountered on quartz, regardless of habit, trace element constituents or variety(e.g., amethyst). Minor faces encountered include the positive right trapezohedron, x(51$\bar{6}$1) and the right trigonal pyramid, s(11$\bar{2}$1). Calculation of cleavage patterns on the basis of reduced surface energy also suggests the low energy requirement for m, r and z cleavage, but much greater values for x and s. Basal pinicoid cleavage, c(0001), is also predicted by this method.

As a consequence of the generation of these exotic Miller-index surfaces and their different energetics, proteins adsorb differently on these surfaces. These produce a range of conformational changes in protein, which may result in altered susceptibility to proteolytic enzyme attack and immunological host response. Experiments will be discussed which indicate specificity of the different planar crystallographic orientations and their protein products. These processes may be the basis of the differing antigenic response in silicosis, and its systemic effects.

M-AM-4M INTERACTIONS OF LIGHT AND CHEMICAL POLLUTANTS IN THE ENVIRONMENT. A. A. Lamola, *Bell Laboratories, Murray Hill, N. J. 07974.*

Life on earth is in balance between the beneficial and detrimental effects of sunlight reaching it. Yet, the role of light as a factor in environmental pollution has been largely ignored. This is, in part, due to the ubiquity of light and the fact that its adverse effects are often subtle or may be indirect. It has become evident, however, that there are several ways in which environmental light and man-made chemicals can interact to alter the equilibrium between environmental light and life. Atmospheric pollution alters the quality and quantity of sunlight reaching the surface of the earth. While climatic changes due to increased atmospheric $CO_2$ have been under consideration for many years, it has only recently been pointed out that the stratospheric ozone concentration could be decreased by the actions of chlorofluorocarbons and excessive amounts of nitrogen oxides introduced into the stratosphere. The concomitant increase in the ultraviolet light intensity at the surface of the earth would certainly lead to an increased incidence of skin cancer in man. However, the effects on lower animals, plants and microbes of both terrestrial and aquatic ecosystems are potentially of greater concern for man. Light can act on chemicals and pollutants in the environment to alter radically their interactions with man and other organisms. The prime example is photochemical smog. However, man releases into the environment many different compounds which are photochemically active towards light found in the terrestrial solar spectrum. There are several examples of sunlight alteration of pesticides. It was recently shown that a heating oil slick on water becomes more toxic as a result of photochemical changes induced by sunlight. Light may also interact with chemicals introduced purposefully or adventitiously into man and animals, causing either injurious or therapeutic effects. Thus a large number of drugs and industrial chemicals have been identified as phototoxic or photoallergic agents in man. These effects are confined mainly to the skin and the cornea. However, the fact that red light can penetrate deeply into the body makes colored drugs and food additives candidates as photosensitizers for organs other than the skin. Finally, man-made chemicals may act on man and other organisms to make them more sensitive to light, and similarly light may act on the organisms to make them more sensitive to chemicals. Examples of the various photobiological interaction modes mentioned above will be discussed.

M-AM-5M ENVIRONMENTAL INTOXICANTS AND HEALTH. I. J. Selikoff, Environmental Sciences Laboratory, Mount Sinai School of Medicine, New York, N. Y. 10029

**M-AM-6M ENZYMIC MODIFICATION OF ENVIRONMENTAL TOXICANTS — THE ROLE OF CYTOCHROME P-450.** W. E. Blumberg, *Bell Laboratories, Murray Hill, N. J. 07974.*

The myriad of molecules of biological origin which appeared on the earth over a period of three billion years pales compared with the great number of other molecules which man has put on his planet during the last century. Most non-biological molecules have been intentionally synthesized, but others are the by-products of technology. For example, polycyclic aromatic hydrocarbons have been found to be present in century-old sediments at 9% of current levels, consistent with the amount that would have been produced by the burning of wood and coal up to that time. A small fraction of these foreign molecules (xenobiotics) are inconsistent with normal life processes so that the innate evolutionary drive for self-preservation mounts a vigorous attempt at their elimination. The most widely employed enzymic attack on xenobiotics first attaches a hydroxyl group to a suitable carbon atom, rendering the molecule more hydrophilic (and therefore more easily excreted) and subject to further attack by conjugating enzymes which might attach such solubilizing groups as mercapturic or glucuronic acid or glycosides. Concomitant with the hydroxylation process many xenobiotics become less toxic; for example, this is the pathway by which many narcotics and other drugs are rendered biologically inactive in humans and is the mechanism by which insects detoxify most insecticides, both natural and man-made. The enzyme system which carries out xenobiotic hydroxylation occurs in various forms throughout the eucaryotic phyla in both plant and animal kingdoms and even occurs in a primitive form in certain bacteria. Cytochrome P-450, a heme enzyme, provides the site at which xenobiotics are hydroxylated. Molecular oxygen is split by this mixed function oxidase, one atom being inserted into the molecule as an epoxide, the other proceeding to water. Another enzyme converts the epoxide into a diol. The cytochrome P-450 system is capable of hydroxylating more than one-third of the compounds found in drinking water in the U.S. Fortunately many aquatic organisms also possess mixed function oxidase activity and serve to detoxify rivers and oceans. Hydrocarbon hydroxylation has been observed in marine environments by bacteria (pseudomonads), by invertebrates (zooplankton and the larger crustaceans), and by teleosts and elasmobranchs. In the case of a few relatively innocuous molecules, such as benzo[*a*]pyrene and 3-methylcholanthrene, the epoxide or diol intermediates are highly toxic, in these cases powerful carcinogens. Thus man's P-450 hydroxylation system may not effectively cope with environmental toxicants in cetrain cases. Drugs, various polycyclic aromatic hydrocarbons, and polyhalogentated hydrocarbons (*e.g.*, PCB's and PBB's) induce increased mixed function oxidase activity in humans, and thus there exists the opportunity for synergistic effects among environmental toxicants.

**M-AM-7M** DETERMINANTS OF BIODEGRADABILITY. Stanley Dagley, Department of Biochemistry, University of Minnesota, St. Paul, MN 55108.

The evolution of earth's living forms depended upon the establishment and continued operation of a carbon cycle, of which a major segment is made up of reactions catalyzed by microorganisms. The exceptional degradative versatility of microbes is due in large measure to enzymes (oxygenases) that incorporate $O_2$ into otherwise biochemically inert chemical structures. When degradation has been started by oxygenases, it is continued by reactions that fall into more common biochemical categories. This principle will be illustrated with reference to seven main channels of catabolism used by microbes to degrade benzenoid compounds after conversion to dihydric phenols. A given species appears to exercise "choice", exerted through highly substrate-specific monooxygenases: only one of the metabolic channels is used for a particular dihydric phenol, althougn the same organism might use others for substrates of quite similar chemical structures. A man-made compound will be degraded immediately if it happens to be susceptible to attack by enzymes used by microbes to degrade natural products, and the closer the resemblance in chemical structure to such a product, the more probable it is that the novel compound will not persist in the environment. However, predictions are of limited value when based on purely chemical considerations; for the capabilities and limitations of microbes are a legacy of their evolution, and questions of biodegradability must be referred to the framework of our knowledge of the biology and enzymology of microbial catabolism. Illustrations will include microbial catabolic pathways for industrial cresols and xylenols, polycyclic hydrocarbons and some of their halogen-substituted analogues. Some limitations of classical techniques, that traditionally use cultures of single strains and focus upon one carbon source, will be mentioned. Questions may arise concerning effects due to mixtures of other compounds that would most probably be present in natural habitats, or to the coexistence of other bacterial populations. Finally, it will be noted that although we rely heavily upon microorganisms to remove man's insults to the environment, their biochemical activities are not invariably beneficial: they sometimes make matters worse.

**M-AM-8M** GENES, POLLUTANTS AND HUMAN DISEASES. J.E. Trosko and C.C. Chang, Michigan State University, E. Lansing, Michigan 48824.

The use of the traditional concepts of diseases has been very successful in "conquering" contagious-related diseases. However, application of these concepts to diseases of contemporary society (i.e., cancer, atherosclerosis, etc.) seems to be ineffective. The role of physical and chemical environmental pollutants in the induction of gene mutations (more or less irreversible changes in the genetic information) and gene modulation (the potential reversible repression or derepression of genetic information) in various human diseases will be discussed. Major concepts (i.e., genetic and environmental determinants of health and disease; the multistage phenomenon of many diseases; the classes of genetic and environmental factors influencing diseases) will be illustrated with the cancer-prone human syndrome of xeroderma pigmentosum serving as a model. Chemical modification of radiation (or chemical)-induced mutagenesis and its role in carcinogenesis will be discussed. Since the role of DNA damage in mutation fixation and various human diseases is well documented, mechanisms will be illustrated by which many non-mutagenic chemicals (and genes) can influence diseases like cancer. These will include the modification of (a) the amount of DNA damage; (b) the repair of that molecular damage; and (c) the expression of the genetic consequences of the DNA damage and its "error-prone" repair. Research supported by NCI grants (CA 13048-5 and CA 21107-01).

PHOTOSYNTHESIS I

REACTION CENTERS

**M-AM-A1** DIRECT MEASURE OF ELECTRON TRANSFER IN BACTERIOCHLOROPHYLL. P. Avouris, K. S. Peters and P. M. Rentzepis Bell Laboratories, Murray Hill, New Jersey 07974.

Picosecond absorption studies have been decisive in elucidating the nature of the primary processes in photosynthesis. Our data show that the first two steps following light absorption by rhodopseudomonas spheroides are an electron transfer reaction from the bacteriochlorophyll dimer $(BChl)_2$ to the bacteriopheophytin (BPh), followed by an electron transfer from $BPh^-$ to the ubiquinone-iron (QFe) system. In this report, we present temperature studies of the above two electron transfer processes. The temperature dependence of the transient-absorptions at 1250 nm and 640 nm induced by 6 psec, 530 nm light pulses was studied. It was found that in the temperature range of 300 K to 4.2 K the rate of the reaction generating the charge (ion pair) transfer species $[BChl_2)^+ - BPh^-]X$ is less than $1.7 \times 10^{11}$ sec; the rate of the next step $[BChl_2) + BPh^-] \rightarrow [B(Cl) + BPh]X^-$ is $6.7 \times 10^9$ $sec^{-1}$ and remains constant throughout this temperature range. These events are interpreted as giving direct evidence for electron tunneling.

**M-AM-A2** DEHYDRATION OF PHOTOSYNTHETIC REACTION CENTERS. R. K. Clayton, Cornell University, Ithaca, NY 14853

Reaction centers (RCs) from Rhodopseudomonas sphaeroides were dried as films in room air onto glass plates. The films could be pumped to remove water; this changed their optical and photochemical properties reversibly. Restoration was complete upon exposure to either $H_2O$ or $D_2O$ vapor. Dehydration of the films shifted all the absorption bands a few nm to shorter wavelengths and attenuated the 860 nm band about 25% with corresponding increase at 795 nm but not at 1250 nm. In dehydrated films about half the RCs were photochemically inactive. The quantum efficiency for bacteriochlorophyll oxidation in the active fraction was 0.5 at 300K, rising to 0.8 or more below 250K. In hydrated (air-dried) films the efficiency was 1.0 ± 0.2 from 300K to 70K. The back-reaction (return of electron from ubiquinone to bacteriochlorophyll) showed a major first-order component of half-time 24 ± 4 ms in dehydrated films from 300K to 70K. In hydrated films, as in aqueous suspensions, the half-time was about 70 ms at 300K, falling to 25 ms between 250K and 200K, and then declining to 17 ms at 70K. The change between 250K and 200K might thus reflect a water-dependent phase transition.

**M-AM-A3** MAGNETIC PROPERTIES OF REACTION CENTERS FROM R. SPHAEROIDES R-26.[†] W.F.Butler, D.C.Johnston,* M.Y. Okamura, H.B.Shore,* and G.Feher. UCSD, La Jolla, CA.

Reaction centers contain one $Fe^{++}$ interacting with the quinones of the electron transfer chain. To determine the strength of this interaction and the electronic structure of the $Fe^{++}$, magnetization measurements were performed with a Faraday magnetometer in the temperature range $0.7°K < T < 170°K$ and magnetic fields up to 10kG. For unreduced RCs the high temperature data yield an effective moment of 5.63 Bohr magnetons/$Fe^{++}$ (i.e., S=2, g=2.30). The low temperature data were fitted with the spin Hamiltonian:

$$\mathcal{H} = g\beta\vec{H}\cdot\vec{S} + D[S_z^2 - \tfrac{1}{3}S(S+1)] + E(S_x^2 - S_y^2)$$

with D=6.0 $cm^{-1}$ and E=2.0 $cm^{-1}$. Data for RCs reduced with dithionite were fitted by adding to the above Hamiltonian a Zeeman term for the quinone and an exchange coupling term $-JS_1\cdot S_2$, where $S_1$ and $S_2$ are the spins of the quinone and $Fe^{++}$, respectively. The best fit was obtained for J=-0.6 $cm^{-1}$. Calculations using this value of J predict the observed broad g=1.8 EPR signal. The sign of J shows that the spins on the quinone and $Fe^{++}$ are antiferromagnetically coupled.

[†]Work supported by grants from the NIH and the NSF.

**M-AM-A4** EPR SIGNALS FROM THE PRIMARY AND SECONDARY QUINONE IN REACTION CENTERS OF R. SPHAEROIDES.[†] M.Y.Okamura, R.A.Isaacson,* and G.Feher. UCSD, La Jolla, CA. 92093.

The proposal that Fe in RCs serves to facilitate the transfer of an electron from the primary quinone $Q_1$ to the secondary $Q_2$ (Okamura, et al., PNAS, 1975) was tested by illuminating RCs having 2.0 quinones with short laser flashes [Wraight, B.B.A.459 (1977); Vermeglio, B.B.A.459 (1977); Vermeglio,Clayton, Biophys.J. 17 (1977)]. The EPR spectra observed after flashes 1 and 3 were similar but had different linewidths, ΔH (ptp of dχ"/dH), supporting the following series scheme:

FLASH 1: $DQ_1Fe^{++}Q_2 \xrightarrow[h\nu]{cyt^{2+}\ cyt^{3+}} DQ_1^-Fe^{++}Q_2 \rightarrow DQ_1Fe^{++}Q_2^-$ ($g = 1.8$, $\Delta H = 450G$)

FLASH 2: $DQ_1Fe^{++}Q_2^- \xrightarrow[h\nu]{cyt^{2+}\ cyt^{3+}} DQ_1^-Fe^{++}Q_2^- \rightarrow DQ_1Fe^{++}Q_2^=$ (No EPR)

FLASH 3: $DQ_1Fe^{++}Q_2^= \xrightarrow[h\nu]{cyt^{2+}\ cyt^{3+}} DQ_1^-Fe^{++}Q_2^=$ ($g = 1.8$, $\Delta H = 300G$)

The position of maximum absorbance (g-value) is the same for $Q_1$ and $Q_2$, showing that both quinones are magnetically coupled (with approximately the same strength) to $Fe^{++}$ (see previous abstract), thus supporting the "Fe-wire" hypothesis.

[†]Work supported by grants from the NSF and the NIH.

**M-AM-A5** THE ROLE OF FE AND $H^+$ IN THE QUINONE ACCEPTOR COMPLEX OF PHOTOSYNTHETIC REACTION CENTERS. C.A. Wraight, University of Illinois, Urbana, Illinois 61801.

Quinones are now known to act as the metastable electron acceptor in the photochemical reactions of many bacteria and of PS II of plants. Two specialized quinones have been proposed to act as a two electron gate between the reaction center (RC) and a quinone pool giving rise to binary oscillations of the semiquinone form in a series of flashes:

$$Q_I\ Q_{II} \xrightarrow{h\nu} \dot{Q}_I^-\ Q_{II} \rightarrow Q_I\ \dot{Q}_{II}^- \text{ (stable)}$$

$$Q_I\ Q_{II}^- \xrightarrow{h\nu} \dot{Q}_I^-\ Q_{II}^- \xrightarrow{2H^+} Q_I\ Q_{II}H_2 + 2H \text{ (pool)}$$

At some stage $2H^+$ are bound and oscillations of $H^+$-uptake also occur. Using RCs from Rps. sphaeroides the electron transfer steps and the involvement of $H^+$ in the disproportionation have been studied via the pH-dependence of the electron transfer kinetics and $H^+$-uptake. One protonation (limiting at pH 7.7) precedes the disproportionation while the second presumably follows it. An Fe atom interacts with the reduced acceptors giving rise to a distinctive ESR signal which is different for $Q_I$ and $Q_{II}$. The Fe is essential for normal functioning of the acceptor complex. Supported by NSF (BMS 75-03127).

**M-AM-A6** PHOTOTRAP ACTIVITY AND TIGHTLY BOUND UBIQUINONE IN CHROMATIUM VINOSUM. J. Runquist* and P. Loach, Northwestern University, Evanston, Il. 60201

Ubiquinone has been shown to be the first stable electron acceptor in R. rubrum(w.t.)[1] and R. sphaeroides(R-26)[2]. However, several recent extraction studies have concluded that ubiquinone is not required for phototrap activity in Chromatium[3,4]. In order to more quantitatively analyze the Chromatium system, we have utilized the technique of growing the bacteria in the presence of a benzoquinone precursor which was labelled with $^{14}C$ and examined the dependency of phototrap activity on ubiquinone content. Extraction of lyophilized Chromatium chromatophores with benzene or petroleum ether resulted in removal of most radioactive material, but left a residual amount of between 3.3 and 10.5% of the initial radioactivity. Ubiquinone was isolated from this residual fraction by extraction with acetone-methanol(1:1) followed by thin layer chromatography. For a sample first extracted with benzene, the ubiquinone remaining per active phototrap was 0.73. Ref: 1. Morrison et al., Photochem. Photobiol. 25, 73 (1977). 2. Okamura et al., PNAS 72, 3491 (1975). 3. Halsey and Parson, BBA 347, 404 (1974). 4. Okamura et al., Biophys J. 16, 223a (1976).

**M-AM-A7** ABSORPTION SPECTRA OF GREEN BACTERIAL REACTION CENTER COMPLEXES AT 5 K. R. M. Pearlstein and W. B. Whitten,* Oak Ridge National Laboratory, Oak Ridge, TN 37830, and J. M. Olson, Brookhaven National Laboratory, Upton, NY 11973

Spectra of reaction center complexes I and II from Chlorobium lim. f. Thiosulfatophilum strain 6230 (Tassajara) were taken from 760 to 860 nm at 5 K. Fourth and eighth derivatives of the spectra were calculated from the digital data. Light minus dark difference spectra were taken with 590-nm actinic light. A shoulder not visible at 77 K appears on the long wavelength side of the 834-nm peak in Complex I. In Complex II, which is derived by guanidine HCl (or L-arginine HCl) treatment of I, the shoulder is much more pronounced; derivative peaks appear at 834 and 838 nm. Features in the difference spectra also appear at 834 and 838 nm, as well as at shorter wavelengths. Other features in the spectra of both complexes occur at roughly the same wavelengths as the peaks in purified Bchl a-protein. We conclude that some of the Bchl in Complex II is in a conformation similar to that of Bchl a-protein.
Sponsored by BES of U.S. DOE under contract with Union Carbide Corp. Work at BNL under auspices of U.S. DOE.

**M-AM-A8** REVERSIBILITY OF CYTOCHROME PHOTOOXIDATION IN RHODOPSEUDOMAS VIRIDIS CHROMATOPHORES. D. Fleischman and D. Limbach*, C. F. Kettering Research Laboratory, Yellow Springs, Ohio 45387.

R. viridis chromatophores contain 2 moles of cytochrome 558 ($E_m$=330mV) per mole of reaction center chlorophyll complex (P985). Illumination of chromatophores in the presence of millimolar orthophenanthroline causes the immediate oxidation of one C558 per P985. After brief (<10 sec) illumination, the C558 recovers in about 1 sec. The rate and temperature dependence of the recovery are approximately consistent with the mechanism $C558^{+2}\ C558^{+2}\ P985\ X \xrightarrow{h\nu} C558^{+2}\ C558^{+3}\ P985\ X^- \rightleftharpoons C558^{+2}\ C558^{+2}\ P985^+\ X^- \longrightarrow C558^{+2}\ C558^{+2}\ P985\ X$, where X is "primary" electron acceptor. During longer illumination the second C558 becomes oxidized in a process following first order kinetics. The reversibility of C558 oxidation is lost in parallel with the oxidation of the second C558, i.e, with the same first order rate constant. In other words, when the second electron is transferred, neither electron can return; in effect the nonreversible C558 oxidation is first order in electron pairs.

**M-AM-A9** CYTOCHROME-REACTION CENTER INTERACTIONS. M. A. Cusanovich, and G. K. Rickle, Tucson, Arizona, 85721

The interaction of reaction centers extracted from photosynthetic bacteria with c-type cytochromes offer an opportunity to investigate biological electron transfer between physiological reactants. We are reporting here on the interaction of reaction centers isolated from Rhodospirillum rubrum (wild type) with horse heart cytochrome c and cytochrome $c_2$ from Rhodospirillum rubrum and Rhodopseudomonas capsulata. The interaction of the cytochromes and reaction centers have been investigated as a function of detergent concentration (LDAO), pH and ionic strength. The photooxidation of the cytochromes was found to be rapid, with second-order rate constants on the order of $10^8$ to $10^9$ $M^{-1}s^{-1}$. Further a change in rate limiting step was observed at high cytochrome concentrations, consistent with the rate of electron transfer after complex formation. The pH and ionic strength studies show that the reaction center dominates the interaction with the structure of the cytochrome at its presumed site of electron transfer relatively unimportant. This research was supported by a grant from the NSF (PCM 75-21009).

**M-AM-A10** PHOTOSYNTHETIC ELECTRON TRANSFER AT MEMBRANE INTERFACE. R.E. Overfield* and C.A. Wraight (Intr. by D. DeVault) University of Illinois, Urbana, IL

A model system consisting of photosynthetic reaction centers (RCs) from Rps. sphaeroides R26 reconstituted into bilayer lipid vesicles has been used to study electron transfer from reduced bacterial cyt $c_2$ and equine cyt c to $P_{870}^+$ following flash excitation. With vesicles of uncharged phosphatidylcholine the electron donation is always slow ($\tau_{\frac{1}{2}}$=1-20 ms). At cyt $c_2$: RC ratios less than one the reaction is first order in cyt $c_2$ and zero order in RCs but at high ratios the reaction is first order in both. Analysis of the lipid gel-fluid phase transition by differential scanning calorimetry suggests that cyt $c_2$ is bound to the reaction center in a fluid lipid environment and is excluded upon crystallization of the membrane. With negatively charged vesicles the slow phase is accelerated and a fast phase of electron transfer appears with $\tau_{\frac{1}{2}}$≤20 μs which increases in magnitude with cyt $c_2$ concentration. These kinetics are similar to the in vivo electron transfer. No fast phase is seen with equine cyt c under similar conditions. A potential energy surface for the cyt-RC interaction is postulated, and the relevance to the in vivo system is discussed. Supported by NSF (BMS 75-03127).

**M-AM-A11** STRUCTURE AND FUNCTION OF RECONSTITUTED REACTION CENTER/LECITHIN MEMBRANES. J.M.Pachence, P.L.Dutton, J.K.Blasie, Univ. of Pa., Phila., Pa. 19174

Reaction centers (RC) were isolated from photosynthetic bacterium Rps. sphaeroides (R26) using the detergent LDAO. Several techniques for removal of LDAO and for incorporation of RC-protein into egg lecithin were developed to prepare protein-lipid vesicles, and subsequently partially dehydrated oriented multilayers. A set of electron density profiles were obtained from lamellar X-ray diffraction of multilayers consisting of purified RC and lecithin at different lipid to protein ratios. These profiles were analyzed to establish the RC structure and distribution in the membrane profile. Oxidation-reduction kinetics were measured in dispersions and multilayers of cytochrome c/RC/lecithin membranes. Cytochrome c, added to preformed vesicles, reduced more than 80% of the laser-oxidized $(BChl)_2$ of the RC with kinetics similar to the in vivo system. The results indicate that the RC protein is distributed asymmetrically in and spans the membrane, lecithin is extensively delocalized on one side of the membrane, and the cytochrome binding site(s) occur predominately on the exterior of the vesicle. Supported by GM 12202

M-AM-A12 FIRST DIRECT DETECTION OF Mg IN PRIMARY PHOTOSYNTHESIS.† J. Norris, M. Bowman,* and M. Thurnauer, Argonne National Laboratory, Argonne, IL 60439.

We have developed a high power electron spin echo (ESE) spectrometer primarily for the study of photosynthesis. Using ESE we have performed the first direct detection of $^{25}Mg$, $^{14}N$ and $^{15}N$ in the photoinduced doublet and/or triplet signals of photosynthetic bacteria. Whereas endor and ordinary epr have not observed $^{25}Mg$ in chlorophyll, another method using $^{25}Mg$ isotope enrichment easily allows the ordinary epr technique to establish the presence of Mg in vitro. Extension of the enrichment technique to in vivo systems gave no indication of the presence of Mg, both in the primary donor and the primary acceptor. The presence of Mg is not expected in the acceptor and the absence of observable Mg in the donor is another consequence of the "special pair" nature of the primary donor. However using ESE we have shown directly that Mg is in the primary donor but again is not detectable in the primary electron acceptor chain. Also a few of the many other applications of ESE in photosynthesis will be discussed with examples including the first ESE study of randomly ordered photoexcited triplets (R. rubrum). †Work performed under BES of DOE.

TRANSPORT SYSTEMS I

M-AM-B1 INTRA-CELLULAR ELECTRICAL PROPERTIES OF CORNEAL ENDOTHELIUM. J.J. Lim and J. Fischbarg, Eye Research Div., Columbia Univ., New York, N.Y. 10032

Intracellular potential difference and input resistance of corneal endothelial cells have been measured by employing microelectrode techniques. Since the cells are small and fragile attempts in the past have failed to yield definitive values for these parameters, i.e., the intracellular potential reported was low (less than 20 mv) in comparison with other epithelial cells. We have, however, measured the intracellular potential difference at 43.2 ± 1.29 mv (n =89, Range: 74 to 18 mv). In addition an endothelial resistance of 140.2 ± 28.4 $\Omega cm^2$ (n= 13) has been measured. Because of the fragility of the cell mentioned above, another difficulty previously reported was that a microelectrode could not be kept in it for more than a few seconds. However, we are able to maintain an electrode in a cell more than 40 minutes by eliminating most of the mechanical and electrical perturbations. Combining the intracellular parameters presently measured with the trans-endothelial electrical parameters previously determined, an electrical model corresponding to the corneal endothelium will be presented.

M-AM-B2 INTRACELLULAR pH REGULATION IN GIANT BARNACLE MUSCLE. W.F. Boron* & A. Roos, Washington University School of Medicine, St. Louis, Missouri 63110.

The intracellular pH ($pH_i$) of giant barnacle muscle fibers is maintained at ∿7.3 by an acid-extruding pump, sensitive to intracellular acid loads. We now report studies on the rate of acid extrusion as a function of $pH_i$, $pH_o$, $[HCO_3^-]_o$, and $[Na^+]_o$. The $pH_i$ of isolated fibers, monitored with pH-sensitive microelectrodes, was lowered to ∿6.7 by the $NH_4Cl$ prepulse technique (Nature 259: 240, 1976). The rate of acid extrusion (M) during the subsequent recovery of $pH_i$ was taken as the product of $dpH_i/dt$ and the previously determined (Am. J. Physiol. 233: C61, 1977) intracellular buffering power. We found that, over a wide range of $pH_o$, M decreased as $pH_i$ rose, approaching zero as $pH_i$ neared ∿7.3. When $pH_o$ was varied by altering $[HCO_3^-]_o$ (0.4% $CO_2$), M, at a given $pH_i$, increased with pH. When $[HCO_3^-]_o$ and $P_{CO_2}$ were increased proportionally (keeping $pH_o$=8.00), M increased; the apparent $K_m$ for $HCO_3^-$ was ∿3 mM. When external $Na^+$ was replaced by choline, M approached zero; preliminary data suggests an apparent $K_m$ for $Na^+$ of ∿20 mM. Supported by NIH grants GM06499, HL00082 and HR-19608.

M-AM-B3 FLUORESCENT PROBES OF MEMBRANE POTENTIAL IN HUMAN RED BLOOD CELLS: CALIBRATION, MECHANISM, AND pH-INTERFERENCE. J.C. Freedman and J.F. Hoffman, Dept. of Physiology, Yale School of Med., New Haven, CT. 06510.

The Jacobs-Stewart theory of ionic equilibria in human red cells, modified for non-idealities, allows accurate calculation of membrane potential ($\Delta\psi$), cell volume (V), and internal pH ($pH_i$) from external solute concentrations. By replacing external NaCl with impermeable Na-tartrate or $MgCl_2$ and adjusting pH and tonicity, $\Delta\psi$ was varied from -5 to +55 mV at constant $pH_i$ of 7.28 and constant V. Also, $pH_i$ was varied from 6.8 to 8.3 at constant $\Delta\psi$ of -5 mV and constant V. Dye fluorescence (F) calibrated at +1.7%$\Delta$F/mV and -20%$\Delta$F/unit$\Delta pH_i$ for diS-$C_3$(5) and +0.6%$\Delta$F/mV and -18%$\Delta$F/unit$\Delta pH_i$ for diI-$C_3$(5). This pH interference explains the 7-8%$\Delta$F/mV we reported when $pH_i$ and $\Delta\psi$ varied simultaneously. Unlike diS-$C_3$(5), F of diI-$C_3$(5) in membrane-free lysates was not quenched, and its absorption was unaltered by hemoglobin and pH. Upon hyperpolarization with valinomycin, diI-$C_3$(5) gives 40%$\Delta$F but shows only red-shifted absorption, indicating that stable dimers and aggregates need not be implicated in fluorescence quenching. (Supported by NIH Grants HL-09906 and AM-17433.)

M-AM-B4 PERMEABILITY OF RBCs TO WATER AND UREA. R. L. Levin and A. K. Solomon, Biophysical Lab., Harvard Med. Sch., Boston, MA 02115

A combined "stop-flow"-multiple non-linear regression analysis technique has been utilized to study the variation with external salt osmolality of the water permeability $L_p$, solute permeability $\omega$, and solute reflection coefficient $\sigma$ of human red blood cells in the presence of the permeable solute urea. The time rate of change in volume of RBCs initially suspended in an isotonic phosphate buffered saline solution (290 mOsm/ℓ) and rapidly mixed with a solution containing both urea and phosphate buffered saline was measured using a redesigned stop-flow apparatus in which the experimental data was fed directly into a mini-computer. The post-mix urea concentration was held constant at ~358 mOsm/ℓ while the extracellular salt osmolality was varied between 235 and 480 mOsm/ℓ. Non-linear "least-squares" analysis was then used to "fit" the experimental data to a modified version of the equations of Kedem and Katchalsky (BBA 27, 229-246, 1958). Increasing the external salt osmolality decreased $\sigma$ from 1.0 to 0.1 and $\omega$ from $1x10^{-14}$ to $1x10^{-16}$ mol/dyne s. $L_p$ was also found to vary with external salt osmolality.

**M-AM-B5** THE PERMEABILITY OF SPECTRIN-ACTIN FILMS TO IONS. M. Blank, L. Soo* and R.E. Abbott*, Dept. of Physiology, Columbia University, New York, N.Y.

Spectrin and actin (S-A) are important extrinsic membrane proteins that are present as a layer on the inner face of the erythrocyte membrane. Using the polarographic technique, we have studied the ion permeability of adsorbed S-A monolayers at the mercury/water interface. The relative permeability of the S-A layer to cations and anions at different pH's is consistent with an isoelectric point (IEP) at a pH between 5 and 6. Below the IEP, the layer tends to impede the flow of cations. Above the IEP, the S-A layer impedes anions. Extrapolating to pH 7.4, it appears that the S-A layer is relatively impermeable to anions in the range where the erythrocyte membrane as a whole is very permeable to anions. Our observations explain the need for specialized anion carriers in the membrane and suggest the existence of a cation rich compartment at the inner surface of the membrane. Supported by NSF-PCM76-11676.

**M-AM-B6** BINDING OF TRITIATED DIHYDRO DIDS TO DOG AND CAT RED BLOOD CELLS. V. Castranova, M. J. Weise*, and J. F. Hoffman. Dept. of Physiology, Yale University School of Medicine, New Haven, Conn. 06510.

The rates of efflux of Cl and $SO_4$ are two-fold higher in dog red cells than in cat erythrocytes, yet their anion exchange systems exhibit many common properties. The dependence of $^{o}M_{SO_4}$ on intracellular sulfate concentration, the inhibition of $^{o}k_{SO_4}$ by chloride and SITS, and the pH dependence of $^{o}k_{SO_4}$ are almost identical in dog and cat red cells (Biophys. J. 16: 170a, 1976). $^3[H]H_2DIDS$ is a potent inhibitor of anion transport exhibiting up to 98% inhibition with a $K_I$ of 0.12μM in both cell types. Binding of $^3[H]H_2DIDS$ to the membranes of dog and cat red cells is almost exclusively limited to the band 3 protein. There are fewer $^3[H]H_2DIDS$ binding sites in the dog than in cat red cells with $0.81 \times 10^6$ sites/cell for dog red cells and $1.19 \times 10^6$ sites/cell for cat erythrocytes at maximum inhibition. The data suggest that either band 3 is heterogeneous or the higher $M_{anion}$ of dog red cells is due to a higher turnover number rather than a greater number of sites. (Supported by USPHS grants HL 09906 and AM 17443).

**M-AM-B7** DNDS: A HIGH AFFINITY, REVERSIBLE PROBE FOR ANION TRANSPORT SITES IN HUMAN RBC MEMBRANES. M. Barzilay*, and Z.I. Cabantchik, NIH, Bethesda, Md.20014.

DNDS(4,4'-dinitro-2,2'-stilbene-disulfonic acid), an effective, reversible, non-penetrating agent was shown to specifically and competitively inhibit sulfate exchange in human RBC(25°C, pH 7.4) at μM levels. Full inhibition was accomplished when $8.0 \pm .7 \times 10^5$ molecules were bound per cell (measured by the Easson-Stedman procedure). Using various analytical procedures which included linear regression plots (modified Dixon and Hunter-Downs) and non-linear regression plots (Levenberg-Marquard) it was demonstrated that the inhibitory effect was exerted on sulfate transport sites ($K_i$=0.45±0.1μM). DNDS effects were asymmetric: no inhibition occurred from the inner surface of resealed ghosts (up to 0.1mM DNDS at pH 7.4, 25°C). Permeability of cells to DNDS was also asymmetric. DNDS did not penetrate into cells or resealed ghosts (over a 2 hr. period) at 25°C or 37°C. DNDS (0.1mM) exited from resealed ghosts at 37°C (30μM/hr.) but not at 25°C (measured over a 2 hr. period). The irreversible inhibitor DIDS blocked DNDS exit, as well as DNDS binding to cells. The above data suggest that the asymmetry of the anion transport system is inherent in the properties of the transport sites themselves.

**M-AM-B8** Na TRANSPORT AND Na-ATPASE OF INSIDE-OUT MEMBRANE VESICLES OF HUMAN RED CELLS. R. Blostein and H.A. Pershadsingh*, Royal Victoria Hospital, Montreal, Canada.

Using inside-out membrane vesicles we measured simultaneously strophanthidin-sensitive $^{22}Na$ uptake and Na-ATPase. With high [Na] and ≥ 0.1 mM [$\gamma$-$^{32}P$] ATP both activities require external K or Rb ($K_{ext}$ ≡ intravesicular K). With 1 mM Na and ≤ 0.5 μM ATP both activities are observed, but $K_{ext}$ or $Rb_{ext}$ decreases both, Na uptake to a greater extent than Na-ATPase. Conversely, $Li_{ext}$ stimulates Na uptake more than Na-ATPase. Thus, the ratio Na pumped/$P_i$ released varies under these conditions suggesting that some Na-ATPase occurs without associated Na pumping. At 0.2 μM ATP, $K_{ext}$ and $Li_{ext}$ decrease the steady-state level of phosphoenzyme, EP, and increase its turnover, presumably via EP.K (or EP.Li) → E.K (or E.Li) + $P_i$. Since $Li_{ext}$ stimulates Na flux and Na-ATPase but $K_{ext}$ inhibits (low [ATP]), it is plausible that at low [ATP] release of K from E.K (E.K → E + K), but not Li from E.Li, is slow and rate-limiting. (Supported by the MRC of Canada).

**M-AM-B9** KINETICS OF Na PUMP INHIBITION BY OLIGOMYCIN. J.R. Sachs. SUNY at Stony Brook, Stony Brook, N.Y. 11794. It has long been known that oligomycin (OL) inhibits the Na pump while promoting the ATP-ADP exchange reactions. This implies that OL combines with an $E_1P$ form of the pump and that the steady state kinetics of pump inhibition by OL should demonstrate that the drug is an uncompetitive inhibitor with respect to both ATP and internal Na; this was found to be true using red cell ghosts and intact red cells. OL is also uncompetitive with respect to outside Na when inhibition of the Na-Na exchange is measured. Taken together, these results indicate that OL combines with an $E_1P$ form of the pump with bound Na. OL does not inhibit the K-K exchange if the cells are free of K, but does inhibit it if the cells contain small amounts of Na indicating that the drug does not combine with $E_2P$ forms of the pump. OL is an uncompetitive inhibitor with respect to K of the Na-K exchange if the measurements are made in Na free solutions but noncompetitive with respect to K if the measurements are made in high Na solutions. Apparently OL combines with $E_1P$ with bound K, bound Na, or both. When the pump is operating as an Na-K exchanger, it appears that K combines with $E_1P$ either with or without bound Na, and that sites for Na and K exist simultaneously at the outside surface of the pump.

**M-AM-B10** A NOVEL METHOD OF ISOLATION OF A LOW MOLECULAR WEIGHT CALCIUM IONOPHORE FROM CALF HEART INNER MITOCHONDRIAL MEMBRANE. Arco Y. Jeng & Adil E. Shamoo, Univ. of Rochester, School of Med. & Dent., Rochester, N.Y. 14642.

A protein has been isolated from calf heart inner mitochondrial membrane based on the relative binding properties of $Ca^{2+}$, $Mn^{2+}$ and $Mg^{2+}$ to the protein. The isolated protein has a molecular weight about 3,000 daltons determined by urea-SDS-gel electrophoresis. This protein has been shown to have two classes of binding affinity for $Ca^{2+}$ by both equilibrium and flow dialysis measurements. The selectivity sequence of the protein determined from organic solvent extraction experiments shows that it favors divalent cations over monovalent cations. The relative selectivity sequence for divalent cations is $Ca^{2+}$, $Sr^{2+}$ > $Mn^{2+}$ > $Mg^{2+}$. $La^{3+}$ and ruthenium red are shown to inhibit the protein-mediated extraction of $Ca^{2+}$ into the organic phase. Other properties of this protein and its significance in mitochondrial $Ca^{2+}$ transport will be discussed.

*This paper is based on work performed under contract with the U. S. Department of Energy at the University of Rochester Department of Radiation Biology and Biophysics and has been assigned Report No. UR-3490-1289.

**M-AM-B11** EFFECT OF $Ca^{++}$ ON PHOSPHORYLATION OF Na-K-ATPase. Edward S. Hyman, Touro Research Institute, New Orleans, Louisiana 70115

Phosphorylation of Na-K-ATPase (E) prepared from rabbit outer renal medulla (Jorgensen, 1974) was studied at 37°C in pH 7.5 imidazole and 140mM $Na^+$, using $ATP{\cdot}P^{32}$ and an electronically controlled buretting system. With 2mM $Mg^{++}$ and below 40μM ATP, $EP^{32}$ formation in 0.3 sec follows a power curve, $EP_{sat} = a\,x^b$, where a and b are constants and x = [total ATP], [Free ATP], or $[MgATP]^{-2}$. $Ca^{++}$ at 4mM does not substitute for $Mg^{++}$ in EP formation. When $Ca^{++}$ at 10mM or 30mM is added to 2mM $Mg^{++}$ and 38.6 μM ATP, $EP_{sat}$ is reduced, and falls on the power curve for either $[MgATP]^{-2}$ or [Free ATP] as determined by simultaneous equations. Raising $Mg^{++}$ stepwise to 100mM reduces $[CaATP]^{-2}$, increases $[MgATP]^{-2}$, further lowers [Free ATP] and incompletely restores $EP_{sat}$ (to $EP_{sat}$ with 100mM $Mg^{++}$ alone-high Γ/2). Thus with this ATPase under these conditions, EP formation parallels $[MgATP]^{-2}$, or the $Mg^{++}$ complex with some other anion in the system such as a negatively charged site of E. $Ca^{++}$ competes with $Mg^{++}$. Since interruption of EP formation by EDTA is delayed in this system beyond the time necessary to chelate $Mg^{++}$, it is suggested that the essential $Mg^{++}$ is complexed with E.

(NIH AM 12718-07)

**M-AM-B12** ELECTROGENIC Na PUMP IN CRUSTACEAN MUSCLE. M.R. Menard*, and J.A.M. Hinke, Vancouver, B. C., Canada.

Following the microinjection of $^{22}Na$ (plus or minus $^{23}Na$) and with the aid of a Na-sensitive microelectrode and an ordinary KCl micropipette, the transmembrane $^{22}Na$ efflux, the myoplasmic Na activity and the resting potential were measured simultaneously in single fibres from the giant barnacle. In some collection periods, ouabain was added to or $K^+$ was omitted in the bathing medium. Na efflux was calculated from the isotope collection and the Na activity data. Evidence for an electrogenic component of the Na pump was obtained by comparing the changes in Na efflux with the changes in resting potential in the experiments. The results are consistent with a model proposed by Moreton, R.B., J. Exp. Biol. 51: 181-201 (1969). The mechanism of charge separation associated with electrogenic pumping is discussed. Using the experimental data and the model, one can calculate $P_{Na}$ permeability to be $0.02 \times 10^{-6}$ cm. $Sec^{-1}$

**M-AM-B13** NEGATIVE COOPERATIVITY OF ATP AND CALCIUM PUMP ATPASE FROM SR. June S. Taylor*, intr. by John Hays.

The hydrolysis of MgATP by the $Ca^{2+}$-dependent ("extra") ATPase of skeletal muscle sarcoplasmic reticulum is biphasic. Micromolar levels of MgATP interact with the membrane-bound enzyme with an apparent $K_M$ of 1 to 6μM, in agreement with published dissociation constants for the enzyme-Mg ATP complex. However, "extra" ATPase activity does not approach a constant maximum rate until MgATP concentrations reach the millimolar range. The activity thus displays strong negative cooperativity with respect to MgATP.

Attempts to resolve these two phases of the ATPase activity profile by variations in assay conditions, by detergent treatment, or by chemical modification failed. Both phases of the $Ca^{2+}$ ATPase kinetic curve appear to be activities of the active ATPase molecule at one or several classes of active sites. The practical effect of the negative cooperative kinetics is to extend greatly the range over which MgATP concentration modulates the rate of ATP hydrolysis. The negative cooperativity does not require that the enzyme be membrane bound, although it may depend on interactions between the $10^5$-dalton peptide chains.

**M-AM-B14** OPTICAL SIGNALS OF MEROCYANINE DYES BOUND TO SARCOPLASMIC RETICULUM (SR) DURING $Ca^{++}$ TRANSPORT. G. Salama*, A. Scarpa, Dept. Biochem-Biophys, U. of Pa., Phila., Pa.

SR isolated from rabbit muscle were suspended in buffered solutions containing dyes sensitive to membrane potential changes. When bound to SR, Merocyanine-540 fluoresces at 585 nm and absorbs at 570 and 530 nm, Merocyanine-Rhodanine (WW 375) absorbs at 720 and 670 nm, and Merocyanine-Oxazolone (NK 2367) at 695 and 640 nm. In the presence of $Ca^{++}$ (10-100 μM) and $Mg^{++}$ (10 mM) addition of ATP stimulates $Ca^{++}$ uptake, producing an increase in absorption at 570 nm and a decrease at 540 nm. Similarly, the non-fluorescent probes exhibit decreases in absorption at 720 and 670 nm with WW 375 and at 720 with NK 2367. Repeated additions of ATP produce little or no further optical response, while $Ca^{++}$ leakage triggered by A23187 reverses the signals. The optical responses are blocked by the prior addition of 2 mM EGTA, $Ca^{++}$ ionophores, or 10% ether. The kinetics of the optical signals are similar and more rapid than the rate of $Ca^{++}$ uptake measured by Arsenazo III. Although the optical signals are related to $Ca^{++}$ transport, further experiments are needed to show a specific dependence on membrane potential.

**M-AM-B15** CALCIUM CONTENT AND NET FLUXES IN SQUID GIANT AXONS. L.J. Mullins, F.J. Brinley, Jr., and J. Requena. Depts. of Physiology and Biophysics, U. of Md. School of Medicine, Baltimore, Maryland 21201 and the Centro de Biofísica y Bioquimica, Instituto Venezolano de Investigaciones Científicas, Caracas, Venezuela

Squid axons freshly dissected from living squid have a Ca content of from 50-70 μmole/kg. axoplasm, as judged from atomic absorption measurements. Treatment of axons with 3 mM Ca choline seawater for one hour or stimulation of axons in 100 mM Ca (Na or Li) seawater at 100 $s^{-1}$ for 10 min. increases their Ca content to 500 or 1600 μmole Ca/kg. axoplasm, respectively. These increases in Ca content can be reversed if the axons are subsequently held in 3 Ca (Na) seawater for 10-60 min.; the Ca content of such axons declines to about 100 μmole/kg. axoplasm. The use of inhibitors (1 mM IAA + 10 μM FCCP) does not interfere with the loss of Ca by loaded axons even though the ATP content of such inhibitor-treated axons is of the order of 25 μM. Axons placed in 40 mM Na (choline) seawater or in 40 mM Na 410 mM K seawater, i.e. conditions where either $Na_o = Na_i$ or where the Na electrochemical gradient is zero, either fail to lose previously loaded Ca-or actually gain further Ca.

**M-AM-B16** $Ca^{++}$ MEASUREMENTS BY ANTIPYRYLAZO III. G. Dubyak, A. Scarpa, and F.J. Brinley. Dept. of Biochem.-Biophys., Univ. of Pa., Phila., PA 19104, and Dept. of Physiol., Univ. of Maryland, Baltimore, MD

$Ca^{++}$--but not $Mg^{++}$ or $Mn^{++}$--causes an appreciable absorbance increase of Antipyrylazo III (bis-antipyrylazo-4,5-dihydroxy-2,7 naphthalene disulfonic acid) in the spectral area 660-800 nm. This facilitates the selection of λ pairs (720-790 nm, 675-690 nm) where $Ca^{++}$ can be monitored without interference by other biologically important divalent ions. In a buffered reaction mixture (pH 7.0) containing 100 mM KCl, AP III - Ca complex has a $\Delta\varepsilon \simeq 7 \times 10^3$ $(cm{\cdot}mol)^{-1}$, a $K_D$ of 120 μM, and a half-time for complex formation of 180 μsec. AP III binds neither to cells nor to subcellular organelles, nor does it affect cellular functions. Examples of $Ca^{++}$ transport by mitochondria, sarcoplasmic reticulum, chromaffin vesicles, and intact cells are shown. In addition to being a "middle range" $Ca^{++}$ indicator which makes possible measurements of $Ca^{++}$ transients at $Ca^{++}$ concentrations where other $Ca^{++}$ indicators are less effective, AP III presents important features with respect to selectivity, response time, and measurement, so as to indicate a wider applicability in biological systems.

ENZYME MECHANISMS I

**M-AM-C1** THE HEME PROTEIN P-450: A STUDY OF THE FORMATION OF ITS FERROUS CARBON MONOXIDE (CO) COMPLEX. Heinz Schleyer, David Y. Cooper*, Otto Rosenthal*, and Pamela Cheung* Harrison Dept. Surg. Res. and Johnson Res. Fdn., Univ. of Pennsylvania, Philadelphia, Penna. 19104

The reactions involved in the formation of the CO complex, P-450 ($Fe^{2+}$)·CO, have been investigated with our soluble P-450 preparation from adrenal cortex (JBC 247, 6103) and membrane-bound preparations from endoplasmic reticulum of rat liver. CO reacts reversibly with high spin (S=2) P-450 ($Fe^{2+}$) to form P-450 ($Fe^{2+}$)·CO with absorption maxima at 367,448 and 550 nm, as previously shown. Markedly different absorption spectra are obtained when this CO complex is prepared by reduction of the $Fe^{3+}$ heme protein in presence of CO, e.g. in the course of reductive titrations (-ΔA∿418nm, +ΔA ∿367 and 448 nm, and well established isosbestic points at 377 and 433 nm). The magnitude of the 448 nm absorption band is pH dependent; it remains constant in the range pH 6.2-7.0, then decreases with increasing pH (half maximal effect ∿ pH 7.6). These findings are presented in relation to the proposed hypothetical structures of the $Fe^{3+}$ and $Fe^{2+}$ forms of the heme protein.

(Supported by Grants AM-04484 and CA-17618 (NIH) and BMS 74-01099 (NSF) ).

**M-AM-C2** EVIDENCE FOR MYOSIN LIGHT CHAIN KINASE AND PHOSPHATASE IN MACROPHAGES. J.A. Trotter and R.S. Adelstein, NIH, NHLBI, Bethesda, Md. 20014

Regulation of actin-activated myosin ATPase activity has been shown in several non-muscle systems, as well as in smooth muscle, to depend on the state of phosphorylation of the myosin. Actin activation of alveolar macrophage myosin has been reported to depend on the presence of a protein "cofactor", the mechanism of action of which is unknown (Stossel and Hartwig, J. Biol. Chem. 250, 5706-5712, 1975). We now report that alveolar macrophages contain myosin light chain kinase capable of transferring approximately one mole of $^{32}P_i$ from [$\gamma$-$^{32}$P]ATP to the 20,000 dalton light chain ($LC_{20}$) of macrophage myosin. This kinase also catalyses the phosphorylation of the isolated $LC_{20}$ of smooth muscle myosin and, at a much lower rate, the isolated $LC_{18.5}$ of rabbit white skeletal muscle myosin. Protein phosphatase activity capable of dephosphorylating the $LC_{18.5}$ of skeletal muscle myosin is also present in macrophages. Together, the kinase and phosphatase represent one potential regulatory system for actomyosin interaction in marophages.

(J.A.T. is a Postdoctoral Fellow of the Muscular Dystrophy Association)

**M-AM-C3** REGULATION OF MYOSIN LIGHT CHAIN KINASES BY $Ca^{2+}$ D.R.Hathaway*, A.Sobieszek*, R.S.Adelstein, NIH, NHLBI. Section on Molecular Cardiology, Bethesda, Md. 20014

Phosphorylation of the 20,000 dalton light chain of platelet and smooth muscle myosin is necessary for actin activation of myosin ATPase activity. Myosin phosphorylation is catalyzed by myosin light chain kinase. $Ca^{2+}$ regulation of myosin kinase activity was studied using the enzyme isolated from human platelets and turkey gizzards. Platelet kinase was prepared from fresh platelet concentrates, as previously described for myoblasts (Nature, 268, 558-560, 1977), but using an extracting solution containing 5 mM EDTA and 2.5 mM EGTA. Partial purification of the kinase was obtained by gel filtration in Sepharose 4B and yielded a kinase that was slightly (10%) inhibited by 1 mM EGTA. Further purification on Sephadex G-100 resulted in a platelet kinase that was markedly (over 80%) inhibited by 1 mM EGTA. In contrast, turkey gizzard myosin kinase was inhibited (>90%) by 1 mM EGTA throughout the entire preparation. Sephadex G-100 gel filtration of the platelet enzyme in 1 M KCl and 5 mM EDTA-EGTA and the gizzard kinase in 0.8 M KCl, 1 mM EGTA, 1 mM $MgCl_2$ resulted in complete recovery of enzymatic activity.

**M-AM-C4** CHANGES IN MYOSIN AND MYOSIN LIGHT CHAIN KINASE DURING MYOGENESIS IN VITRO. S.P.Scordilis and R.S. Adelstein, N.I.H./N.H.L.B.I., Bethesda, Md. 20014

Myosin and the myosin light chain kinase (MLCK) were isolated from a cloned cell line (Yaffe L5-810) of rat myoblasts while they were proliferative cells (PMB), early myotubes without sarcomeres (EMT), and myotubes with sarcomeres (MTS). Fusion was effected by lowering of the serum concentration in the growth medium which otherwise maintained the myoblasts as dividing cells. The myotubes with sarcomeres beat spontaneously. The myosin from each of these cell types has a heavy chain of 200,000 daltons. The light chain patterns changed: PMB, 20,000 and 15,000; EMT, 20,000; MTS, 23,000, 19,000 and 16,000 daltons. The PMB MLCK is not $Ca^{2+}$-dependent, whereas approximately 75% of the MTS MLCK does require $Ca^{2+}$ for activity. If any MLCK is present in the EMT, it must be present in extremely low amounts, as it has not been detected. Neither has any MLCK inhibitor been demonstrated in the EMT. The 19,000-20,000 dalton light chains of all three myosins are phosphorylatable. (S.P.S. is a Post-doctoral Fellow of the Muscular Dystrophy Association of America).

**M-AM-C5** ACANTHAMOEBA MYOSINS. H. Maruta,* J.H. Collins,* H. Gadasi,* and E.D. Korn. NIH, Bethesda, MD 20014

Acanthamoeba extracts contain at least four "myosins". Three have been purified: myosin IA, a one-headed molecule with peptide chains of about 130,000, 17,000 and 14,000 daltons (ratio about 1:1:0.5); myosin IB, a one-headed molecule with peptides of about 125,000, 27,000 and 14,000 daltons (about 1:1:0.5); and myosin II, a 400,000-dalton, two-headed myosin with peptides of about 170,000, 17,500 and 17,000 daltons (1:1.5:1). A fourth "myosin", slightly larger than myosin I and which may be derived from myosin II, occurs in cell extracts but has not been purified. Myosins IA and IB have much greater (K+,EDTA)ATPase activities than $Ca^{2+}$ATPase activities; the reverse is true for myosin II. The $Mg^{2+}$ATPase activities of myosins IA, IB and II are only about 2-fold activated by actin. However, the $Mg^{2+}$ATPase activities of myosins IA and IB, but not of myosin II, are highly actin-activated after phosphorylation of their heavy chains by a specific Acanthamoeba myosin kinase (cofactor) that does not phosphorylate myosin II. Myosins IA and IB may be proteolytic products of a common precursor. However, all presently available data indicate, but do not prove, that myosins I and II are isozymes.

**M-AM-C6** THE TEMPERATURE DEPENDENCE OF RIBONUCLEASE A CATALYSIS: ANALYSIS BY USE OF TRANSITION STATE THEORY. M. Eftink* and R. Biltonen,* Intro. by J. Ogilvie, Dept. of Biochem., U. of Virginia, Charlottesville, VA 22903

Interpretation of the magnitude of the activation enthalpy ($\Delta H^{\dagger}$) for enzyme catalyzed reactions has in the past been limited. The transition state formalization (Wolfenden, Acc. Chem. Res. 5, 10) provides a means for more clearly analyzing activation parameters. The $\Delta H^{\dagger}$ for the second order rate constant ($k_c/K_m$) for an enzymatic reaction minus the $\Delta H^{\dagger}$ for the corresponding nonenzymatic reaction is equal to $\Delta H_{ts}$, the enthalpy change for the "binding" of the transition state to the enzyme. This parameter can be compared to the $\Delta H$ for the interaction of various transition state analogs with the enzyme. This relationship has been employed in studying the RNAse A catalyzed hydrolysis of cCMP. The $\Delta H_{ts}$ is found to be of the same order to magnitude as the $\Delta H$ for the association of the transition state analog 2'-CMP. Mechanistic implications will be discussed.

(Supported by NSF Grant PCM75-23245-A02)

**M-AM-C7** A THEORETICAL STUDY OF BENZO[A]PYRENE BINDING BY CYTOCHROME P-450. W. B. England and L. L. Shipman, Chemistry Division, Argonne National Laboratory, Argonne, Illinois 60439

Benzo[a]pyrene (BP) is a ubiquitous carcinogenic and mutagenic environmental pollutant formed primarily from incomplete combustion of organic material. BP is oxidized by membrane-bound cytochrome P-450 to just a few of the total number of possible epoxide metabolites. We have investigated the possibility that cytochrome P-450 one-electron oxidizes BP and that BP orientation in the enzymatic site is dominated by the anisotropic coulombic force between the net negative charge on the iron protoporphyrin IX-dioxygen complex and the delocalized positive charge on BP cation. In particular, contour maps have been computed for the interaction energy and force between a negative test charge and the charge distribution of BP cation radical. Features in these contour maps have been interpreted in terms of their significance for the enzyme-substrate interaction.

This work was performed under the auspices of the U. S. Department of Energy.

**M-AM-C8** COMPLEMENTATION OF MUTANT AND INACTIVATED NUCLEASE FROM HAEMOPHILUS INFLUENZAE. M. Yaqub* and J.K. Setlow, Brookhaven National Laboratory, Upton, N.Y.11973

Complementation between certain pairs of extracts of mutants deficient in ATP-dependent nuclease can result in enzyme activity, provided the extracts have not been dialysed. The factor lost on dialysis is labile and has a molecular weight between 2,000 and 12,000, as judged by filtration. It can be provided to a dialysed mutant extract through a dialysis bag by a crude mutant but not a crude wild type extract. The sensitivity of the mutant extracts to heat depends on the complementation group of the other partner, indicating that the heated extract provides a particular one of the three known subunits that is defective in the unheated partner. Wild type enzyme inactivated by urea or heat can be reactivated by reaction with a mutant extract, but independently of the mutant's complementation group. We postulate that the dialysable factor is a fourth subunit of the enzyme, necessary for activity, tightly bound in the wild type but loosely bound in the mutant, and that it is supplied by the mutant extracts to inactivated wild type enzyme.
(Supported by the U.S. Department of Energy)

**M-AM-C9** THE KINETICS OF Mg-STIMULATED OUABAIN BINDING TO PURIFIED $Na^+,K^+$-ATPase. F. Mandel, E. T. Wallick and A. Schwartz, Pharmacology & Cell Biophysics, Univ. of Cincinnati College of Medicine, Cinti, OH 45267

The following model for the Mg-induced ouabain (oub) binding to $Na^+,K^+$-ATPase (E) has been studied:

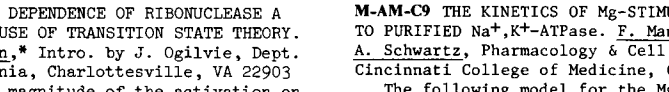


where Ka, bKa, $K_i = k_{-2}/k_2$ and $bK_i = k_{-1}/k_1$ are dissociation constants of various enzyme complexes. The rates of association to the enzyme are denoted by $k_1$ and $k_2$ and the dissociation rate constants by $k_{-1}$ and $k_{-2}$. Assuming that Mg reacts with the enzyme at a much faster rate than ouabain reacts with the enzyme, the fraction bound as a function of time is given by:

$$B(t) = 2[Oub]_{tot} / \{q^{\frac{1}{2}} \cdot (e^{\delta t} + 1)/(e^{\delta t} - 1) - \beta\}$$

where $\beta = [E]_{tot} + [Oub]_{tot} + K^{app}$,
$K^{app} = bK_i \cdot (Ka + Mg)/(bK_a + Mg)$, $q = \beta^2 - 4\,[Oub]_{tot} \cdot [E]_{tot}$

and $\delta = q^{\frac{1}{2}} \cdot \dfrac{k_1 K_a + k_2\,[Mg]}{K_a + [Mg]}$ .

The data are consistent with this equation.

**M-AM-C10** METAL AND ATP INTERACTIONS WITH ADENYLATE CYCLASE. R. Harris,* R. Cruz,* and A. Bennun, Rutgers University, Newark, N. J. 07102

The effect of several hormones on the kinetics of adenylate cyclase from fat cell membranes were studied for $Mg^{2+}$ concentration curves at 5mM ATP. Hill plots were calculated and values for Hill coefficient ($^nH$) and $K_{0.5}$ (mM) for total Mg ($Mg_t$), free $Mg^{2+}$ ($Mg^{2+}$) and 50% inhibition by free ATP (ATP) were obtained for: Basal (B), 50 $\mu$M l-epinephrine (E), 40 $\mu$g/ml ACTH and 35 $\mu$g/ml glucagon (G). $^nH$ ($Mg_t$): B=2.6; E=4.6; ACTH=4.2 and G=3.5. $K_{0.5}$ ($Mg_t$): B=16.5; E=6.1; ACTH=4.5 and G=6.8. $^nH$ ($Mg^{2+}$): B=1.2; E=1.1; ACTH=1.4 and G=1. $K_{0.5}$ ($Mg^{2+}$): B=11.5; E=1.2; ACTH=0.35 and G=1.8. $^nH$ (ATP) from negative slopes: B=1.2; E=1.1; ACTH=1.6 and G=1.0. $Ki_{0.5}$ (ATP): B=0.03; E=0.25; ACTH=0.62 and G=0.16. The effect of MgATP, $Mg^{2+}$ and ATP is cooperative for total Mg with single interacting sites for free Mg and free ATP. The hormones effect is to increase the affinity for activatory free $Mg^{2+}$ and decrease the affinity for inhibitory free ATP rather than (with the exception of ACTH) to modify the number of interacting sites for these compounds.

**M-AM-C11** $^{31}$P-NMR OF BOUND SUBSTRATES OF PHOSPHORYL TRANSFER ENZYMES. B. D. Nageswara Rao and M. Cohn, University of Pennsylvania, Philadelphia, Pennsylvania 19104

Kinases are phosphoryl transfer enzymes that catalyze the reaction ATP + S → ADP + SP, where S is a second substrate. A divalent cation, usually $Mg^{2+}$, is an obligatory component of these reactions. In the present work several different kinases are studied by observing $^{31}$P-NMR spectra of enzyme-bound substrate complexes. These experiments provide information on the enzyme-substrate interactions and the role of the $Mg^{2+}$ ion in terms of effects on the NMR-spectral parameters, chemical shifts and spin-spin coupling constants, in the bound complexes. An analysis of the spectra of equilibrium mixtures of bound substrates allows the determination of the rate of interconversion of reactants and products on the surface of the enzyme and of equilibrium constants at high enzyme concentrations that may be physiologically significant. Such equilibrium constants might differ by as much as $10^3$ from those at catalytic enzyme concentrations. Some of the results obtained on arginine kinase, creatine kinase, pyruvate kinase, adenylate kinase and 3-phosphoglycerate kinase will be presented and compared.

**M-AM-C12** HISTIDINE IN THE NUCLEOTIDE BINDING SITE OF TPN-SPECIFIC ISOCITRATE DEHYDROGENASE. Robert S. Ehrlich and Roberta F. Colman. Chem. Dept., Univ. Del., Newark, DE.

Incubation of pig heart TPN-specific isocitrate dehydrogenase with ethoxyformic anhydride at pH 5.8 results in an 8-fold greater rate of loss of dehydrogenase than oxalosuccinate decarboxylase activity. Rate constants for loss of dehydrogenase and decarboxylase activities depend on the basic form of ionizable groups with pKs 5.67 and 7.05, respectively, suggesting that inactivation of the two catalytic functions results from reaction with different amino acids. The rate of loss of dehydrogenase activity is decreased only slightly by manganous-isocitrate, but is reduced up to 10-fold by coenzymes or coenzyme analogues, such as 2'-phosphoadenosine 5'-diphosphoribose (PADPR). Modified enzyme fails to bind TPNH, but exhibits manganese-enhanced isocitrate binding typical of native enzyme, implying that reaction occurs at the nucleotide binding site. Measurements of ethoxyformyl-histidine formation at 240 nm and incorporation of $^{14}C$-ethoxy groups in the presence and absence of PADPR indicate that inactivation may be related to modification of a single histidine. The critical histidine appears to be located in the nucleotide binding site.

MUSCLE PROTEINS I

**M-AM-D1** DIVALENT CATIONS AFFECT THE ROTATIONAL MOBILITY OF THE HEADS OF HEAVY MEROMYOSIN (HMM). Stefan Highsmith CVRI, Univ. of Cal., San Francisco, CA. 94143.

Divalent cations were removed from fluorescently labeled HMM in 0.15 M KCl, 10 mM Tes, pH 7 at 4°C with EDTA. Titration with $Mg^{2+}$ or $Mn^{2+}$ greatly increased the rotational mobility of the heads as measured by fluorescence depolarization. $Ca^{2+}$ had no effect. The mobility of myosin subfragment-1 (S-1) was unaffected by EDTA or divalent cations. This indicates that HMM's enhanced mobility reflects increased flexibility rather than a more compact structure. The divalent cations probably bind to light chain 2 (MW 18K) which is thought to be near the swivel where S-1 joins S-2. The difference in head mobility for $Mg^{2+}$ and $Ca^{2+}$ may have a regulatory role. However, the association constant for HMM and $Mg^{2+}$ was estimated from titration curves to be $> 10^8\ M^{-1}$. Thus, the site would be saturated with $Mg^{2+}$ *in vivo* and its function in skeletal muscle is probably structural rather than regulatory. The $[Mg^{2+}]$ dependency of the mobility is quantitatively similar to that for EDTA activation of myosin ATPase activity. (Offer(1964)BBA89,566). This suggests that removal of tightly bound $Mg^{2+}$ on myosin causes EDTA activation. (Grants: USPHS HL-16683, AHA CI-60).

**M-AM-D2** THE INTRINSIC SEGMENTAL FLEXIBILITY OF THE S1 MOIETY OF MYOSIN. R.A. Mendelson and P.H. Cheung*, CVRI Univ. of Calif., San Francisco, CA 94143.

The fluorescence depolarization of 1,5 IAEDANS labelled single headed myosin (SHM) has been investigated. Over the time range studied the polarization decay of soluble myosin (M) and SHM were almost identical [$\phi(SHM) \simeq .9\phi(M)$] thus demonstrating that earlier measurements on M were primarily probing the intrinsic rotation of the S1 moiety. This and ancillary results verify the notion of a localized, highly flexible region between S1 and S2 which allows S1 to tumble within almost $4\pi$ sr. SHM synthetic filaments gave the same large immobilization found in M filaments (with or without DTNB LC) and relaxed myofibrils, demonstrating that motion is hindered by the lattice alone. Monte Carlo simulations indicated that the half angle of motion within an assumed cone-shaped lattice boundary was less than 12.5 deg. No physiologically important combination of ligands significantly affected lattice immobilization, HMM flexibility, or S1 shape, supporting the notion of S1's reaching actin by translational diffusion with concomitant increase in rotational freedom. (Supported by NIH HL-06285, NIH HL-16683 and NSF PCM76-11491.)

**M-AM-D3** THERMODYNAMIC STUDIES OF THE BINDING OF ADENOSINEDIPHOSPHATE (ADP) AND CALCIUM TO BEEF CARDIAC MYOSIN. S.K. Banerjee* and E. Morkin. University of Arizona Health Sciences Center, Tucson, Arizona 85724

Thermodynamic quantities for the binding of ADP and $Ca^{2+}$ to purified beef cardiac myosin have been determined by flow calorimetry at 25°C and equilibrium dialysis at 4°C in 0.5 M KCl, 20 mM Tris-Cl, pH 7.5. The results indicate that: 1) there are about 2 mol high affinity $Ca^{2+}$ binding sites per mol myosin with an affinity constant of $10^5\ M^{-1}$; 2) the enthalpy of $Ca^{2+}$ binding is about zero; 3) about 2 mol ADP are bound in the presence of either $CaCl_2$ or $MgCl_2$; 4) free energy of binding of MgADP and CaADP is -6.7 and -5.7 kcal/mol, respectively; 5) enthalpy of binding of MgADP and CaADP is -12.5 and -19.0 kcal/mol, respectively. These results show that CaADP binds to cardiac myosin with a much greater negative enthalpy than MgADP. Also, the free energy of ADP binding to cardiac myosin is similar to values reported for skeletal myosin. However, the enthalpy of binding is much less negative than the value obtained for skeletal myosin by Kodama and Wooledge (J.Biol.Chem.(1976)252,7499). The latter results suggest a subtle difference in the nucleotide binding sites of these myosins.

**M-AM-D4** CRYSTAL STRUCTURE OF TROPOMYOSIN. G.N. Phillips, Jr., E.E. Lattman*, P. Cummins*†, J.J. Bloom, K.Y. Lee*, and C. Cohen, Rosenstiel Ctr., Brandeis U., Waltham, MA.

The three-dimensional structure of rabbit cardiac tropomyosin has been determined by x-ray diffraction using data to 20 Å. Phase information was obtained from electron microscopy, model building, flattening solvent space, and single isomorphous replacement. The molecules are bonded end-to-end to form an open meshwork of cross-connecting filaments in the crystal. Rabbit cardiac tropomyosin is known to be a coiled-coil of two identical α-helical chains--each with one cysteine residue. Difference Fourier projections of a Hg derivative show a single peak per tropomyosin molecule. Since the Hg is a marker for the single cysteine residue, this suggests that the SH groups of each chain are closely aligned. The location of the Hg atom is also critical since it can be used to place the entire amino acid sequence along the filament path, including the molecular ends and cross-connecting sites. These studies are being extended to crystals containing the components of the troponin complex. This work was supported by NIH, No. AM17346, RCDA, No. HL00161 and grants from the MDAA.

†University of Birmingham, England.

**M-AM-D5** $Mg^{2+}$-DEPENDENT INTERACTION BETWEEN TROPOMYOSIN AND MUSCLE ACTIN-ACANTHAMOEBA ACTIN COPOLYMERS. Y.Z. Yang, E.D. Korn, and F. Eisenberg. NIH, Bethesda, MD 20014

Acanthamoeba actin (aA) differs from muscle actin (mA) in the $[Mg^{2+}]$ required for binding tropomyosin (TM). $Mg^{2+}$-dependent binding patterns of copolymers with varying ratios of the two actins indicate that mA and aA are randomly distributed in the copolymers. Furthermore, TM binds to the copolymers in a molar ratio of 1 TM to 7 actins as it does to homopolymers. For homopolymers, bound TM inhibits the mA-activated heavy meromyosin (HMM) ATPase but has no effect on the aA-activated HMM ATPase. If TM exerted the same effect on 7 consecutive actin monomers in an actin filament, then as the ratio of aA to mA in the copolymer is increased, the effect of TM will change abruptly from maximal inhibition of the ATPase to no inhibition at all. In contrast, we find that as the ratio of aA to mA is increased, the inhibition by TM is gradually reduced as if the aA is never affected by tropomyosin. This result can not be attributed to TM being unable to inhibit aA since with troponin present (in the absence of $Ca^{2+}$), the aA-activated HMM ATPase is strongly inhibited. We conclude that TM can have an independent effect on adjacent aA and mA monomers in the copolymer.

**M-AM-D6** FLUORESCENT PROBES STUDIES OF BINDING OF ACTIN WITH MYOSIN SUBFRAGMENT-1. T.-I Lin, S. Carlile*, R.M. Dowben, UTHSCD, TX 75235.

F-actin labeled with various fluorescent probes, dansyl aziridine (DAZ), 2-(4'-maleimidylanilino) naphthalene-6-sulfonic acid (MIANS), and 4-dimethylamino-4'-maleimido-stilbene (DMAMS) was used to study its binding interaction with S-1. On adding S-1 to MIANS and DMAMS labeled actin a small fluorescence enhancement (5-10%) occurs instantaneously (within a few seconds), followed by a very slow (takes several hours) but larger enhancement (20-35%). On the other hand, the fluorescence of DAZ-actin was slightly quenched (7%) immediately after adding S-1, followed by a very slow but large enhancement. Adding ATP to the complexes reverses these effects. These results suggest that the binding of actin with S-1 involves two conformational changes. Presumably, the small changes reflect the direct perturbation of the probes by S-1 and the second changes reflect the slow interactions between the residues at the binding interface of the complex. The binding behavior of S-1 with various labeled actin will be compared.

Supported by Texas Heart Association.

**M-AM-D7** FLUORIMETRIC STUDIES OF TROPOMYOSIN AND F-ACTIN LABELED WITH 3-PYRENEMALEIMIDE. T.-I Lin, C. Ford*, and R. Dowben, UTHSCD, Dallas, TX 75235 (Spon. By G. Weiss).

3-Pyrenemaleimide (PM) was attached to sulfhydryls of tropomyosin (TM) and F-actin in molar ratios of 1.95 and 0.83, respectively. The ratios of fluorescence intensity at various emission peaks relative to that at 377 nm max vary only slightly in various denaturing media but the quantum yield depends strongly on the solvent. Our study suggests that in actin PM is exposed on the surface but in TM PM may be located at a hydrophobic patch. The succinimido ring of PM undergoes aminolysis, as labeled proteins aged or denatured in urea, shown by the progressive decrease of emission peaks at 376, 396 and 416 nm and gradual increase of new peaks at 386 and 405 nm. The fluorescence of both labeled proteins changes significantly as the proteins depolymerize which is useful for monitoring the depolymerization. Adding actin to PM-TM induces new excitation peaks at 287 and 291 nm suggesting a Trp residue in actin is close to PM in TM upon binding. The binding behavior of TM with actin will be compared with the results obtained by using other probes.

Supported by NIH 16678 and Texas Heart.

**M-AM-D8** THE EFFECTS OF pH ON CALCIUM BINDING TO THE $Ca^{2+}$-$Mg^{2+}$ AND THE $Ca^{2+}$-SPECIFIC SITES OF RABBIT SKELETAL TnC. Steven P. Robertson, J. David Johnson and James D. Potter, Pharmacology & Cell Biophysics, Univ. of Cincinnati College of Medicine, Cincinnati, OH. 45267

$Ca^{2+}$ binding to rabbit skeletal TnC was measured indirectly in solutions containing 2mM EGTA or EDTA, 10mM $PO_4$ and 90mM KCl. The calcium induced enhancement of tyrosine fluorescence (0.15 mg/ml TnC) was unchanged between pH 7.5 and 6.0 suggesting that $Ca^{2+}$ binding to the $Ca^{2+}$-$Mg^{2+}$ sites is independent of pH in this range. $Ca^{2+}$ binding to the $Ca^{2+}$-specific sites, inferred from the $Ca^{2+}$ dependence of dansylaziridine (DANZ) labelled TnC fluorescence (54μg/ml $TnC_{DANZ}$) was pH dependent. The pCa values (± 95% confidence limits) at which the fluorescence enhancements are half maximal are shown below. Note that pH dependence of $Ca^{2+}$ binding to the $Ca^{2+}$-specific sites is similar to the pH dependencies of $Ca^{2+}$ activated myofibrillar ATPase and tension.

| pH | $TnC_{DANZ}$ | Tyrosine |
|---|---|---|
| 7.5 | 6.04 ± .12 | 7.16 ± .03 |
| 7.0 | 5.74 ± .06 | 7.05 ± .13 |
| 6.5 | 5.52 ± .12 | 7.04 ± .06 |
| 6.0 | 5.33 ± .12 | 6.97 ± .09 |
| 5.5 | 5.05 ± .15 | 6.62 ± .09 |

Supported by AHA 75818. JDP is an E.I. of AHA. JDJ is a Fellow of the MDA.

**M-AM-D9** FLUORESCENCE STUDIES OF $CA^{++}$-INDUCED CHANGES IN TROPONIN-C. H. C. Cheung and F. Garland, Biophysics Section, Department of Biomathematics, University of Alabama in Birmingham, Birmingham, AL 35294

Troponin-C (TNC) has been studied with two fluorescent probes. Probe I(1,5-IAEDANS) is sensitive to $Ca^{++}$ binding to the high affinity $Ca^{++}$-$Mg^{++}$ sites, but not to the low affinity $Ca^{++}$-specific sites. The binding causes a 30% increase in quantum yield and a blue shift of 5 nm. Two lifetimes are observed when $Ca^{++}$ is absent and only one lifetime is detected when $Ca^{++}$ is present. Identical spectral parameters are obtained when $Ca^{++}$ is replaced by $Mg^{++}$. The rotational correlation time of TnC(I) is 20% longer in $Mg^{++}$ than in $Ca^{++}$. In contrast to probe I, probe II(dansylaziridine) in TnC(II) responds differently to $Mg^{++}$ and $Ca^{++}$. $Mg^{++}$ binding results in a 20% decrease in quantum yield and a red shift of 8 nm. $Ca^{++}$ binding is accompanied by 200% increase in quantum yield and a blue shift of 19 nm to 501 nm. Without bound cations,two lifetimes (ca. 9 and 17 nsec.) are observed. Both lifetimes increase with increasing $Ca^{++}$ level. The results suggest that dansylaziridine is useful for probing conformational changes induced by specific $Ca^{++}$ binding to the low affinity sites.

**M-AM-D10** CROSS INNERVATION: A COMPARISON OF EFFECTS ON $Ca^{2+}$ AND $Sr^{2+}$ ACTIVATION, MYOSIN LIGHT CHAINS, AND HISTOCHEMISTRY IN RABBIT SOLEUS. D.J. Secrist, P.E. Hoar, & W.G.L. Kerrick, Dept. of Physiology and Biophysics, University of Washington, Seattle WA 98195

Two kinds of cross innervation surgeries were performed: (1) suturing of a fast nerve to the sarcolemma of soleus and (2) nerve cross union. The rabbits were sacrificed between 6 and 18 months post-operative. To evaluate the extent of cross innervation, histochemical staining of muscle cross-sections, SDS polyacrylamide gels, and single fiber (mechanically skinned) tension measurements were performed. $Ca^{2+}$ and $Sr^{2+}$ activated tension measurements made on single fibers showed that in successfully crossed slow twitch soleus muscle some or all fibers had $Ca^{2+}$, $Sr^{2+}$ sensitivities characteristic of a fast twitch muscle. In single fibers from normal soleus, a direct correlation was observed between the myosin light chains appearing on SDS gels and the characteristic sensitivity to $Ca^{2+}$ and $Sr^{2+}$. Successfully cross innervated single fibers showed a banding pattern consisting of both slow and fast light chain components.

(Supported by PHS GM 00260, NS 05082, & HL 05527; Muscular Dystrophy Association; Graduate School - University of Washington.)

**M-AM-D11** NANOSECOND DECAY STUDIES OF FLUORESCENT LABELED TROPOMYOSIN. C. Ford*, J. Bunting, R. Dowben and T.-I Lin, UTHSCD, Dallas, TX 75235.

Tropomyosin (TM) has been labeled with the sulfhydryl specific fluorescent probes 3-N-pyrenemaleimide, dansylaziridine (DAZ), and 4-dimethylamino-4'-maleimidostilbene (DMAMS). Labeling ratios between 1.5 and 2.0 were commonly observed suggesting more than one binding site on TM. Fluorescence lifetime data was analyzed by a method of momments which can determine the number of components by use of the determinants of the I-curve moments. The fluorescence decay of DAZ-TM was composed of two components with time constants of 12.3 nsec and 2.5 nsec. PM-TM analyzed for three components with values of 75.1 nsec, 27.1 nsec and 4.4 nsec. DMAMS-TM had a single decay time of 0.95 nsec. The multiple lifetimes most likely result from labeling at different sites with different environments. PM-TM and DMAMS-TM lifetime values did not change significantly when the labeled TM was bound to F-actin. Although energy transfer has been observed between actin tryptophan and these three probes, the absence of change in lifetime values is consistent with the picture of the probes as acceptors. Supported by NIH 16678 and Texas Heart.

**M-AM-D12** DISSOCIATION OF THE ACTIN-SUBFRAGMENT-ONE COMPLEX BY AMP-PNP AND ADP. L.E. Greene* and E. Eisenberg. NELBI, NIH, Bethesda, Maryland 20014

The ability of AMP-PNP and ADP to dissociate acto-subfragment-one was studied using an analytical ultracentrifuge with UV optics. Particularly below 0.1 M ionic strength, the maximum dissociation induced by either ADP or AMP-PNP at saturating nucleotide concentration is considerably less than the dissociation induced by ATP under identical conditions. At 0.22 M ionic strength, pH = 7.0, 22° with saturating nucleotide concentration present, ADP weakens the binding of actin to S-1 about 100-fold ($K \simeq 10^5\ M^{-1}$), while AMP-PNP weakens it about 1000-fold ($K \simeq 10^4\ M^{-1}$). This 10-fold stronger dissociating effect of AMP-PNP compared to ADP correlates with data indicating that AMP-PNP binds about 10 times more strongly to S-1 than does ADP. On the other hand, the binding constants of ADP and AMP-PNP to acto·S-1 are nearly identical ($K \simeq 5 \times 10^3\ M^{-1}$). These data are consistent with actin and nucleotide both binding to S-1 simultaneously to form a ternary complex. ADP and AMP-PNP both weaken the binding of actin to S-1 with AMP-PNP acting more like ADP than ATP in this respect.

**M-AM-D13** ACTIN SEQUENCE REPEATS INDICATE POSSIBLE ACTIVE SITE COMPONENTS. Michael Gallagher* and Vincent D'Aco* Dept Biochem SUNY Downstate Med Cent, NY 11203, and Hydroscience Inc, Emerson, NJ. (Intr. by Alfred Stracher)

Sequence repeats within rabbit muscle actin were detected by a visual analysis of those short sequence lengths found to compare favorably by computer methods (Gallagher + D'Aco JCellBio 75:326a, 1977). This led to a pattern consistent with triplication of sequence information (residues 1-74, 146-218, 300-374; eg elements 1,2,3).Each element appears to contain an internal duplication, roughly dividing the element into two major subsections (a+b) of equivalent length. We have correlated this pattern of replication with the published actin chemical and enzymatic modification literature, and have developed a model for the actin active site (ATP binding/hydrolysis) containing discrete sequence lengths. We propose that homologous residues 32-40 and 366-374, along with $Cys_{10}$, are active site componenets. $Cys_{373,10}$ coordinate adenine in monomer and polymer, respectively. $Arg_{37,39,371}$ coordinate ATP phosphate. $His_{40}$ participates in hydrolysis. This model accounts for the experimentally determined parameters of monomeric and polymeric actin, as well as the transitional processes of polymerization and depolymerization. (Supported in part by GM19626 to A. Stracher)

**M-AM-D14** EFFECTS OF DEUTERIUM OXIDE ($D_2O$) ON CALCIUM TRANSIENTS AND MYOFIBRILLAR RESPONSES IN FROG SKELETAL MUSCLE. R. E. Godt, D. G. Allen*, and J. R. Blinks; Dept. of Pharmacology; Mayo Foundation, Rochester, MN 55901.

The mechanism by which substitution of $D_2O$ for $H_2O$ suppresses contraction was studied in intact aequorin-injected fibers and in mechanically skinned fibers of R. temporaria at 10°C. The log apparent affinity constant of CaEGTA, determined with aequorin, was 6.38 in $H_2O$ and 5.20 in $D_2O$ (pH=pD=7.0); 99.8% $D_2O$ reduced aequorin light output for any $[Ca^{++}]$ no more than 50% in vitro. In intact fibers $D_2O$ substitution decreased twitch and tetanic tension in a dose-dependent fashion; in all-$D_2O$ (99.8%) Ringer, aequorin signals and tension development were essentially abolished. $[Ca^{++}]$-tension relations were determined in skinned fibers at pH 7.0 ($H_2O$) and pD 7.0 and 7.6 ($D_2O$). Maximal $Ca^{++}$-activated tension was 20% higher and relaxation markedly slowed in $D_2O$ (both pD levels). $D_2O$ shifted the $[Ca^{++}]$-tension curves to the right (i.e., more $Ca^{++}$ required) by 0.3 log unit at pD 7.6 and 0.5 unit at pD 7.0. We conclude that in intact muscle $D_2O$ inhibits contraction both by decreasing $Ca^{++}$ release and by decreasing the $Ca^{++}$ sensitivity of the contractile system. Support: NIH (AM17828 and HL12186); American Heart Association; British Heart Foundation.)

**M-AM-D15** VARIABLE CONTRACTILITY OF CARDIAC CONTRACTILE PROTEINS. G. B. McClellan and S. Winegrad, Dept. of Physiology, Sch. Med., Univ. Pa., Philadelphia, PA 19104

In rat ventricular strips that have been made hyperpermeable by exposure to EGTA, it is possible to directly probe the properties of the contractile proteins with $Ca^{++}$ in the presence of many of the cells' normal regulatory systems. The nature of the contractile system, with respect to both contractility and Ca sensitivity, is different in strips prepared from hearts immediately after sacrifice of the animal from those taken from hearts that have been perfused with Krebs for 10 min after sacrifice, presumably because the former are still under the influence of the large release of catecholamines during sacrifice. The contractile system of the bundle from the non-perfused or "catecholamine-treated" heart has a lower Ca sensitivity, and its Ca-activated force responds to cyclic nucleotides in a different way from the perfused or "non-catecholamine-treated" heart. In the perfused heart cGMP inhibits force development, but in the nonperfused it can enhance force development.

(Work supported by grant PHS HL 15835.)

HEMOGLOBIN I

**M-AM-E1** SUBUNIT DISSOCIATION IN TADPOLE HEMOGLOBIN. D.H.Atha and A. Riggs, Zoology Dept., Univ. of Texas, Austin, Texas 78712.

The tetramer-dimer dissociation constant for phosphate free $HbO_2$ from the bullfrog tadpole (Rana catesbeiana) increases from 5 μM near pH 7.5 to 4 mM at pH 10.0 at 20° C. The results, obtained by sedimentation velocity and gel chromatography are similar to those for human $HbO_2$ except that the tadpole $HbO_2$ dissociation occurs at much lower pH. The corresponding constant for deoxy Hb increases from 3 x $10^{-11}$ M at pH 7.5 to 0.1 mM at pH 10.0. The results indicate that dissociation of oxy and deoxy tetramers is accompanied by the release of 2 and 4 protons respectively in the pH range 9-10. Additional dissociation to monomer also occurs with high dilution. The weight fraction of monomer is almost 0.30 at pH 8.7 and is 0.65 at pH 10.5 at a heme concentration of 0.22 μM. The Bohr effect of the dimer appears to be near zero. The observed decrease in the Hill coefficient, n, with pH can be accounted for partly by subunit dissociation and by the known heterogeneity of the unfractionated hemoglobin.

This work was supported by NSF grant PCM-76-06719 and Robert A. Welch Foundation grant F-213.

**M-AM-E2** STRUCTURE-FUNCTION RELATIONSHIPS IN THE HEMOCYANIN SYSTEM OF LIMULUS POLYPHEMUS. Joseph Bonaventura and Celia Bonaventura, Duke University Medical Center and Duke University Marine Laboratory, Beaufort, North Carolina 28516

The hemocyanin system of the horseshoe crab, Limulus polyphemus, is a particularly interesting example of a macromolecular assembly containing diverse subunits. The intact molecule is a protein of 3.3 x $10^6$ daltons which shows a strong negative Bohr effect, allosteric interactions with chloride ions, and marked cooperativity in oxygen binding. This molecule can be dissociated into electrophoretically distinct functional subunits of about 75,000 daltons. These subunits can be fractionated by ion exchange chromatography. The isolated subunits have distinct functional and structural properties. Natural and artificial mixtures of subunits can be reassembled to the 3.3 x $10^6$ dalton structure. The various subunits play diverse roles in the reassembly. Electron microscopy of assembly products (work done in collaboration with E. Van Bruggen, University of Groningen, The Netherlands) suggests a model for the reassembled structure.

**M-AM-E3** ANIONIC CONTROL OF HEMOGLOBIN FUNCTION. Celia Bonaventura and Joseph Bonaventura, Duke University Medical Center and Duke University Marine Laboratory, Beaufort, North Carolina 28516

Human hemoglobin is in a state of dynamic equilibrium between high and low affinity forms. The oxygen affinity can be modulated by the concentration of anions in the external medium. Detailed studies of the structural and functional properties of human hemoglobin variants has provided greater insight into the mechanism by which cofactor binding is linked to oxygen binding. The mutant hemoglobins whose structural and functional modifications are particularly relevant to the question of anionic control mechanisms are those which involve the diphosphoglycerate binding site. Studies on the oxygen binding behavior of Hb Raleigh (β1 Val→AcAla), Hb Deer Lodge (β2 His→Arg), Hbs Providence (β82 Lys→Asn and Asp), Hb Leiden (β6 deleted), Hb Hope (β136 Gly→Asp) and Hb Abruzzo (β143 His→Arg) are consistent with the interpretation that the positive charge cluster of the DPG binding site de-stabilizes the low affinity conformation. The anionic control of hemoglobin's oxygen affinity is, accordingly, hypothesized to result from neutralization of repulsive interactions associated with the positive charge cluster. Predictive aspects of this hypothesis are discussed.

**M-AM-E4** QUANTUM EFFICIENCY CHANGES: A NEW MANIFESTATION OF CONFORMATIONAL CHANGE IN HEMOGLOBIN. C.A. Sawicki* & Q.H. GIbson* (Intr. by L.J. DeFilippi) Cornell Ithaca, New York 14853.

A combined stopped flow-laser photolysis apparatus, with a mixing dead time of 1 msec, was used to measure the relative quantum efficiency for removal of bound carbon monoxide at a series of time delays after mixing pH7 phosphate buffer solutions of deoxyhemoglobin and carbon monoxide at 20°C. Using the quantum yield of carboxymyoglobin (Bücher, T. and Negelein, E. (1942) Biochem. 7, 311, 163-187) as a standard, the quantum yield for fully liganded COHb is found to be 0.48 ± 0.02 while the quantum yield shortly after mixing when only 10% of the heme sites are liganded is found to be 0.9 ± 0.1. As ligand binding proceeds the observed quantum yield decreases monotonically to the fully liganded value. Similar flow-flash experiments with myoglobin showed no changes in quantum yield following mixing. It is suggested that the observed dependence of the quantum yield on the degree of ligation results from conformational changes linked to ligand binding. (Supported by NIH Grant GM-14276-12).

**M-AM-E5** KINETICS OF OXY-HEMOGLOBIN TETRAMER - DIMER ASSOCIATION BY LIGHT-SCATTERING STOPPED-FLOW. T. M. Zamis*, D. P. Flamig, and L. J. Parkhurst. Dept. of Chemistry, University of Nebraska, Lincoln, NE., 68588

Four concentrations of hemoglobin ranging from 30 to 11 μM in heme, initially at pH 10.8 were dropped to pH's 6, 7, and 8 and the association reaction to form tetramers studied with and without added IHP. The data could not be fit with a simple $2D \rightleftharpoons T$ mechanism, suggesting the need for a conformational change between two types of dimers and two types of tetramers. The latter model gave good fits to the data. The fitting required the use of a Runge-Kutta -Newton-Gauss minimization program with 6 variable parameters for the 4 concentrations at each pH. The final equilibrium constants calculated were: 7.85μM, 7.03μM, and 6.2μM for pH's 6, 7, and 8, respectively, in the absence of IHP. IHP had a small effect on the calculated equilibrium constants but accelerated the overall reaction. Overall half-times for the IHP reactions ranged from 20 msec at pH 6 to 40 msec at pH 8 compared to approximately 60 msec at pH 6 and 80 msec at pH 8 with no IHP present.

Grant Support: NIH HL 15284-06, Research Corporation, Research Council, University of Nebraska

**M-AM-E6** RESONANCE RAMAN STUDIES OF METHEMOGLOBIN DERIVATIVES AT ROOM TEMPERATURE AND 77°K*. K.C. Cho, R.D. Remba*, and D.B. Fitchen. Laboratory of Atomic and Solid State Physics, Cornell University, Ithaca, N.Y. 14853.

**Resonance Raman spectra in the Soret region are reported for the following methemoglobin derivatives: fluoromet, cyanate-met, thiocyanate-met, hydroxymet, and azidomethemoglobin at 285°K and 77°K. For the mixed spin derivatives (at room temperature), the spin state marker bands are observed to shift from the typical high spin position to the typical low spin position upon cooling to liquid nitrogen temperature. The results strongly suggest that contrary to the steric repulsion argument, the iron atom spin state is an essential parameter in governing the iron atom-heme plane geometry.**

*Work supported in part by NIH grant #AM18048-03 and an NIH traineeship (RDR).

**M-AM-E7** MÖSSBAUER SPECTROSCOPY OF HIGH SPIN FERROUS HEME COMPLEXES* T. A. Kent, Physics Dept., The Pennsylvania State University**

The Mössbauer spectra of deoxyhemoglobin, deoxymyoglobin, and two model compounds have been observed at high fields and various temperatures. In each case the temperature dependence, sign, and asymmetry parameter of the quadrupole interaction have been deduced and the internal field has been parameterized. In the case of deoxymyoglobin this information, combined with published single crystal measurements, determined the EFG orientation. We find that above 30K all four materials are characterized by similar EFG and magnetic parameters, with $\Delta E$ negative, $\eta \simeq 0.7$, and the internal magnetic field opposing the applied field for all molecular orientations. The severe restrictions which these observations place on any crystal field model will be described and discussed.

*Submitted by George Lang.
**Supported by NIH Grant (HL-16860-04).

**M-AM-E8** MÖSSBAUER SPECTROSCOPY OF LOW-SPIN FERRIC HEME COMPOUNDS.* D. Rhynard, Physics Department, The Pennsylvania State University**

Mössbauer spectra of several low spin ferric heme protein and model compounds have been recorded at various temperatures and magnetic fields. The results are interpreted using a crystal field model with axial field $\Delta$, rhombic distortion V and orbital reduction factor k as variable parameters. The principal axes of the rhombic field are rotated from the cubic frame, defined by the six ligands of $Fe^{+3}$, by Euler angles $\alpha$, $\beta$, $\gamma$. The set of parameters $\Delta$, V, k, $\alpha$, $\beta$, $\gamma$ determines the g-tensor, the hyperfine tensor A and the quadrupole tensor P, as well as the relative orientations of the tensors' principal axes. The parameters thus obtained for myoglobin azide and the model compound heme-$(Py)_2$ yielded g-tensors that are in good agreement with EPR measurements.

*Submitted by George Lang.
**Supported by grant HL 16860-04 from the National Heart and Lung Institute.

**M-AM-E9** MÖSSBAUER SPECTROSCOPY MEASURES SPIN FLUCTUATION RATES IN ($Fe^{2+}$,S=2) IRON PROTEINS. H. Winkler, University of Hamburg, C. Schulz* and P. G. Debrunner, University of Illinois, Urbana, Illinois 61801

$^{57}$Fe-Mössbauer measurements on several high-spin ferrous proteins yielded spin Hamiltonian and hyperfine parameters that characterize the electronic ground state of the iron in detail.[1,2] Transitions occur between the 5 states of the spin quintet, S=2, due to spin-phonon coupling and in an applied field $\vec{H}$ the spin expectation value $\langle\vec{S}\rangle$ and thus the magnetic hyperfine interaction $\langle\vec{S}\rangle \cdot \vec{A} \cdot \vec{I}$ will fluctuate. In Kramers systems such dynamical effects can be studied via EPR relaxation measurements. We show that under favorable conditions it is possible to determine the spin-lattice interaction of the non-Kramers paramagnetic center from Mössbauer spectra. This effect is analyzed in the Mössbauer spectra of reduced cytochrome P450[1] and reduced rubredoxin[2] and it is shown that in the latter the one-phonon direct process dominates up to 150K. Supported in part by USPH GM 16406 and NSF PCM 76 81025.

[1]P. Champion et al. Biochemistry 14 4151 (1975).
[2]C. Schulz and P. G. Debrunner. J. Physique 37 C6-153 (1976).

**M-AM-E10** INTERPRETATION OF HEMOGLOBIN OPTICAL SPECTRA. W.A. Eaton and L.K. Hanson*, Laboratory of Chemical Physics, N.I.H., Bethesda, Md. 20014; P.J. Stephens*, J.C. Sutherland, and J.B.R. Dunn*, Department of Chemistry, U.S.C., Los Angeles, Calif. 90024

The optical spectra of oxy- and deoxyhemoglobin (oxyHb and deoxyHb) have been investigated between 1800 nm and 300 nm using the techniques of polarized single crystal absorption spectroscopy and solution natural and magnetic circular dichroism. In addition to the porphyrin $\pi \rightarrow \pi^*$ transitions, 7 electronic transitions of oxyHb and 4 transitions of deoxyHb have been characterized. Most appear in the near infrared spectral region. To interpret the spectra iterative extended Hückel molecular orbital calculations were carried out on model chromophores. Assignments are proposed for all of the transitions in terms of one-electron excitations between single configurations. 5 of the 7 bands of oxyHb are interpreted as arising from transitions into the lowest empty molecular orbital, which is delocalized over the $FeO_2$ unit. 3 of the 4 bands of deoxyHb are assigned to porphyrin($\pi$) $\leftrightarrow$ iron(d) charge-transfer transitions. The remaining bands are assigned to d $\rightarrow$ d transitions of the iron.

**M-AM-E11** ANALYSIS OF MODELS FOR EXPLANATION OF $^{14}$N HYPERFINE SPLITTING PATTERNS IN R AND T FORMS OF NITROSYLHEMOGLOBIN. S. K. Mun, J. C. Chang, and T. P. Das, Department of Physics, SUNY, Albany, NY 12222

In an attempt to test the proposed models in the literature for the explanation of the three and nine-line $^{14}$N hyperfine patterns associated with the chains of nitrosylhemoglobin in different environmental conditions, we have investigated the electronic wave-functions and spin densities at the $^{14}$N nuclei in nitrosyl and the imidazole nitrogen($N_\epsilon$)ligand of iron belonging to the proximal histidine for different structural situations, such as bent and straight NO bonds, protonated and deprotonated imidazole and elongated Fe-$N_\epsilon$ bond. Our results indicate that in all the situations studied, the unpaired electron resides on the $d_{z^2}$-like orbital and only nine-line hyperfine patterns are expected, although the ratio of the isotropic $^{14}$N hyperfine constants for the nitrosyl nitrogen and $N_\epsilon$ varies for different situations, about 1.5 for both protonated and deprotonated imidazole cases with straight NO bond, 1.2 for bent NO and 2.3 for extension of 0.5 Å of Fe-$N_\epsilon$ bond. The effects of other possible structural changes such as bending of Fe-$N_\epsilon$ bond from the heme normal will be discussed. Grant support:NIH HL15196.

**M-AM-E12** PROTON RELAXATION STUDIES OF SURFACE HISTIDINE RESIDUES IN NORMAL AND SICKLE CELL HEMOGLOBIN. I. M. Russu and C. Ho, Dept. of Life Sciences, Univ. of Pittsburgh, Pittsburgh, PA. 15260

Proton NMR relaxation techniques have been used to determine both spin-lattice and spin-spin relaxation times ($T_1$ and $T_2$) of histidyl protons in human normal adult and sickle cell hemoglobins (Hb A and Hb S) in the deoxy form. These measurements were obtained from a Bruker HXS-360 NMR spectrometer at 27°C. The hemoglobin concentration was 6.2 mM in 0.1 M Bis-Tris buffer in $D_2O$ at pH 6.9. There are 10 readily resolvable C2 proton resonances of histidyl residues, which are believed to be located on the surface of the Hb molecule. There is a distribution of $T_1$ and $T_2$ values suggesting that each of these surface histidyl residues has an unique environment. Furthermore, four histidyl residues in Hb S have relaxation times different from the corresponding ones in Hb A. Two of them have been assigned to the C2 proton resonances of β2 and β146 histidyl residues. These results strongly suggest that there are specific surface conformational differences between Hb A and Hb S and that proton relaxation times of the histidyl residues are valuable dynamic probes to investigate these differences. (Supported by research grants from NIH and NSF.)

**M-AM-E13** GELATION OF SICKLE CELL HEMOGLOBIN IN MIXTURES WITH NORMAL OR FETAL HEMOGLOBIN. H.R. Sunshine*, J. Hofrichter*, and W.A. Eaton, Intr. by E.A. Padlan, Laboratory of Chemical Physics, NIH, Bethesda, Md. 20014

The kinetics and thermodynamics of the gelation of sickle cell deoxyhemoglobin (Hb S) in hybridized mixtures with normal deoxyhemoglobin (Hb A) or fetal deoxyhemoglobin (Hb F) have been investigated. At a constant, initial total Hb concentration, the delay time for gelation increases approximately exponentially with increasing mole fraction of Hb A or Hb F in the range 0 to 0.5. For a 50-50 mixture of Hb S and Hb A the delay time is increased by a factor of $10^4$ relative to pure Hb S. This factor is between $10^7$ and $10^8$ for a 50-50 mixture of Hb S and Hb F. Interpretation of the equilibrium data on the total Hb concentration in the solution phase (i.e. the supernatant obtained after sedimentation of polymers) requires a model in which non-copolymerizing species act to decrease the $\alpha_2\beta_2^S$ solubility through their excluded volume effect. The large kinetic effects of Hb A and Hb F support our previous hypothesis that the delay time of intracellular gelation relative to the capillary transit time is the primary determinant of clinical severity in sickle cell disease.

THEORETICAL BIOLOGY I

**M-AM-E14** MECHANISM OF SICKLE CELL HEMOGLOBIN GELATION. J. Hofrichter*, J.S. Gethner, and W.A. Eaton, Laboratory of Chemical Physics, N.I.H., Bethesda, Md. 20014

The kinetics of sickle cell deoxyhemoglobin gelation have been studied in order to elucidate both the initial polymerization process and the kinetics of monomer addition to existing polymers. Intensity light scattering experiments with a neodymium laser have been used to examine the progress curve for the nucleation-controlled polymerization reaction. Despite the >100-fold increase in sensitivity over turbidity and birefringence experiments, a characteristic delay followed by almost purely autocatalytic polymerization is observed. Temperature jump birefringence experiments on previously gelled samples have been used to obtain rate parameters for the polymerization and alignment processes in the absence of nucleation. Most of the kinetic results can be rationalized using a mechanism based on equilibrium nucleation of individual polymers, followed by polymer growth until solubility equilibrium is achieved. The mechanism predicts that the extreme sensitivity of the delay time to initial concentration, equilibrium solubility, and temperature is due in large part to the non-ideality of the concentrated protein solutions required for gelation.

**M-AM-E15** LOW-TEMPERATURE KINETIC STUDIES OF MODIFIED MYOGLOBINS. M. Sharrock and T. Yonetani, Physics Dept., Gustavus Adolphus College, St. Peter, MN 56082 and Dept. of Biochem. and Biophys.,Univ. of Penn., Phila.,PA 19104

Low-temperature flash photolysis studies have revealed an unsuspected complexity in the ligand-binding of heme proteins such as myoglobin (1) and cytochrome oxidase(2). In the case of myoglobin, the path of CO from the solvent to the heme iron appears to involve surmounting at least four free-energy barriers. The observation of all four processes requires measurements over large ranges of temperature (10K-320K) and time ($\mu$sec-many sec). Comparative studies of myoglobin containing the natural protoheme prosthetic group and synthetic myoglobins incorporating deuteroheme and mesoheme are presented. We conclude that modifications of the heme group affect mainly the innermost barrier and have little, if any, effect on the outer three barriers. These findings support the view that the innermost barrier is related to properties of the heme group itself, while the other barriers are related to properties of the protein and/or solvent.

(1)Austin, et al.,Biochemistry 14, 5355 (1975)
(2)Sharrock and Yonetani, BBA, in press

**M-AM-F1** A SECTOR RULE FOR ELECTRIC-DIPOLE-ALLOWED TRANSITIONS, O. E. Weigang, University of Maine, Orono 04473.

The earliest models for the origins of optical activity invoked the mechanism of "coupled electric oscillators." Werner Kuhn considered the juxtaposition required of two "coupled" oscillating electric dipoles within the molecule so that circularly dichroic absorption would arise. J. G. Kirkwood and I. Tinoco have pursued a similar line of theory. The easiest measurements to make and, to date, the preponderence of data on rotatory strength have been for transitions strongly magnetic-dipole-allowed. With the most recent improvements in instrumental sensitivities for CD measurements there is a growing body of data for rotatory strengths of strong electric-dipole-allowed transitions. No sector rules have been advanced for these cases, at least none with a firm theoretical basis. Sector rules are probably the only theoretical construct that can be used in a broad survey of cases to establish whether a given intramolecular coupling mechanism is important for the optical activity. Experimental data will be given that illustrates the form of a theoretical sector rule where the orientation of anisotropic matter at a point is important along with the point of location.

**M-AM-F2** CRYSTAL FIELD CALCULATION OF g VALUES AND ZERO-FIELD SPLITTING FOR HIGH SPIN FERRIC COMPLEXES OF RHOMBIC CHARACTER. A.S. Rispin, M. Sato and H. Kon, NIAMDD, NIH, Bethesda, Md., 20014, Intr. by M.R. Bunow

For high spin ferric ions in rhombic symmetry, we have used a crystal field model to relate term splittings of the $^4T_1$, $^2T_2$ and $^4T_2$ excited states to zero-field split energies and g values of the $^6A_1$ term. Five crystal field parameters were used: one cubic parameter, two tetragonal parameters and second and fourth order rhombic parameters. In tetragonal symmetry with only three crystal field parameters, a simpler model including only the $^4T_1$ and $^2T_2$ excited states is adequate to relate term energies to g values and zero-field split energies. No higher lying terms other than $^4T_2$ can influence the $^4T_1$ term directly through the tetragonal or rhombic crystal field. We show that the fourth order rhombic crystal field parameter is a key parameter. We have performed a computer diagonalization of the spin-orbit, electrostatic and crystal field perturbation matrix for seventeen high spin ferric mixed crystalline species of varying rhombicities and for metmyoglobin and cytochrome P-450.

**M-AM-F3** THE PHOTOSYNTHETIC CLOCK IN ACETABULARIA. G. L. Clark,* and A. G. De Rocco, Department of Physics and Astronomy, and The Institute for Physical Science and Technology, University of Maryland, College Park, Md. 20742

The physiological model proposed by Sweeney for the photosynthetic rhythm in Acetabularia minor is given a genetic model and provided with a suitable diffusion-dependent mathematical format. We propose that a small polypeptide passively diffuses outwards from within the organelles alternatively with a threshold-dependent active transport inwards. The active transport is in turn allosterically autoregulated by the transported polypeptide. Under certain conditions the kinetics of the overall process demonstrate a hysteresis loop (metastable states) from which follows a relaxation oscillation of the sort anticipated by Sweeney. The "paradox" arising from the action of actinomycin D on nucleate and anucleate cells, and the observed effects of rifampicin, cycloheximide, puromycin, and chloramphenicol can be incorporated into the model if the moiety undergoing flux is coded for by organelle DNA, translated on cytosol 80S ribosomes, and degraded by two proteases whose m-RNA's, one nuclear the other organelle, exhibit differential stability.

**M-AM-F4** KINETICS OF BACTERIAL SPORE GERMINATION. G.M. Lefebvre,* Introduced by Adel F. Antippa, Trois-Rivières Québec G9A 5H7 Canada.

When a suspension of bacterial spores germinates, the extent of germination, measured as a loss of turbidity, describes a sigmoidal time dependence. The experimental results can be described exactly over the entire time span by a simple two step 5 parameter model. In this model, change in refractivity occurs mostly in the second step, and, in a single spore, is considered to be instantaneous and randomly distributed in time. In the first step, the transition from the initial state to the intermediate state requires a small increase in refractivity. This increase, readily observed at temperatures below optimum, permits an accurate analysis of micro-lag time, and suggests that the differences in efficiency of various germinants may be more apparent than real.

**M-AM-F5** MATHEMATICAL SIMULATIONS OF INTERACTION OF ANTINEOPLASTIC DRUGS INHIBITING DNA SYNTHESIS. A. Belmont,* M. Grattarola,* E. Milgram,* C. Nicolini. Temple University Health Sciences Center, Philadelphia, Pennsylvania 19140

Several models, with increasing degree of complexity, of DNA synthesis based on Michaelis-Menten enzyme kinetics are examined. They are open systems which incorporate complex biochemical feedback controls. Computer studies of these models yield simulations of multiple drug actions and interactions in both the steady state and transient situations. In many cases the results encountered parallel specific drug synergism and antagonism reported in the literature. Such a mathematical approach, which utilizes also real numerical values of feedback constants and maximum velocities, as outlined above, used in conjunction with experimental results may prove successful in designing optimal combination chemotherapy, which could bypass the inherent limitations of empirical trials. (This work was supported by Grant CA20034 from the National Cancer Institute).

**M-AM-F6** TRANSIENT ELECTRON PAIRING IN ENZYME CATALYSIS AND THE CONDITIONS FOR ITS OCCURRENCE. M. Conrad, Dept. of Computer & Comm. Sci., Univ. of Michigan 48109

A coupling interaction between parallel spin electrons arises indirectly from constraints imposed on these electrons by van der Waals' and other weak interactions between the complementary surfaces of enzyme and substrate. This interaction is small, but sufficient to give a high probability for the occurrence of a pairing event on a catalytic time scale, thereby constructing from the antisymmetric wave function of two electrons a short-lived symmetric wave function for an electron pair. During its lifetime the pair is free from the external applicability of the Exclusion Principle, thus drops to a low energy (e.g. hydrogen-like) orbit belonging to many nucleii, then breaks up and re-establishes a Pauli-consistent electronic structure. However, the energy released by falling and delocalization causes a nuclear motion capable of disrupting the weak interactions responsible for holding the complex together. Transient electron pairing thus allows both for high specificity (requiring close fitting, hence sharp attraction between enzyme and substrate) and high reaction speed (requiring rapid break-up, hence instability of the complex).

**M-AM-F7** GENERALIZED HARVESTING IN ITERATIVE,DENSITY DEPFNDENT MODELS. M. Witten, Dept. of Biometry, Med. Univ. of South Carolina, Charleston, S.C. 29403

In this paper, we examine the constuction of a generalized, iterative density dependent harvesting model containing; time and density dependent harvest, a time lag term, and a term incorporating management feedback. The general form of equation studied is given by

$$(1)\quad x_{n+1} = x_n \Phi(x_n) T(\tfrac{1}{n}, x_{n-k}) - H(\tfrac{1}{n}, x_n) M(n)$$

We examine some behaviors of (1) in relation to the shift of the equilibrium. And we discuss the management feedback concept for continuous density dependent models of the form

$$(2)\quad \frac{dx(t)}{dt} = x(t)\Phi(x(t))T(\tfrac{1}{t}, x(t-\tau)) - H(\tfrac{1}{t}, x(t))M(t)$$

This particular form,(2), has some interesting parameter sensitivities when analyzed on the analogue computer.

**M-AM-F8** PHYSIOLOGICAL FUNCTIONS EXPRESSED AS THE DIFFERENCE BETWEEN GROWTH AND AGE-RELATED INVOLUTION TERMS. Richard P. Spencer. Nuclear Medicine, Univ. Connecticut Health Ctr., Farmington, CT. 06032.

A number of physiological functions increase monotonically during early portions of the life span, but then decrease with advanced age. Description of this phenomonon is facilitated by treating it in 2 parts: a growth expression and an age-related involution term. Such an approach has been used to describe various organs. The growth portion is conveniently described as an approach to an asymptote (such as a modified exponential). Age related involution can be set directly proportional to the life span expended. It would be useful to analyze each contributing factor in such terms; for example, in cardiac output: ventricular volume, ejection fraction and heart rate. The approach gives a reasonable description of age associated changes in the cardiac output. By viewing such events in terms of distinct growth and involution terms, there may be a stimulus to their identification. (Supported by USPHS CA 17802, National Cancer Institute).

**M-AM-F9** A RANDOM MODEL OF TUMBLING REGULATION IN BACTERIAL CHEMOTAXIS. A. M. Portis and D. E. Koshland, Jr., University of California, Berkeley, CA 94720

Tumbling behavior is characterized by an integer X, which is taken to denote the state of a response regulator. In the X = 0 state the bacterium tumbles, while for X > 0 tumbling is suppressed. X increases randomly at a mean formation rate $v_f$ stimulated by the occupation of chemoreceptors and decreases randomly at a mean disappearance rate $v_d$. A bacterium is then in the tumbling state for a mean time $1/v_f$. The mean time $t_s$ for smooth swimming is equal to the recurrence time and is given by $1/(v_d - v_f)$. The distribution in tumbling times is exponential. The recovery time $t_R$ following stimulation by attractant is the first passage time. The distribution in recovery times for X initially large is expected to be gaussian with variance $(v_d + v_f)t_s^2 t_R$. Comparison is made with the observed response times of individual tethered bacteria under repetitive stimulation by attractant.[1] The observed behavior is qualitatively in agreement with the model so long as regulator formation is suppressed for X > 0. Then, both smooth-swimming and tumbling times should be exponentially distributed.

[1] J. L. Spudich and D. E. Koshland, Nature 262, 467 (1976)

**M-AM-F10** THEORETICAL TREATMENT OF CRYSTALLIZATION IN MACROIONIC SOLUTIONS. R. Hastings, North Dakota State University.

The formation of a crystalline structure in aqueous solutions of heavily ionized polystyrene spheres and in solutions of spherical viruses will be discussed within the framework of the Kirkwood-Poirier theory of electrolytic solutions. Approximate solutions to a set of coupled integral equations for the various interion effective potentials will be given. The theory exhibits a mean field transition to a crystalline phase as the critical ionic strength is approached. The predicted crystal lattice spacing is found to be on the order of several macroion radii, in qualitative agreement with experimental observations. Techniques currently being applied to obtain numerical solutions to the integral equations will be discussed. Non-linear corrections to the theory will also be discussed.

**M-AM-F11** THEORETICAL STUDIES OF DNA CONFORMATION IN CHROMATIN STRUCTURE AND INTERCALATION COMPLEXES. G. Pack, G. Loew. Stanford Univ., Stanford, CA 94305

A number of changes in DNA conformation have been proposed to account for chromatin structure. The energetics of two of these have been calculated and shown to be dependent on crucial base-backbone interactions which are modulated by the degree of neutralization of the phosphate groups. Histones which cause such neutralization thus allow a stabilization of the kinked forms of DNA relative to DNA-B. Conformation changes which occur in helical segments when small molecules intercalate have been determined by X-ray analysis and appear to involve changes in base-backbone interactions similar to those proposed for the kinked structure of DNA. The energetics of such changes have also been calculated and can account for the pyrimidine-3'-5'-purine sequence isomer specificity observed in the binding of ethidium bromide, a known DNA intercalator. The calculations further indicate that it is base-backbone interactions rather than ethidium interactions with the bases that account for the major part of the observed specificity. The combined results of these studies indicate that perturbations of base-backbone interactions underlie changes in DNA structure induced by both endogenous and exogenous molecules.

**M-AM-F12** REGULATION OF TISSUE GROWTH: A MATHEMATICAL MODEL. J.D. Dasgupta* and D.P. Dubey. Panjab University India, and Sidney Farber Cancer Institute, Boston, Mass.

A mathematical model of cellular growth control by negative feedback mechanism has been proposed. It assumes that all cells in a tissue synthesize the mitotic inhibitor 'chalone.' For division to occur, the intracellular concentration should be less than a critical value ($n_c$), above which the cells would stop dividing. The values of $n_c$ are distributed over the cell population in Gaussian manner. The rate equations governing the inter- and intracellular chalone concentration have been solved for different conditions. The effect of chalone production, decay rate and the cell membrane permeabilities to its transport, on the mode of rise of its concentration in the intra- and intercellular spaces have been investigated. Computer simulation technique was employed to study the effects of sudden fall in intra and intercellular chalone concentration on the cell proliferation and death rate in a tissue. The proposed model has been applied to predict the distribution of cell cycle time and the process of malignant growth.

## MICROTUBULES AND FILAMENTS

**M-AM-G1** THE VINBLASTINE-INDUCED SELF-ASSOCIATION OF TUBULIN. C. Na, and S. N. Timasheff, Dept. Biochemistry Brandeis University, Waltham, MA 02154

The self-association of calf brain tubulin induced by the antimitotic drug vinblastine was investigated in PG buffer (0.1M NaPi, $10^{-4}$GTP, pH 7.0) using velocity sedimentation. Schlieren profiles suggested that tubulin undergoes an isodesmic association. Weight average sedimentation coefficients ($\bar{s}$) were determined at vinblastine concentrations between $2.5 \times 10^{-5}$M and $2 \times 10^{-4}$M and at tubulin concentrations up to 10 mg/ml where unimodal sedimentation patterns prevail. These experimentally obtained $\bar{s}$ can be fitted well to the $\bar{s}$ calculated for an isodesmic association model. Association constants, obtained at different vinblastine concentrations, indicate that the binding of one vinblastine molecule per tubulin dimer with a ligand-protein association constant of $2.5 \times 10^4 M^{-1}$ was involved in the tubulin association, which itself has an intrinsic association constant of $9.8 \times 10^4$ $M^{-1}$ at 20°C. Experiments as a function of temperature resulted in an enthalpy change of 13.0 kcal/mole and an entropy change of 67 e.u. at 20°C, indicating that the self-association is entropy-driven. (Supported by NIH Grants GM-14603, CA-16707, and CA-05538).

M-AM-G2 REVERSIBLE DISSOCIATION OF THE $\alpha\beta$-DIMER OF BOVINE BRAIN TUBULIN. H.W. Detrich,III* and R.C. Williams, Jr., Dept. of Biology, Yale University, New Haven, CT 06520, and Dept. of Molecular Biology, Vanderbilt University, Nashville, TN 37235.

Equilibrium ultracentrifugation was used to demonstrate that the $\alpha\beta$-dimer of bovine brain tubulin (purified by phosphocellulose chromatography after two cycles of an assembly-disassembly procedure) dissociates reversibly, with a dissociation constant $\leq 8 \times 10^{-7}$ M (at 4.7° in 0.1 M PIPES buffer, 2 mM EGTA, 1 mM $MgSO_4$, 0.1 mM GTP, 2 mM DTE, pH 6.9). This result was confirmed by observation of an appropriate dependence of the sedimentation coefficient of tubulin on its concentration. Small zone gel filtration experiments on Bio-Gel P-150 also demonstrated an increase in peak elution volume with decreasing column load concentration. Reversibility of the dissociation was demonstrated directly by measurement of sedimentation velocity and peak elution position of tubulin reconcentrated from dilute solution by pressure ultrafiltration. This tubulin retained both its ability to form microtubules and more than 70% of its colchicine-binding capacity under the conditions of the experiments. (Supported by Grants HL12901 and HD00032 of the NIH)

M-AM-G3 INCORPORATION OF FLUORESCENTLY LABELED ACTIN INTO LIVING CELLS. Yu-Li Wang* and D. Lansing Taylor, Biol. Labs. Harvard University, Cambridge, MA 02138

Actin labeled with 5-iodoacetamidofluorescein has been incorporated into the functional pool of actin in C. carolinensis and P. polycephalum by direct microinjection. The functional activity of the labeled actin has been analyzed at three levels of organization as: (a) the purified actin, (b) in motile extracts of cells, and (c) in living motile cells. The labeled actin exhibited normal polymerization and activated myosin ATPase to a similar extent as unlabeled controls. Labeled actin and endogenous actin was incorporated into contracted pellets to approximately the some extent in motile cell extracts. After microinjecting labeled actin into single C. carolinensis the fluorescent actin spread into both the endoplasm and ectoplasm without forming distinct fibrils. In contrast, fluorescent bundles developed in the ectoplasm of P. polycephalum following microinjection of labeled actin. This new experimental method in conjunction with fluorescence spectroscopic techniques could become a powerful tool for studying the intracellular distribution, and structural changes of cellular components in living cells.

M-AM-G4 QUANTITATIVE ANALYSIS OF THE INTERACTION OF MICROTUBULES WITH ACTIN AND WITH EACH OTHER. L. Griffith* and T. Pollard, Harvard Med. Sch., Boston, MA.

We have studied the interaction of purified brain microtubules with purified skeletal muscle actin using two quantitative methods. 1) At low shear, the viscosities of actin and microtubules combined for 20 min at 37° can be as much as ten to twenty times greater than the sum of the viscosities of the individual proteins. These mixtures are thixotropic, and their viscosities increase as a function of protein concentration and the duration of incubation at 37°. 2) Microtubules sediment with actin conjugated to agarose beads. We have also studied the interaction of microtubules with each other using viscometry. The viscosity of purified microtubules after 20 min at 37° is not a linear function of protein concentration; above 11 mg/ml it ascends sharply to greater than 1,000 cp. These solutions are thixotropic. In contrast, at up to 20 mg/ml microtubules treated with trypsin to cleave microtubule associated proteins or microtubules assembled from pure tubulin in DMSO have viscosities below 100 cp after 20 min at 37°. This suggests that the interaction of microtubules with each other is facilitated by microtubule associated proteins. (NIH GM23531.)

M-AM-G5 VISUALIZATION OF ACTIN FILAMENT POLARITY IN THIN SECTIONS. D.A. Begg* and L.I. Rebhun, Department of Biology, Univ. of Virginia, Charlottesville, VA 22901.

The binding of heavy meromyosin (HMM) or myosin subfragment 1 ($S_1$) is used to identify cytoplasmic actin microfilaments and to determine their polarity with respect to anchoring sites. This method has been used successfully to study highly ordered arrays of microfilaments; however, the microfilaments in most cells are loosely organized and are frequently labile. Although these filaments "decorate" with HMM or $S_1$, their polarity is difficult to determine. We have studied the association of 60-80 A° filaments with cortices isolated from fertilized sea urchin eggs. Fixation of $S_1$-decorated filaments in a medium containing .1M phosphate buffer, 1% gluteraldehyde and 0.2% tannic acid dramatically enhances their arrowhead configuration. Filaments which attach to the membrane display a clear, uniform polarity with the arrowheads pointing away from the membrane. The improved ability to detect actin filament polaity afforded by this technique should be applicable to the study of the relationship between actin filament polarity and cell motility in a wide variety of cell types.

M-AM-G6 10 nm FILAMENTS: SMOOTH MUSCLE AND SQUID AXOPLASM. Priscilla F. Roslansky* and Robert V. Rice. Carnegie Mellon University, Pittsburgh, Pa. 15213; Marine Biological Laboratory, Woods Hole, Mass. 02543.

10 nm filaments from the smooth muscle of chicken gizzard have been compared with 10 nm neurofilaments from extruded axoplasm of the giant axon of Loligo pealei. Morphologically, these filaments appear similar when viewed with transmission electron microscopy using 2% uranyl acetate as a negative stain. The 55,000D protein associated with the intermediate filament of smooth muscle and the 63,000D and 200,000D proteins associated with neurofilaments have been isolated. Peptide maps of these proteins using thin layer chromatography and high voltage electrophoresis have been prepared. These studies indicate that these filaments are biochemically different. (Supported by NIH grant AM 02809-18).

M-AM-G7 ACTIN AND MYOSIN FROM THE HIGHER PLANT LYCOPERSICON ESCULENTUM. M. Vahey*, R. Trautwein*, S. P. Scordilis, Dept. of Biological Sciences, The University at Albany, Albany, N.Y. 12222 and The Section on Molecular Cardiology, NHLBI-NIH, Bethesda, MD. 20014.

Extracts of parenchyma cells from the fruit of tomato were examined for the presence of myosin and actin-like molecules. High ionic strength extracts exhibit a myosin like enzyme whose ATPase activity in 0.5 M KCl is maximal in the presence of $K^+$-EDTA, 1/4 maximal in the presence of $Ca^{++}$, and is least active with $Mg^{++}$. The protein elutes immediately after the void volume on gel filtration through Cl-Sepharose 4B and it forms a complex with rabbit skeletal muscle F-actin which is dissociated by MgATP. In 20 mM KCl the activity of the Mg activated ATPase is increased ten fold by rabbit F-actin. Low ionic strength extracts exhibit a band which co-migrates with rabbit actin on SDS PAGE indicating a molecular weight of 45,000 daltons. Such preparations polymerize in the presence of 0.1 mM $CaCl_2$, 0.5 mM ATP when warmed to 27°C and made 2.0 mM with respect to $MgCl_2$. Crude extracts show 6 nm thin filaments which become decorated with rabbit myosin subfragment-1 to form arrowheads of uniform polarity and with a periodicity of 32 to 37 nm. This complex is dissociated by MgATP.

**M-AM-G8** WATER-CYTOSKELETON INTERACTIONS IN HUMAN CANCER CELLS. P.T. Beall, B.R. Brinkley‡ B.B. Asch‡ and C.F. Hazlewood. Baylor College of Medicine, Houston, TX 77030.

In a study of 11 established human breast cancer cell lines, a correlation has been found between (a) doubling time; (b) the mobility of cellular water molecules; and, (c) the substance and structure of the cytoskeleton. Nuclear magnetic resonance spin-lattice relaxation times, $T_1$, for cellular water protons were determined by a 180°-τ-90° pulse sequence at 30 MHz and 25°C. $T_1$ values lower than 3000 ms are indicative of restricted freedom of mobility for water protons. Cytoplasmic microtubules of the cytoskeleton were visualized by the indirect immunofluorescent antibody technique. Doubling times of 24 hr-28 days correlated with $T_1$ values from 930 ms - 260 ms. Fast dividing (1-3 days) cells had a diffuse transformed cytoplasmic microtubule pattern, intermediately (3 days-1 wk) dividing cells had a combination of assembled microtubules and diffuse fluorescence, and slowly dividing cells had a full microtubule complex. These data suggest that a portion of the differences in mobility of water molecules among a group of similar cancer cells is associated with elements of the cytoskeleton. (Supported by ONR N0014-76, Welch Q-390, NIH grants CA-21624, CA-23022, CA-11944, RR-00188, and GM-20154.

**M-AM-G9** A PARTIALLY PURIFIED MODEL SYSTEM OF GELATION AND CONTRACTION FROM D. DISCOIDEUM. S.B. Hellewell* and D.L. Taylor. The Biol. Labs. Harvard Univ., Cambridge, Ma.

The proteins involved in gelation and contraction have been partially purified from the contracted pellets of a previously reported cell free extract (Condeelis & Taylor 1977). The contracted pellets were solubilized with 0.6 M KI and subsequently desalted into a low ionic strength actin depolymerization buffer. The initial cell extract contained ca.28 separate proteins while the contracted pellet consisted of eight major polypeptides which represented 60-70% of the total protein (actin, myosin, 250 k, 95k, 75k, 55k, 28k, 20k daltons). Removal of myosin prevented the extract from contracting, while the remaining proteins formed a gel in 2.5 mM Pipes buffer, 2.5 mM EGTA, 1 mM Mg-ATP, 20 mM KCl, pH 7.0. Gelation was inhibited by $>10^{-6}$ M free ($Ca^{++}$). The reincorporation of purified Dictyostelium myosin reconstituted pH and $Ca^{++}$-regulated contractions. Gelation has been quantitated by assaying strain birefringence and light scattering.

**M-AM-G10** GELATION OF ACANTHAMOEBA EXTRACTS. S. MacLean,* H. Kaufman,* and T.D. Pollard (Intr. by M. Kushmerick), Harvard Medical School, Boston, MA 02115.

We have studied the gelation of Acanthamoeba extracts quantitatively using a low shear rolling ball microviscometer. The extract is a 140,000 g supernate containing the cell's soluble components in a sucrose-ATP-EGTA buffer. When the cold extract is warmed to 25° its viscosity increases, after a brief lag, from about 1.5 cp to greater than 1400 cp in 30 s or less. Gelation of extract desalted on Sephadex G-25 requires the addition of both $Mg^{++}$ (≥1 mM) and ATP (≥0.2 mM). ITP, but not ADP, ADP-N-P or ADP-C-P, will substitute for ATP. AMP causes a small increase in viscosity but no gelation. Neither $Mn^{++}$, $Ca^{++}$, $Ba^{++}$, $Na^{+}$ nor $K^{+}$ will substitute for $Mg^{++}$. Incubation at 0° with both $Mg^{++}$ and ATP increases the rate of the subsequent viscosity increase at 25°. The extent of this potentiation increases over about 15 min at 0°. In the presence of 2 mM $Mg^{++}$ and 1 mM ATP the optimal free $Ca^{++}$ concentration for gelation is about $10^{-8}$M. At lower $Ca^{++}$ concentrations the rate of the viscosity increase is less, while at $Ca^{++}$ concentrations greater than $10^{-7}$M the viscosity change is completely inhibited. (NIH Grant GM-19654)

**M-AM-G11** COMPARISON OF α-ACTININ WITH A 100,000 DALTON PROTEIN IN THE BRUSH BORDER. M. Mooseker*and R. Stephens, Dept. of Anat., Harvard Med. Sch., Boston, MA. & M.B.L., Woods Hole, MA. (Intr. by R. Linck).

The brush border of intestinal epithelial cells contains a protein with the same molecular weight as α-actinin (100,000 daltons). An enriched fraction of the 100,000 dalton protein was obtained by gel filtration of a high salt extract of brush borders from chicken. This protein was further purified by preparative SDS gel electrophoresis. We compared the tryptic peptides of the brush border protein with those of chicken gizzard α-actinin. The maps were made on silica gel thin layer plates chromatographed in methanol-ammonia and electrophoresed at either pH 3.5 or 6.5. The peptides were visualized with fluorescamine. Maps with 0.3-0.5 nmoles of either the brush border or smooth muscle protein each had 55-60 spots. When the peptides were co-run on the same plate, 45% of the spots were co-incident indicating limited homology between these proteins. These results add credence to the suggestion from antibody localization studies that an α-actinin like protein is present in nonmuscle cells. Supported by M.D.A. Fellowship (M.M.), N.I.H. GM-15500 (R.S.) and N.I.H. GM-19654 to T.D. Pollard.

**M-AM-G12** MICROTUBULE-MEMBRANE INTERACTIONS IN CILIARY MOTILITY. W. L. Dentler,* R. E. Stephens, and M. M. Pratt,* Dept. Physiol. and Cell Biology, U. of Kansas, Lawrence, KS 66044, and Marine Biological Laboratory, Woods Hole, MA 02543.

Structures bridging outer doublet microtubules and the membrane occur in cilia at 16 nm intervals along the length of the axoneme. Cytochemistry has demonstrated ATPase at this location. A high molecular weight protein, solubilized with the membrane fraction, has certain properties in common with dynein. The lipophilic, photoactivatable reagent 4,4'-dithiobisphenylazide cross-links this protein with membrane tubulin and two other membrane proteins of ∿45,000 and ∿65,000 daltons. Upon cross-linking, the microtubule-membrane bridge and the associated region of the membrane become more resistant to detergent solubilization. Cross-linking discoordinates, then prevents ciliary motion in gill tissue, implying that free translation of microtubule-membrane linkages within the fluid bilayer is involved in normal ciliary movement. It may be relevant that demembranated cilia, when reactivated, beat in a spiral rather than in the typical monophasic, planar fashion. Supported by USPHS Grants AM 24,179 and GM 20,644

**M-AM-G13** BULL SPERM MOTILITY AND CALCIUM BINDING. L. Nelson and M. Young*, Department of Physiology, Medical College of Ohio, Toledo, Ohio 43699

The divalent cation fluorescent probe, chlortetracycline, emits a signal when calcium ions are added to washed bull sperm cell suspensions that is saturable when the concentration exceeds 10 mM. Ultrasonic disruption of the cells for 30 seconds increases the output by about 25-30%. Lanthanum reduces the signal by about 2/3, but this decrease may be partially reversed by supplementation of the medium with more calcium. Acetylcholine and physostigmine each enhance the fluorescent signal by about 10%, while decamethonium, the cholinergic receptor depolarizer decreases the signal by nearly 12%. On the other hand, nicotine, a cholinomimetic substance, causes a 25% drop at millimolar concentration. The local anesthetic procaine has a relatively minor effect, while dibucaine at the same concentration brings about a 40% decrease. Other cholinergic agents are in the process of being tested to elucidate a proposed interaction between calcium transport and acetylcholine in sperm motility control.

**M-AM-G14** SWIMMING SPEED DISTRIBUTIONS OF BULL SPERMATOZOA AS DETERMINED BY QUASI-ELASTIC LIGHT SCATTERING. F. R. Hallett, T. Craig,* and J. Marsh,* Department of Physics, University of Guelph, Guelph, Ontario, Canada N1G 2W1.

Eighty-eight semen samples from thirty-nine bulls have been investigated by the quasi-elastic light scattering technique. Normal, defective and dead cells each yielded characteristic autocorrelation functions. The form of these functions indicates that the swimming speed distribution of normal cells is a gamma distribution with two degrees of freedom while that for defective or circular swimmers is a gamma distribution with one degree of freedom. The resulting analysis of the experimental autocorrelation functions yields the fraction of the sample which is normal, the fraction which is defective and the average speed of each group. The average helical swimming speed of normal cells was found to be 384 $\mu ms^{-1}$ while the average trajectory speed of the circular swimmers was found to be 103 $\mu ms^{-1}$. The overall quality of each of the semen samples as determined by light scattering is compared to quality determination on the same samples by technicians from the artificial insemination industry. We would like to acknowledge the support of the National Research Council of Canada.

## LIPID BILAYERS I

**M-AM-H1** MORPHOLOGY OF THE HEMOCYANIN CHANNEL IN LIPID BILAYERS. T.J. McIntosh, G.A. Zampighi, J.D. Robertson, and H.P. Ting-Beall, Dept. of Anatomy, Duke University School of Medicine, Durham, North Carolina 27710.

Keyhole limpet hemocyanin (KLH) has been shown to form conductance channels in black lipid membranes (Latorre, et al.). We have performed experiments in an attempt to visualize how the large (300Å by 500Å) KLH molecule associates with lipid films to form channels. KLH was injected under monolayers of various lipids. Bilayers were formed by the Langmuir-Blodgett dipping technique and studied with the electron microscope both in face view by negative staining and in cross sectional view in thin sections. The large KLH molecules were not seen. However, many small donuts, approximately 70Å in diameter with a 20Å stain-filled central region, were associated with the lipid bilayers. Similar results were obtained when phospholipid vesicles were incubated with KLH. Preliminary data indicate that the number of donuts seen in the microscope is related to the number of conductance channels formed in black lipid membranes. We believe that KLH, in the presence of polar lipids, dissociates into 70Å donuts which form a complex with the lipid.

**M-AM-H2** INFLUENCE OF DOUBLE-LAYER and DIPOLAR SURFACE POTENTIALS ON IONIC CONDUCTANCE OF GRAMICIDIN CHANNELS. G. Szabo and D. McBride† Dept. Physiol. & Biophysics, UTMB, Galveston, TX 77550

The conductance (g) of single gramicidin A channels in lipid bilayer membranes increases with salt concentration (NaCl or KCl, 0.01M to 1M) when membranes are formed from the neutral lipid monoolein. In contrast, g's are nearly independent of salt concentration when membranes are formed from negatively charged lipids such as phosphatidyl inositol. This result indicates that the double layer potential induced at the membrane surface by the presence of negative surface charge is affecting the cations that enter the channel. Comparison of independently determined double layer surface potentials and gramicidin single-channel conductances indicates that a large fraction of the surface potential is acting on cations entering the channel. Similar comparisons of lipids having no net charge (phosphatidyl choline, monoolein, cholesterol) indicate that only a small fraction of the potential that originate from dipolar surface groups may act on cations entering the channel.

Supported by USPHS grant HL 19639

**M-AM-H3** BLOCKING OF GRAMICIDIN CHANNEL CONDUCTANCE BY $Ag^+$ D. McBride* and G. Szabo(intr. by D. Baker) Dept. Physiol. & Biophysics, UTMB, Galveston, Texas 77550.

The ion conductive channels formed by gramicidin A in lipid(monoolein) bilayer membranes are found to be highly permeable by the monovalent $Ag^+$ cation. For example, single channel conductances in pure solutions of $Ag^+$ (g = 16 pS for 0.1M $AgNO_3$) are larger than those measured in pure solutions of $Na^+$ (g = 5.5 pS for 0.1M $NaNO_3$). Despite its considerable permeability, $Ag^+$ is found to block the movement of alkali metal cations through gramicidin channels. The presence of 10mM $Ag^+$, for example, is found to reduce g's from 25 pS to 17 pS in 1M $NaNO_3$ and from 46 to 39 pS in 1M $KNO_3$. The blocking of gramicidin single-channel conductance by $Ag^+$ is qualitatively similar but quantitatively stronger than that observed for $Tl^+$ by others. The molecular mechanisms of blocking will be discussed in light of the large polarizabilities of both $Ag^+$ and $Tl^+$. A theoretical framework, with a minimal number of adjustable parameters, will be considered in order to describe the detailed blocking properties of $Ag^+$. Supported by NIH HL-19639

**M-AM-H4** $^{13}C$ AND $^{23}Na$ NMR STUDIES OF GRAMICIDIN - CATION SYSTEMS, Arthur Kowalsky, Biophysics Dept., Albert Einstein College of Medicine, Bronx, New York 10461.

The interaction of gramicidin (GR) with NaSCN is being studied with $^{23}Na$ and $^{13}C$ NMR. The association constant in ethanol, determined from the broadening of the Na resonance is 17 ± 1 $M^{-1}sec^{-1}$. The data are best fit by assuming a 1:1 complex. In $[CH_3]_2SO$ solution (GR is ca 85% monomer) there is no broadening of the Na resonance by GR indicating essentially no complex. The $^{13}C$ spectrum of GR in $CH_3OH$ (ca 80% dimer) changes with Na content and, as Na content increased, approaches but never becomes identical with the monomer spectrum in $[CH_3]_2SO$. In dioxane (ca 98% dimer) Na causes a broadening of the N-formyl carbon resonance and a shift downfield. A $^{13}C$ resonance tentatively assigned to GLY carbonyl changes markedly. Other carbonyl resonances broaden. This indicates Na causes either a conformation change or a dissociation and a disturbance of the GR structure as the Na travels the channel (suggested previously by others). Complexes in dioxane were formed first in ethanol, the solution was lyophilized and the solid dissolved in dioxane. Since comparable concentrations of NaSCN are insoluble in dioxane without GR, $K_{assoc}$ in this solvent is very large. Only 1 Na appears to be complexed per dimer in dioxane.

**M-AM-H5** SYNTHETIC REPLACEMENT OF THE N-TERMINAL AMINO ACID OF GRAMICIDIN A: EFFECT ON TRANSMEMBRANE CHANNEL CONDUCTANCE. J.S. Morrow, Department of Pathology, Yale Medical School, New Haven, Conn. 06510, W.R. Veatch, Department of Pharmacology, Harvard Medical School, Boston, Mass. 02115 and L. Stryer, Department of Structural Biology, Stanford Medical School, Stanford, Calif. 94305.

Gramicidin A is a linear polypeptide antibiotic which forms dimeric transmembrane channels selective for small monovalent cations. After cleavage of the N-formyl blocking group, a modified Edmund degradation was used to remove L-Valine$_1$. A formylated amino acid was then recoupled with DCCI. (1) An alternating LD sequence is essential: When equal concentrations of the D-Val$_1$ analog and of L-Val$_1$ are added to the membrane forming solutions, the total conductance of the lipid bilayer membrane containing D-Val$_1$ is less than 0.01 of the membrane containing L-Val$_1$. (2) A hydrophobic side-chain is required: The L-Cys$_1$ analog is inactive (<.001), but conversion to S-methyl-L-Cys$_1$ restores activity (0.2). (3) The single-channel conductance depends on the nature of the side-chain, probably due to its dipole moment: The relative single-channel conductance of L-Val$_1$, S-methyl-L-Cys$_1$, and p-iodo-Phenylalanine$_1$ is 1.0 : 1.0 : 0.65.

**M-AM-H6** SINGLE-FILING MULTI-BARRIER MODELS FOR GRAMICIDIN CHANNELS. J. Hägglund, J. Sandblom*, B. Enos and G. Eisenman, Physiol. Depts., UCLA, Ca. and Uppsala U., Sweden.

Schagina, Grinfeldt and Lev's demonstration of single-filing with 2-ion occupancy from .001 to 0.1 M RbCl in gramicidin channels motivated us to examine models for the channel containing 2 inner sites not in equilibrium with the solution. We have explored Heckmann-Chizmadjev-Eyring type single-filing models with 2 or 3 barriers and 2 or 4 sites to reconcile the concentration dependence of flux ratio, conductance, I-V characteristic and permeability for Li, Na, K, Rb, Cs and Tl. A 3 barrier 2 site model fails to produce the conductance and flux ratio data simultaneously for RbCl at low concentrations; and we find it necessary to introduce an additional site at each end of the channel in equilibrium with the solution and interacting with the inner sites. We conclude that the general model is of the 3-barrier 4-site class, of which previous models like Sandblom, Eisenman and Neher's 1-barrier 4-site model and Hladky's 3-barrier 2-site model are special cases, representing high and low concentration limits, respectively.

Supp. by NSF (PCM7620605) and USPHS (NS09931, FO5 TW-2468)

**M-AM-H8** ALCOHOL ANESTHETICS FLUIDISE LIPID MEMBRANES WITHOUT NECESSARILY LOWERING PHASE TRANSITION TEMPERATURE. M.J. Pringle, * L. Chang * and K.W. Miller, Depts. of Anesthesia and Pharmacology, Harvard Medical School, Massachusetts General Hospital, Boston, Mass. 02114.

Lipid theories of anesthesia suggest that anesthetics act by (a), increasing membrane fluidity or (b), lowering the lipid gel-liquid crystalline transition temperature. To evaluate these theories on model systems, the alcohols $C_{14:0}$, $C_{16:0}$, cis- and trans- $C_{14:1}$ and $C_{16:1}$, were studied. Anesthesia was measured using tadpoles immersed in alcohol solutions. Membrane fluidity was measured with spin-labelled 7,6-phosphatidyl choline in egg lecithin/cholesterol (1:1), whilst dipalmitoyl lecithin phase transitions were monitored using the membrane/buffer partitioning of the spin label TEMPO. Of the alcohols, $C_{14:0}$ and $C_{16:0}$ were non-anesthetic, while $C_{16:1}$ and $C_{14:1}$ were partial and full anesthetics respectively. All the compounds fluidised PC/cholesterol liposomes but with magnitudes which reflected their relative anesthetic potency. However, only the cis-unsaturated alcohols lowered, whilst the trans-unsaturated and saturated alcohols raised the DPL phase transitions even though cis and trans isomers were of comparable potency.

**M-AM-H9** INACTIVATION OF ALAMETHICIN-INDUCED CONDUCTANCE BY QUATERNARY AMMONIUM IONS AND LOCAL ANESTHETICS. J. Donovan, Department of Biophysics, University of Chicago, and R. Latorre, Department of Physiology, Harvard Medical School, Boston, Ma. 02115.

Quaternary ammonium ions (QA) having a long alkyl chain and the local anesthetics (LA) lidocaine and tetracaine cause inactivation of the alamethicin-induced conductance in lipid bilayer membranes. The alamethicin-induced conductance undergoes inactivation only when QA or LA are added to the side containing alamethicin. The concentration of QA required to produce a given amount of inactivation depends on the length of the alkyl chain present in the QA and follows the sequence $C_9 > C_{10} > C_{12} > C_{16}$. The observed time course of the inactivation is well predicted by a model similar to that of Heyer et al. (J.G.P. 67:703(1976)). In this model QA or LA pass through the alamethicin channel, bind reversibly to the other membrane surface changing the transmembrane potential and turn the conductance off. The extent of inactivation depends on the binding characteristics of the QA or LA to the membrane surface. The measured binding constants were found to be: 10000 for $C_{16}$; 80 for $C_{12}$; 4.5 for $C_{10}$ and 1.5 charge $nm^{-2}M^{-1}$ for $C_9$ and tetracaine.

Supported by NIH-GM grant # 25277

**M-AM-I** ION ENTRY INTO GRAMICIDIN A CHANNELS. O.S. Andersen and J. Procopio*. Dept. Physiology and Biophysics, Cornell Univ. Med. Coll., New York, N.Y. 10021.

Current-voltage characteristics of Gramicidin A (Gram A) single channels in phospholipid bilayers have been studied at low aqueous concentrations of $Na^+$, $K^+$, $Rb^+$, $Cs^+$, $NH_4^+$, $Tl^+$, and $Ag^+$. At high potentials (0.3 - 0.5 V)the current reaches a limiting value, independent of the applied potential. The magnitude of the limiting current (1-5 pA in 0.1 M salt)is consistent with the notion that ion entry into Gram A channels is limited by (electro)diffusion in the aqueous phases. It is, in general, not correct to assume that ions moving through the channel are in distribution equilibrium with the aqueous phases. The current-voltage characteristics observed with the alkali metal ions and $NH_4^+$ are similar, and the limiting currents appear to be scaled by the aqueous diffusion coefficients of the ions. The current-voltage characteristics for $Ag^+$ and $Tl^+$ show quite different behavior. They are sigmoidal, and the limiting currents are "much" larger than predicted from the alkali metal ion behavior. It is possible that this is due to a structural change in the Gram A channel induced by these ions.

**M-AM-H10** ANION SELECTIVE PERMEATION OF LIPID BILAYERS MEDIATED BY A NEUTRAL CARRIER WITH ONLY OXYGEN LIGANDS. R. Margalit and G. Eisenman, Physiol. Dept., UCLA Medical School, Los Angeles, Ca. 90024.

We find the neutral, non-cyclic $Li^+$ selective ionophore of Ammann et al. (Anal. Lett. 8, 857, 1975) to produce anion selective permeation of GMO or PE bilayers by a carrier mechanism in the equilibrium domain, with anion ($A^-$) carrier (S) complexes of the type $AS^-$, $AS_2^-$, $A_2S_2^{2-}$ deduced from studies of the dependence of membrane conductance and dilution potentials on ligand and anion concentration. The membrane potential in mixtures of cations and anions obeys the Goldman-Hodgkin-Katz equation with concentration- and voltage-independent permeability ratios. The membrane conductances for single ions are hyperbolic functions of voltage and agree with the permeability ratios. The permeability ratios for 2:1 carrier:ion complexes relative to $Li^+$ are $ClO_4^-(2.3) > Li^+(1) \approx SCN^-(1) > I^-(.20) > NO_3^-(.046) \approx Br^-(.046) > Cl^-(.018) > F^-(.009) > Ac^-(.002)$ for anions and are $Li^+(1) > Na^+(.12) > K^+(.046) > Rb^+(.032) > Cs^+(.018)$ for cations. Since the carrier molecule does not contain an intrinsic anion-binding group, an interposed water molecule is proposed as the anion binding site.

Supp. by NSF PCM 7620605 and USPHS NS09931.

**M-AM-H11** RECONSTITUTION OF $Ca^{2+}$ - $Mg^{2+}$-ATPase IN GIANT VESICLES. T. J. Murphy and A. E. Shamoo, U. of Rochester, School of Med. & Dent., Rochester, N.Y. 14642.

Giant vesicles with diameters in the 60-300 micron range were formed by the method of Paul Mueller (personal communication; based on the earlier work of Reeves and Dowben, J. Cell Physiol. 73: 49, 1968). These vesicles are unilammelar, contain no organic solvent, are stable for of the order of weeks, and can readily be impaled with glass micro-electrodes--thus making them potentially ideal for reconstitution studies. Vesicle membrane electrical properties have been characterized in single micro-electrode voltage and current clamp studies and preliminary studies have been carried out on giant vesicles doped with $Ca^{2+}$ + $Mg^{2+}$-ATPase from rabbit skeletal muscle sarcoplasmic reticulum. The relationship between the properties of ATPase doped Bangham vesicles and black lipid membranes and those of ATPase doped giant vesicles will be discussed.

Supported by U.S. DOE contract and assigned Report #UR-3490-1287 and also supported in part by NIH.

**M-AM-H12** DISCRETE-ION EFFECT IN LIPID BILAYERS. C.-C. Wang* and L. J. Bruner. Department of Physics, University of California, Riverside, CA 92521.

The magnitude of membrane surface charge density, $|\sigma_s|$, due to adsorbed dipicrylamine anions ($DpA^-$) has been measured as a function of aqueous phase $DpA^-$ concentration using a high field voltage step technique. Accompanying low field measurements have determined the transient current relaxation time, $\tau_o$, governed by the height of the central energy barrier which $DpA^-$ ions must surmount in moving from one interfacial potential minimum to the other. A highly simplified model of the discrete-ion effect predicts that the central barrier height will be modulated by adsorbed charge, yielding the relation,

$$\tau_o(|\sigma_s|) = \tau_o(0)\exp[\frac{e\ell|\sigma_s|}{\varepsilon\varepsilon_o kT}]$$

where $\ell$ is the separation between the $DpA^-$ adsorption plane and the counterion image plane, and $\varepsilon$ is the effective dielectric constant in the vicinity of the adsorption plane. The above relation has been confirmed experimentally, yielding $(\ell/\varepsilon)=0.25$Å. This value is insensitive to variation of aqueous phase ionic strength and of membrane lipid composition. This work has been supported by the United States Army Research Office.

**M-AM-H13** ALTERATIONS OF MEMBRANE CONDUCTANCES BY MEROCYANINE AND MEROCYANINE-RHODANINE DYES. S. Krasne. Dept. of Physiology, UCLA Med. Sch., Los Angeles, Calif. 90024.

The effects of the voltage-sensing dyes merocyanine 540 (MC540) and a merocyanine-rhodanine (WW444) in altering the conductance properties of phosphatidyl ethanolamine bilayers in the absence and presence of the ion carrier nonactin were investigated. The following observations were made: Both dyes produced only small conductances in bilayers in the absence of nonactin. Addition of these dyes in the presence of nonactin and either KCl or $NH_4Cl$ (0.1M) caused dramatic increases in the carrier-mediated, zero-current, bilayer conductances, however (e.g. 1μM MC540 and 5μM WW444 increased this conductance by 2.5 and 1.7 orders-of-magnitude, respectively). MC540 decreased the conductance mediated by the permeant anion tetraphenylborate. These results suggest that the dyes induce large negative potentials near the bilayer surface. In addition, the normally non-linear current-voltage properties mediated by nonactin in these bilayers become increasingly linear upon addition of these dyes, and these dyes induce fast ($\bar{\tau}$=20-35μsecs) voltage-dependent, relaxation processes in the nonactin-mediated bilayer conductances. For all observations, MC540 is about 10x more potent than WW444. (Supported by USPHS HL20254.)

**M-AM-H14** EVIDENCE THAT VALINOMYCIN AND ITS PROLINE CONTAINING ANALOGS DIFFER ONLY IN SLOWER CONFORMATIONAL REARRANGEMENTS BETWEEN THE INTERFACE AND THE INTERIOR OF A GMO BILAYER. B. Enos and G. Eisenman. Physiol. Dept., UCLA, Los Angeles, CA 90024

Cyclo-(D-val-L-lac-L-val-D-pro)$_3$, Ivanov's analog of valinomycin in which proline replaces hydroxyisoval. was characterized as to steady-state G vs. V, G vs. C, and V°. A domain of 1:1 stoichiometry exists in which C- and V-independent perm. ratios are Rb(4.8)>Cs(1.2)>K(1.0)>$NH_4$(.28)>Tl(.08)>$CH_3NH_3$(.004)>Na(.00002)>Li(.000004). No p.d. occurs in a carrier gradient. Unlike val, the same "hyperbolic" G-V characteristic is found at low concentrations for all ions and conc.-dependent kinetic effects of unprecedented size become apparent for Rb, Cs, and K above .00005M. Despite the conclusion (BBA 455, 665) that a proline substituted analog acts via solution-complexation, it is possible to understand the proline series of analogs entirely within the interfacial-reaction scheme by including an unfolded conformational state at the interface which must be traversed in bringing the carrier or complex into the membrane, and which becomes rate determining with increasing proline content.

Supp. by NSF PCM 7620605, USPHS NS09931, F32 GM05786.

**M-AM-H15** A MEASUREMENT OF MEMBRANE VISCOSITY. R. Hochmuth, P. Worthy,* E. Evans, Washington University, St. Louis, MO. 63130 and Duke University, Durham, N.C. 27706

A theory of membrane viscoelasticity developed by Evans and Hochmuth in 1976 is applied to the particular case of red cell relaxation in which an elongated cell is allowed to return (relax) to its original biconcave shape. It is shown that the theory describes the relaxation behavior of red cells extremely well for a single fixed value of the time constant of 0.099±.0.013 sec. The time constant is the ratio of membrane surface viscosity to membrane elasticity. Thus, when the time constant is multiplied by a recent measurement for membrane elasticity of 0.0061±0.0012 dyne/cm, a value for the surface viscosity of $(6\pm2)\times10^{-4}$ dyne sec/cm (poise·cm) is obtained. When this value for surface viscosity is substituted into Saffman's theory for Brownian motion in a two-dimensional sheet, a value of approximately $10^{-10}$ $cm^2$/sec is calculated for the lateral diffusion coefficient.

**M-AM-H16** PARINARIC ACID AS A MEMBRANE PROBE: ROTATIONAL MOTION, ENERGY TRANSFER AND BIMOLECULAR PHOTOCHEMISTRY. B. Hudson, P. Wolber,* E. Tecoma,* C. G. Morgan,* and R. D. Simoni,* Stanford University, Stanford, California 94305

The rotational motion of parinaric acid in phospholipid bilayers has been studied by polarized nanosecond fluorimetry. The anisotropy decays to a constant nonzero value due to the restricted nature of the motion. Models describing this motion will be discussed. At high parinaric acid concentrations a bimolecular photochemical reaction results in loss of fluorescence. The use of this reaction to measure translational diffusion will be discussed. DMPC bilayers containing M-13 coat protein have been prepared by detergent dilution. The M-13 coat protein tryptophan fluorescence is efficiently quenched by Förster transfer to parinaric acid. This transfer is so efficient that even in the absence of knowledge of the dipole orientation factor it can be shown that the acceptor must associate with the protein and that the protein must be aggregated in both fluid and solid DMPC.

**M-AM-H17** LATERAL DISTRIBUTION OF FLUORESCENT LABELED PHOSPHOLIPIDS IN MEMBRANES AS MEASURED BY ENERGY TRANSFER. B.K. Fung,* L. Stryer, Department of Structural Biology, Stanford Medical School, Stanford, California 94305

Energy transfer between four different donor-acceptor pairs of fluorescent-labeled phosphatidylethanolamine in phosphatidylcholine membrane vesicles was investigated. The efficiency of energy transfer was measured as a function of the surface density of the acceptor for donor-acceptor pairs with Ro distances ranging from 20 to 50Å. Good agreement was found between the observed transfer efficiencies and theoretical values calculated according to Förster theory assuming a statistical distribution of donors and acceptors in the plane of the membrane. These studies indicate that fluorescence energy transfer can be used to accurately measure lateral distances between protein molecules and between proteins and lipids in biological membranes.

S Y M P O S I U M

# BIOPHYSICS OF BACTERIAL CHEMOTAXIS

**M-PM-1S** BACTERIAL CHEMOTAXIS. Howard C. Berg, Department of Molecular, Cellular and Developmental Biology, University of Colorado, Boulder, Colorado 80309

Bacteria can accumulate in regions that are hot or cold, light or dark, or of favorable chemical content: they exhibit "thermotaxis", "phototaxis" and "chemotaxis". They swim by rotating helical flagella. They back up or choose new directions at random by reversing the sense of the rotation: they have reversible rotary motors. The probability of a reversal depends on the way in which the intensities of sensory stimuli change with time: in chemotaxis, on the time rate of change of the occupation of specific receptors. A review will be given of recent work on bacterial chemotaxis, including the biochemistry and genetics, as an introduction to the talks on the physics that follow.

**M-PM-2S** PHYSICS OF THE BACTERIAL ENVIRONMENT. Edward M. Purcell, Lyman Laboratory, Harvard, University, Cambridge, Massachusetts 02138.

In the neighborhood of a bacterial cell in water Brownian motion and viscosity dominate the scene. Inertial forces are utterly negligible. Diffusive transport is rapid, with characteristic times in milliseconds. Statistical fluctuations in local concentration, hence in receptor occupancy, are considerable. How can the bacterial cell measure the concentration of an attractant? What are the physical limitations on its ability to sense a gradient? Why does it swim? Considering such questions, we are led to certain general conclusions. Solving the problem of the diffusive current to a cell with N receptors specific for some solute molecule X shows that the cell's intake of X molecules can almost equal that of a perfect absorber even when X-receptors cover only a small fraction of its surface. In a uniform medium access to solute cannot be significantly increased by swimming or stirring. Swimming at speed v for a distance less than D/v (D = diffusion coefficient) is an empty exercise in the cell's evanescent environment. Consideration of random noise in chemoreceptor occupancy indicates that in gradient sensing E. coli performs about as well as physics permits.

M-PM-3S BIOPHYSICS OF FLAGELLAR MOTION. R.M. Macnab,* Yale University, New Haven, Connecticut 06520.

The net migration of bacteria in response to chemical gradient stimuli results, not from a steering mechanism as in higher species, but from modulation of the occurrence of non-specific direction changes. The motor organelles, termed flagella, are thin protein filaments possessing an intrinsic, crystalline helicity. Helical wave propagation could, in principle, derive from either conformational or rotational phase change. The evidence in support of a rotational mechanism, capable of reversal, will be reviewed. In some of the commonest bacterial species, such as E. coli or Salmonella, an arbitrary number of flagella originate randomly around the cell body. When the motors are rotating in a counterclockwise sense, the filaments coalesce into a coordinately propagating bundle with resulting translational cell movement ("running"). The differential geometry and hydrodynamics of the individual rotating helices in overlapping domains will be discussed. Reversal of the motors to clockwise rotation is responsible for the directional changes alluded to previously; the cell undergoes a chaotic motion ("tumbling") which randomizes its orientation. Tumbling is not, however, a simple consequence of reversed rotation, but involves remarkable changes in filament structure, from the normal left-handed helices to a distinctly different right-handed form. The structural basis for these different forms, and the reason why motor reversal causes interconversion, will be discussed. Documentation of these phenomena is technically difficult because the filaments, being so thin (20 nm), scatter light very weakly in the microscope. Recent records made with a silicon intensifying target vidicon camera will be shown.

## M I N I S Y M P O S I U M

## PRIMARY EVENTS IN RADIATION BIOLOGY

M-PM-1M MOLECULAR PHYSICS OF PRIMARY EVENTS IN RADIATION ACTION ON MATTER. M. Inokuti. Argonne National Laboratory, Argonne, Illinois 60439

Much progress has been made in the detailed analysis of the delivery of energy on matter by ionizing radiations on the molecular level. The analysis stems from the earlier work by Fano, Platzman, and Spencer, and has been extensively developed by their co-workers. The effort has so far been concentrated on electron incidence on simpler molecular substances, i.e., the basic prototype problem. The analysis consists of two principal ingredients. First, the comprehensive cataloging of all inelastic-collision cross sections for electrons with molecules (including secondary-electron energy distribution in a single collision), and second, the evaluation of cumulative consequences of many electron collisions for electrons as well as for medium molecules. For the first task, a set of semiempirical methods of assessing data reliability and accuracy devised by Platzman is highly effective. For the second task, there are two classes of approaches, i.e., the method of transport theory originally due to Spencer and Fano and the Monte-Carlo method. These approaches are complementary to each other in the insight they give into the intricate physics involved in the radiation-energy absorption process. The discussion will concern not only traditional topics of radiation physics such as stopping power and ionization yields, but also some special consequences of chemical and biological interest.

M-PM-2M REVIEW OF THE PRIMARY PROCESSES OF IRRADIATED AQUEOUS SOLUTIONS. Edwin J. Hart. Argonne National Laboratory, Argonne, Illinois 60439

The primary species of irradiated water, sub-excitation electrons ($e^-_{se}$), hydrated electrons ($e^-_{aq}$), hydrogen atoms (H), hydrogen ions ($H_3O^+$), oxygen atoms $O(^3P)$ and hydrogen ($H_2$) are created in less than $10^{-12}$ s of the passage of the ionizing particle. Specie recombination reactions require much longer periods. The time scale of these events, the yields of the primary species, the products of these radical reactions, their rate constants, and the mechanism of water radiolysis are quite adequately known. In addition, thousands of radical-radical reaction rate constants have been established by radiation chemists. Thus, a sound basis has been provided for productive research in quantitative biology. LET, oxygen and pH profoundly alter the distribution and reactivity of these primary species and produce major qualitative and quantitative changes in the resulting products. Less fully known and appreciated are the effects of radiation on concentrated solutions. If the concentrated solute has no effect on primary specie production, then the yields of products are generally increased, since radical-radical reactions are suppressed. But entirely new chemical reactions may be initiated by $e^-_{se}$ in aqueous solutions above 0.01M and contribute substantially to product formation. Some examples of LET, oxygen, pH, and $e^-_{se}$ effects will be discussed.

M-PM-3M MOLECULAR BIOLOGY OCCURRING AS A CONSEQUENCE OF PHYSICAL AND CHEMICAL PROCESSES. F. Hutchinson, Yale University, New Haven, Connecticut, 06520

The most significant effects of ionizing radiations on living cells which have been identified are: the loss of ability of the cell to replicate, the induction of mutations, carcinogenesis, and teratogenesis, or alterations in the pattern of development of embryonic cells. A number of lines of evidence implicate radiation-produced lesions in the cellular DNA as the major cause of these effects. These lesions include: DNA double-strand breaks, single-strand breaks, alkali-labile bonds, damaged DNA bases, cross-links between the complementary strands of the DNA double helix, and cross-links between DNA and other cell constituents such as proteins. DNA is unique among cellular constituents in being subject to repair systems which remove lesions from the molecules. Single-strand breaks and alkali-labile bonds are efficiently repaired by enzymes which apparently use the complementary strand as a template to repair the damaged strand. Chemically altered bases are excised, and presumably the breaks so created are repaired by similar processes. DNA double-strand breaks are also repaired, although apparently less efficiently. In bacteria, this repair requires the presence of gene products involved in genetic recombination, as well as homologous DNA having the same base sequence. The double-strand break appears to be a major lesion determining the ability of a cell to be able to continue replication. The lesions which induce mutagenesis have not yet been identified. However, there is strong evidence that many mutations are introduced as a result of errors in repair of radiation-induced lesions.

M-PM-4M PRIMARY EVENTS IN CELLULAR RADIOBIOLOGY. C. A. Tobias, Lawrence Berkeley Laboratory, University of California, Berkeley, California 94720

Studies of accelerated heavy ions of various atomic numbers (1 to 34) and with different kinetic energies (up to 800 Mev/amu) aimed at understanding the mechanisms of the effects on mammalian cells in culture are reviewed. Contrary to a widely held belief, lethal effects are not proportional to the energy deposited or to the LET of the particles. The effects are also dependent on the spatial patterns of energy transfer and on fast radical interactions. Three convenient parameters are: particle flux density, physical charge state, and kinetic energy. The primary biological lesions are not formed at the time the particles pass through the cell, but develop later as a result of the interactions between diffusing free radicals and essential biomolecules (e.g., DNA). Final biological effect depends on the number and kinds of lesions and their enzymatic repair. Single-strand scission of DNA appears unimportant. Double-strand scission is lethal to Φ X174 phage; it is repaired relatively slowly in mammalian cells. Inability to repair and misrepair of double-strand lesions appear to be correlated with cell lethality.

**M-PM-5M** CELL IRRADIATION WITH MOLECULAR IONS. Harald H. Rossi*, Columbia University, New York, New York 10032

The theory of dual radiation action postulates that the effects of ionizing radiation on the cells of higher organisms are due to the pairing of labile alterations (termed sublesions) to produce permanent injuries (termed lesions). It is also postulated that the interaction distance of sublesions is of the order of one micrometer. In order to test the theory and to evaluate the combination probability of sublesions as a function of their separation, molecular ions ($D_2^+$) are employed to irradiate cells attached to a thin mylar window which separates them from the vacuum chamber. When impinging on the window, the ions are stripped of their electron and the two deuterons are separated by multiple coulomb scattering as they traverse the mylar sheet. The separation depends on sheet thickness but is of the order of a few tenth of a micrometer. The effects of such paired deuterons are compared with those of randomly incident deuterons which are obtained by stripping of the ions at a considerable distance before they reach the foil. As expected, the biological effect of paired ions is greater than that of random ions and the difference depends on the phase of the cell in its reproductive cycle. Initial data have been obtained on the dependence of the interaction of sublesions on their separation.

This investigation is supported by Grant Number CA 15307, DHEW, and by Contract EY-76-C-02-3243 from ERDA.

**M-PM-6M** THE USE OF CHEMICAL MODIFIERS TO STUDY FUNDAMENTAL ASPECTS OF RADIATION BIOLOGY. J. D. Chapman, Department of Radiation Oncology, Dr. W. W. Cross Cancer Institute and Department of Radiology, University of Alberta, Edmonton, Alberta. T6G 1Z2

The technique of pulse radiolysis has made possible the direct measurement of several absolute rate constants for free radical reactions of potential importance in cellular radiobiology. Several compounds have been shown to be selective scavengers of specific free radicals produced in the radiolysis of water and also protect mammalian cells against inactivation by either X-rays or heavy-charged particle radiation. These studies indicate that the indirect action of hydroxyl radicals (and possibly hydrogen atoms) produced in the cellular water results in at least 60 to 80% of all cell inactivation. To date no component of cell inactivation can be attributed to solvated electrons. This may only reflect the fact that the selective scavengers of solvated electrons in use today are much too toxic to use with mammalian cells at the high concentrations needed to produce protection. When cell inactivation is resolved kinetically into single-hit and double-hit components, the concentrations of radical scavenger required to protect against single-hit and double-hit events are significantly different. This result indicates that the hydroxyl radical concentration in the vicinity of the cellular targets resulting in single-hit events is higher than the concentration required to produce double-hit events. Conversely the distance hydroxyl radicals must diffuse to cause single-hit damage is considerably shorter than the diffusion distance of the same radicals which result in double-hit lesions. The time-scale of these radical events in mammalian cells is approximately $10^{-9}$ seconds. For cell inactivation at high-LET's produced with the heavy-charged particle beams at the BEVALAC at Lawrence Berkeley Laboratory, the indirect action of hydroxyl radicals and hydrogen atoms appears to be as important at the maximum RBE as it was for X-irradiation. For radiations of LET's greater than those resulting in maximum RBE the importance of indirect effect appeared to diminish. It is only with the very densely ionizing particle tracks that direct action becomes the dominant form of cell inactivation in mammalian cells. For much of the LET spectrum of importance in radiobiology the cellular radiation chemistry appears to be qualitatively similar.

**M-PM-7M** A SEARCH FOR FUNDAMENTAL CONSTANTS IN CELLULAR DOSE-RESPONSE RELATIONSHIPS. Paul Todd, Paul S. Furcinitti, James C.S. Wood, W. R. Garrett, and M. G. Payne. The Pennsylvania State University, University Park, Pennsylvania 16802 and Oak Ridge National Laboratory, Oak Ridge, Tennessee 37830

Several conceptual models of cell inactivation by ionizing radiation lead to a similar mathematical form of the dose response function:

$$S = \exp\left\{-CD-AR^2\tau^2\{-1+(D/R\tau)+\exp(-D/R\tau)\}\right\}$$

S is the fraction of surviving cells; D is the dose; R is the dose rate; and $\tau$ is the recovery mean time for sublethal events. The constants A, C, and $\tau$ should be derivable from more fundamental data from radiation chemistry, molecular biology, and cell science. By proceeding from the assumption that the lethal event in cells is the unrepaired double-strand DNA break, data were abstracted from biochemical and radiation studies on virus, bacterial, and mammalian DNA and from radiation chemical and repair studies with synchronized and asynchronous mammalian cells inactivated by radiations of varying LET. On the basis of the above assumption, the constants A and C should be determined from the number of nucleotides per cell, the probabilities per unit dose of DNA strand-break induction, the break-repair capacity of the cell, the LET dependence of strand-break induction, and the geometry of the sensitive sites. Some of these data are known only within a factor of two, so preliminary calculations of A and C, although of the proper magnitude, are limited by the accuracy of the available numerical data. Work supported by USPHS Grant RO1-CA-17536 from the National Cancer Institute.

BIOENERGETICS I

**M-PM-A1** ENDOR FROM CYTOCHROME OXIDASE. H.L. Van Camp‡ Y.H. Wei‡ T.E. King, and C.P. Scholes, Lab of Bioenergetics & Dept. of Physics, SUNY/Albany, Albany, NY 12222

ENDOR was done at 2.1 K on the "copper" signal of cytochrome oxidase. Samples contained 25-50 mg/ml protein and 10 nmole heme a/mg protein. Enzymic activity was determined by $O_2$ consumption in the presence of cytochrome c and ascorbate. Small amounts of "adventitious" copper occurred in some samples, but there was no dependence of ENDOR intensity or frequency on it. All samples yielded similar spectra. For example, at g = 2.00 (H= 3241 G) ENDOR was seen near the free proton precession frequency and as well at 7.8, 9.8, 19.5, and 23.1 MHz. A change in Zeeman field and/or microwave frequency showed the 7.8 and 9.8 MHz lines to be from at least one nitrogen, but the 19.5 and 23.1 MHz lines are from inequivalent protons with couplings of 11.6 and 18.9 MHz. Except for the weakly coupled protons, the ENDOR spectra were remarkably isotropic. A preliminary deuteration experiment showed no exchangeable protons. Variations in proton hyperfine couplings with respect to enzymic activity were less than 4%. We have not yet detected ENDOR characteristic of the copper nucleus itself.

**M-PM-A2** RESONANCE RAMAN SPECTROSCOPY OF CYTOCHROME OXIDASE. G. T. Babcock, I. Salmeen† and L. Rimai†, Dept.of Chem., Michigan State Univ., East Lansing, MI 48824 and †Res. Staff, Ford Motor Company, Dearborn, MI 48121.

We have obtained resonance Raman spectra ($\lambda_{ex}$=4416Å) of cytochrome oxidase under various conditions of pH, reduction and ligand binding. We have also taken spectra of monomeric heme a when the 5th and 6th ligands to iron are imidazole. Our results confirm earlier observations of Salmeen et al who showed that the reduced protein has several unusual features when compared with other heme proteins. We have established that the unusual aspects of the oxidase spectra are the result of interactions between heme a and the protein moiety and are not intrinsic to heme a itself. These interactions are labile and are destroyed at moderately alkaline pH (pH>9.5). Specific bands in the spectrum of the reduced protein, notably those at 1670 $cm^{-1}$ and 215 $cm^{-1}$, are assigned to cytochrome $a_3^{2+}$. The 1670 $cm^{-1}$ band is attributed to the cytochrome $a_3^{2+}$ formyl group whose position relative to the plane of the porphyrin ring appears to be sensitive to the redox and spin state of cytochrome $a_3$. (Research supported, in part, by the Research Corporation.)

**M-PM-A3** PHOTOREDUCTION OF COPPER CHROMOPHORES IN RHUS VERNICIFERA LACCASE AND PORCINE CERULOPLASMIN. Y. Henry* and J. Peisach, Institut de Biologie Physico-chimique, Paris, France, and Albert Einstein College of Medicine, Bronx, New York.

The low temperature (77 K) irradiation of oxidized ceruloplasmin or laccase at the 330 nm absorption which arises from Type 3 copper leads to the reduction of the blue, Type 1 copper as demonstrated by the bleaching of the 610 nm chromophore and the decrease of the EPR signal associated with this species. The optical absorption of Type 3 copper also decreases. The EPR of Type 2 copper remains unaffected. Concomitant with the Type 1 copper reduction, a new EPR signal, possibly that of a biradical, appears. These optical and magnetic changes are wavelength specific. No effect is observed when the proteins are irradiated near 610 nm. Irradiation at 280 nm produces an axial radical unlike that formed at 330 nm. Upon thawing the bleached protein in the presence of oxygen or ferricyanide, the optical absorptions of Types 1 and 3 copper are completely restored, the EPR signal of the radical species disappears, and the EPR of Type 1 copper is now indistinct from that of the untreated protein. These studies demonstrate that energy is transferred between Type 3 copper and Type 1 copper in the blue oxidases.

**M-PM-A4** HEME ELECTRONIC STATES IN MIXED-VALENCE CYTOCHROME OXIDASE BY MCD. L. Vickery, G. Babcock, L. Garcia-Iniguez and G. Palmer. Univ. California-Irvine, Michigan State Univ.-East Lansing and Rice Univ.-Houston.

A mixed valence (MV) species of cytochrome oxidase in which cyt a is oxidized and cyt $a_3$ is reduced can be formed in the presence of carbon monoxide. We have used MCD spectroscopy in the Soret region to determine the redox and spin states of each heme in the MV-CO complex of the purified enzyme from 10° to -110° and in its photolysis product at -180°. The MV-CO complex exhibits a *C*-type MCD spectrum like that observed for low spin ($S = \frac{1}{2}$) cyt $a^{3+}$ in the fully oxidized enzyme and a weaker *A*-type spectrum arising from diamagnetic cyt $a_3^{2+}$·CO. This indicates that reduction and ligation of cyt $a_3$ to an $S = 0$ state does not affect the spin state of cyt $a^{3+}$. Photolysis of the complex below -140° is essentially irreversible and yields an MCD spectrum with *C*-term contributions from low spin $a^{3+}$ and high spin $a_3^{2+}$. Difference MCD spectra clearly establish that cyt $a^{3+}$ remains completely low spin, being unaffected by the $S = 0 \rightleftharpoons S = 2$ transition of cyt $a_3^{2+}$ at low temperatures. [Supported in part by NIH Grant GM-21337.]

**M-PM-A5** ORIENTATION OF IRON SULFUR CENTERS IN THE MITOCHONDRIAL MEMBRANE. J.C. Salerno, H. Blum*, J.S. Leigh, and T. Ohnishi, Johnson Foundation, Dept. of Biochemistry and Biophysics, University of Pennsylvania, Phila., PA.

Iron sulfur chromophores in the NADH dehydrogenase succinate dehydrogenase and cytochrome b-$c_1$ region of the respiratory chain exhibit orientation dependent EPR spectra in preparations of oriented multilayers. Several binuclear Fe/S clusters such as Center S-1 in SDH, Rieske's center and at least one of the Fe/S centers in NADH dehydrogenase are oriented with the x axis of the g tensor parallel to the membrane normal. That is, the Fe-Fe is probably parallel to the membrane plane. This is not unexpected for intrinsic membrane proteins with the Fe-S clusters held between membrane penetrating α-helices. The tetranuclear Fe/S clusters are all also highly oriented in the membrane, with the exception of "Center 5", which is associated with a soluble flavoprotein. A variety of effects on EPR spectra of several Fe/S centers and flavin semiquinone can be observed in SMP after addition of dysprosium EDTA.

**M-PM-A6** ELECTRON TUNNELING IN BIOMOLECULES. M. J. Potasek and J. J. Hopfield, Princeton, N. J. 08540

The vibronically coupled theory of electron transfer between biomolecules describes a situation in which the electron tunnels from donor molecule to acceptor and includes vibronic coupling in each molecule. Many electron transfers in photosynthesis and oxidative phosphorylation occur in membranes where "sites" are closely packed and differences in redox energies are minimal. For photon or oxidative energy to be converted to useable chemical energy, directionality in electron transfer must be maintained. This tunneling model of electron transfer provides directionality by requiring relatively short transfer distances. Experimental verification of electron tunneling in photosynthetic and respiratory systems will be presented. Some of the examples from respiration will include cytochrome peroxidase, cytochrome c and cytochrome $c_1$.

**M-PM-A7** SEQUENCE OF EVENTS IN THE REDUCTION OF $O_2$ BY CYTOCHROME OXIDASE, H.J. Harmon, Dept. of Biochemistry & Biophysics, Univ. of Penn., Phila. (currently - School of Biol. Sci., Oklahoma State Univ., Stillwater,OK,74074.)

Studies of the events associated with oxygen reduction by cytochrome c oxidase via low temperature spectroscopy indicate the sequence of oxidation. At -117°C following the binding of $O_2$ to fully reduced oxidase, a decrease in 594-635nm absorption (loss of $\underline{a}^{2+}O_2$) occurs before an increase in 830-940 absorption ($Cu^{+}\rightarrow Cu^{++}$) and the decrease in 612-635nm absorption ($\underline{a}^{2+}\rightarrow\underline{a}^{3+}$). The sequence of oxidation is $\underline{a}_3^{2+}$, $Cu^{+}$, and lastly cyt $\underline{a}^{2+}$. Studies of the effects of pH on the formation of oxygen compounds confirm the uniqueness of the 594 and 612nm signals. No decrease in 594nm absorption occurs with decreasing pH while Cu and cyt $\underline{a}^{2+}$ oxidation continue, although slowed. The oxidation of $Cu^{+}$ is not decreased significantly at low pH and suggests its interaction with cyt a. These and other results suggest: 1) two $2e^{-}$ steps are not involved in $O_2$ reduction, 2) protonation of bound $O_2^{-n}$ occurs early in the sequence, this compound capable of either re-reducing the oxidase or resisting further oxidation, 3) 594 and 612nm identify separate chromophores, the latter being cyt a. (Supported by NIH Grant GM 01997-02)

**M-PM-A8** RESPIRATORY ACTIVITIES OF MITOCHONDRIA AND SUBMITOCHONDRIAL PARTICLES FROM SKELETAL MUSCLE. D.M. Scott*, E.T. Storey, and C.P. Lee. Univ. of Pa., Philadelphia, PA, and Wayne State U., Detroit, MI.

Rabbit skeletal muscle mitochondria (RMM) show uncoupled respiratory rates with pyruvate/malate, succinate and L-3-glycerol phosphate (GP) of ca. 60 nmol $O_2$/min-mg protein; the rate with NADH is nil. Submitochondrial particles (SMP) prepared from RMM show rates with NADH, succinate and GP of ca. 70 nmol $O_2$/min-mg protein; the same rate with NADH is found with RMM treated with 6% cholate. The respiratory rate of SMP with NADH is not stimulated by cholate. Respiratory control ratios (uncoupler/oligomycin) in SMP are 1.8-2.0 for all substrates. Since NADH oxidase and GP oxidase are on opposite sides of the inner membrane, and since GP is impermeable to the inner membrane (Klingenberg, Eur. J. Biochem. 13:247, 1970), the results suggest that these SMP are not simply inside-out vesicles and that energy conservation can occur in the membrane in the absence of a transmembrane electrochemical gradient.
(Supported by NIH-HL19737 and the Muscular Dystrophy Assn.).

**M-PM-A9** THE EFFECT OF BULK WATER STRUCTURE ON THE TEMPERATURE DEPENDENCE OF THE REDUCTION POTENTIAL OF CYTOCHROME C. G. P. Kreishman, C. W. Anderson,* C.-H. Su,* H. B. Halsall, and W. R. Heineman,* Department of Chemistry, University of Cincinnati, Cincinnati, Ohio 45221.

The temperature dependence of the reduction potential ($E^{o'}$) of cytochrome c in NaCl and KCl-$H_2O$ solutions exhibited a biphasic behaviour with a transition temperature at 42°C. $dE^{o'}/dT$ was larger above 42°C than below. This biphasic behaviour was not observed in NaBr, NaF and NaI-$H_2O$ solutions or in NaBr and NaCl-$D_2O$ solutions. These results are consistent with the previously noted bulk water destructuring at 42°C which has been observed only in $Cl^{-}$-$H_2O$ systems (Kreishman, Foss, Inoue and Leifer, Biochemistry, (1976) 15, 5431). In the less structured bulk solvent, the larger oxidized form is favored as indicated by the large decrease in the reduction potential. The transition temperature at which the destructuring occurs can be altered by varying the amount of $D_2O$ in the sample.

**M-PM-A10** THERMODYNAMICS AT NONEQUILIBRIUM STEADY STATES. J. Keizer*, Intr. by R. E. Harrington, University of California, Davis, California, 95616.

A generalization of the entropy function, called the σ-function, is used to characterize the thermodynamics of far from equilibrium steady states. The construction of the σ-function requires the introduction of new extensive variables which measure the distance a system is away from equilibrium. The σ-function is related to molecular fluctuations in the traditional extensive variables and the stability of the steady state just as the entropy is at equilibrium. Its application to several models of biological transport processes is discussed.

**M-PM-A11** PROTECTION OF HIGH-ENERGY PHOSPHATE LEVELS IN HEARTS DURING SEVERE HYPOXIA. E.T.Fossel* and J.S. Ingwall, Biophysical Laboratory and Dept. of Medicine Harvard Medical School, Boston, Mass. 02115.

$^{31}P$ Nuclear Magnetic Resonance (NMR) can be used to moniter levels of the high-energy phosphate containing molecules,Adenosine Triphosphate (ATP) and Creatine Phosphate (CrP) in isolated perfused rat hearts. We find that during periods of 10 min and 20 min of severe hypoxia levels of CrP and ATP fell but upon reoxygenation recovered to control levels of 32 and 26 μmoles/g dry weight respectively. However, upon reoxygenation following 30 min of severe hypoxia CrP and ATP fell to 25% and 10% of control values respectively and recover only to 35% and 30% of control values on reoxygenation. Inclusion of the salvage pathway substrate, inosine, in perfusate at 0.4 mM decreased the level to which CrP and ATP fell (to 18% and 75%) and upon reoxygenation levels of CrP and ATP returned to control values. Thus, availibility of purine nucleosides to the salvage pathway permits recovery of high-energy phosphate levels following 30 min of severe hypoxia.

**M-PM-A12** RATES OF REDUCED CYTOCHROME C-FERRICYANIDE BINDING AND ELECTRON TRANSFER. J.A.McCRAY and T.KIHARA*, Dept.of Physics and Atomos.Sci.,Drexel Univ., and The Johnson Research Foundation,Univ.of Pa.,Phila.Pa

We have found the rates of binding and electron transfer between ferrocytochrome c and ferricyanide using the continuous flow technique, which enabled us to use high concentrations of ferricyanide so that binding sites could be saturated and subsequent electron transfer observed. The extent of the reactions were measured at fixed times(e.g.700μs after mixing). In $H_2O$ buffer the binding rate of ferricyanide to ferrocytochrome c was found to be $1.18 \times 10^7\ M^{-1}s^{-1}$. The electron transfer rate was $2.53 \times 10^3 s^{-1}$. These reactions were also measured in $D_2O$ buffer. The ratio of the rates of binding in $H_2O$ to that in $D_2O$ was found to be 1.34 and the corresponding ratio of the electron transfer was 1.55. Our work has shown that a ferrocytochrome c-ferricyanide complex forms before electron transfer occurs, and the rates of both reactions are slower in $D_2O$. The ratios of these rates in $H_2O$ and $D_2O$ are close to $\sqrt{2}$ suggesting that hydrogen atoms of water are involved in the in vitro electron transfer and that reorientation of solvation water molecules is necessary before the complex can be formed.

**M-PM-A13** HYDROXYL RADICAL PRODUCTION INVOLVED IN NADPH-DEPENDENT LIPID PEROXIDATION OF RAT LIVER MICROSOMES. C. S. LAI* and L. H. PIETTE, Cancer Center of Hawaii, University of Hawaii, 1997 East-West Road, Honolulu, Hawaii 96822

The spin traps, 5,5'-Dimethyl-1-pyrroline-1-oxide and phenyltertiarybutylnitrone were used to investigate the primary free radical involved in NADPH-dependent lipid peroxidation of rat liver microsomes. We previously reported that a NADPH-dependent hydroxyl radical (OH·), which may be the primary free radical that initiates lipid peroxidation, is generated in liver microsomes ( Lai and Piette, Biochem. Biophys. Res. Comm., 78:51, 1977 ). The hydroxyl radical production is correlated well with the malonaldehyde production in lipid peroxidation during NADPH oxidation. Factors such as pH, ferrous ion, ferric ion, ethylenediaminetetraacetate and sodium chloride affecting the hydroxyl radical production in liver microsomes are discussed. In addition, using a fast ESR flow system we describe the relationship between lipid peroxidation and drug hydroxylation in liver microsomes.

## PHYSICAL PROBES OF MEMBRANE STRUCTURE

**M-PM-B1** HIGH-FIELD NMR OF MEMBRANES AND PROTEINS. E. Oldfield, R. Jacobs,* M. Meadows,* D. Rice,* and R. Skarjune.* Department of Chemistry, University of Illinois, Urbana, Illinois 61801.

$^2H$ NMR spectra of dimyristoylphosphatidylcholines (DMPC) specifically labelled in positions 2', 3', 4', 6', 8', 10', 12', and 14', of the 2-chain and of $3\alpha d_1$ cholesterol, have been obtained as a function of temperature and cholesterol composition. Data on the specifically deuterium labelled cholesterol molecule (in nonsonicated membrane systems) permits evaluation of the order parameter ($S_0$) describing rigid body motions in the bilayer. Segmental order parameters derived from the data presented allow calculation of individual chain segment projections onto the director axis. Mathematical models which include chain tilt as well as those which neglect this type of rigid body motion give essentially identical results. Results of calculations of chain length and membrane thickness of a DMPC-30 mole % cholesterol membrane system at 23° are in excellent agreement with distance determinations made using high-resolution neutron diffraction. We have also constructed a sideways-spinning probe for highfield NMR spectrometers which provides very high S/N ratios. Results on a variety of proteins will be shown.

**M-PM-B2** $^{13}C$-NMR STUDIES OF RHODOPSIN:PHOSPHOLIPID INTERACTIONS. N. Zumbulyadis, D. F. O'Brien, and R. A. Ott,* Eastman Kodak Company Research Laboratories, Rochester, New York 14650

High-resolution $^{13}C$-NMR spectroscopy was used to probe details of lipid-protein interactions in rhodopsin:phospholipid recombinant vesicles and sonicated rod outer segment discs. The variations in the linewidths of the individual carbon resonances were used to monitor the effects of rhodopsin on the motional state of lipid molecules. It is found that rhodopsin restricts the mobility of the various parts of the lipid molecules to a differing extent. The results indicate that in recombinants, even at low concentrations, rhodopsin effectively broadens the $^{13}C$ resonances of the glycerol backbone. Furthermore, it is found that in systems with a high degree of unsaturation in the β-acyl chain, such as the disc lipids, it is the α-chain that is preferentially immobilized.

**M-PM-B3** CARBON-13 NMR STUDIES OF THE CHOLERA TOXIN RECEPTOR, GANGLIOSIDE GM1. L.O. Sillerud*, J.H. Prestegard*, R.K. Yu*, D.E. Schafer, and W.H. Konigsberg* (Intr. by S.M. Baylor). Yale University, New Haven CT 06510, and VA Hospital, West Haven CT 06516.

The glycosphingolipid membrane-bound receptor for cholera toxin, ganglioside GM1, has been isolated in high purity (greater than 99%) and sufficient quantity to afford natural-abundance 13-C NMR spectra of excellent signal-to-noise ratio at 67.88 MHz. The resonances in the proton-decoupled spectrum of aqueous GM1 micelles have been completely assigned through the use of model compounds, measurement of spin-lattice relaxation times (T1), and binding of diamagnetic calcium and paramagnetic europium ions. T1 values for most of the GM1 carbons in the micelle are short, reflecting a large micelle size (MW ca 250 kD), strong intermolecular interactions, and limited local motion. Broadening and shifting of 13-C resonances by europium and calcium, respectively, were exploited to determine the details of the cation-binding site. In addition to sialic acid the terminal galactose and N-acetylgalactosamine were found to be involved, apparently explaining why the affinity of GM1 for cations is higher than that of monomeric sialic acids.

**M-PM-B4** PHYSICAL STUDIES OF THE INTERACTION OF CHOLERA TOXIN WITH PHOSPHOLIPID VESICLES CONTAINING GANGLIOSIDE GM1. L.O. Sillerud*, D.E. Schafer, R.K. Yu*, and W.H. Konigsberg*, Yale University, New Haven CT 06510, and VA Hospital, West Haven CT 06516, and T.K. Lim* and V.A. Bloomfield, University of Minnesota, St. Paul MN 55101

In an effort to understand how ganglioside GM1 acts as a receptor for cholera toxin and aids the protein in penetration of the plasma membrane, we have undertaken a variety of physical studies of the influence of the toxin on the properties of dimyristoyllecithin vesicles containing 2.5 mole per cent GM1. Proton NMR with the aid of Pr(III) showed that both inner and outer monolayers were perturbed by the toxin, implying that the protein penetrates the bilayer and does not form Pr(III) channels through the membrane. The gel-to-liquid-crystalline transition of these vesicles, as revealed by differential scanning calorimetry, is strongly perturbed by binding of the toxin, a result consistent with a lack of temperature dependence of the NMR properties of the vesicles. Thus GM1 may effectively aid toxin penetration of the bilayer even below the transition temperature. We have also performed laser light scattering studies to determine the effects of GM1 and toxin on vesicle size.

**M-PM-B5** IN VITRO CATABOLISM OF VERY LOW DENSITY LIPOPROTEINS: STRUCTURAL ALTERATIONS MONITORED BY $^{13}C$-NMR. J. Brainard*, P. Kinnunen*, A. Catapano*, E. Cordes*, A. Gotto*, L. Smith and J. Morrisett, Dept. of Chem., Indiana Univ., Bloomington, Ind. and Dept. of Med. and Biochem., Baylor College of Med., Houston, TX

Normal human VLDL was treated with purified lipoprotein lipase sufficient to hydrolyze all the constituent triglycerides (TG) in <1 hr. The extent of lipolysis was limited by the amount of albumin (BSA) present to scavenge released fatty acids (FA). After the first 60 min digestion, the mixture was chromatographed on G-150 to separate BSA-bound FA from modified VLDL. Three cycles of digestion-chromatography produced 3 different particle populations which were studied by 63.4 kG $^{13}C$-NMR. A large intensity loss of resonances attributable to TG C$\alpha(\gamma)$, C$\beta$, $CH_2OC{=}O$, and CHOC=O was observed; in addition there appeared 2 new resonances in the glyceride region of the spectrum and a new carbonyl resonance attributable to FA. These studies demonstrate the feasibility of monitoring VLDL metabolism by NMR and suggests a method for studying the relative location of the lipid metabolites within the remnant particle. (Supported by HL-17269-03 and HL-15648-05.)

**M-PM-B6** ESR DETERMINATION OF MEMBRANE ORDER IN YEAST STEROL MUTANTS.* F.W. Kleinhans, N.D. Lees,* M. Bard,* IUPUI; and R.A. Haak, I.U. Med. Ctr., Indianapolis, IN.

Yeast sterol mutants[1] were subjected to ESR analysis in an attempt to elucidate how altered sterol composition correlates with the membrane order parameter S. The measurements were made at 25° on intact cells of Sacharomyces cerevisiae harvested during the exponential phase of growth and spin labeled with 5 doxyl steric acid (5N10). The wild type and a double mutant, erg 6/2, were found to have significantly different order parameters of S = 0.595 ± 0.005 and S = 0.626 ± 0.005, respectively. The higher order parameter of erg 6/2 is consistent with measurements[2] showing a higher percentage of sterols (by dry weight) in erg 6/2. An increase in membrane sterol content is expected to result in a more rigid membrane. Two single mutants, erg 2 and erg 6, have order parameters intermediate between the wild type and erg 6/2 values.

*Work supported in part by the I.U. and Purdue Research Foundation

[1]Derek H.R. Barton, et. al., J.C.S. Perkin I, 88 (1975)
[2]S.W. Molzahn and R.A. Woods, J. Gen. Microbiol, 72, 339-348, (1972)

**M-PM-B7** THE IDENTITY OF THE LOW AFFINITY $Ca^{++}$ BINDING SITES IN MITOCHONDRIA AS DETERMINED BY THE RESONANCE RAMAN SPECTRUM OF RUTHENIUM RED BOUND TO MITOCHONDRIA. J. M. Friedman, G. Navon,† P. Glynn,* and K. B. Lyons,* Bell Laboratories, Murray Hill, New Jersey 07974

The resonance Raman (RR) spectrum of ruthenium red displays frequency shifts and intensity changes when ruthenium red goes from a free to a bound configuration. These spectral changes are different for protein bound versus phospholipid bound ruthenium red. Furthermore on the basis of changes or absence of changes in the RR spectrum, it is apparent that ruthenium red only binds to the negatively changed phospholipids such as cardiolipin and phosphatidylserine. From RR titration curves we establish that ruthenium red can bind up to three cardiolipin molecules or six phosphatidylserine molecules indicating that each ruthenium atom has an effective charge of +2. The RR spectrum of ruthenium red bound to mitochondria at concentrations that saturate the low affinity $Ca^{++}$ binding sites indicates that ruthenium red is bound to a negatively charged phospholipid. A survey of the concentrations of the various phospholipids in the inner membrane indicates that the binding site is almost certainly cardiolipin.

†Perm. address: Tel-Aviv Univ., Ramat-Aviv, Israel.

**M-PM-B8** ORDER AND MOBILITY OF THE MEMBRANE LIPIDS OF ACHOLEPLASMA LAIDLAWII AS MONITORED BY $^2H$ AND $^{13}C$ NMR. Ian C. P. Smith, K. W. Butler, K. G. Johnson,* A. Joyce,* A. P. Tulloch,* G. W. Stockton,* J. H. Davis,* and M. Bloom,* Div. Biol. Sci., NRC, Ottawa, Canada and Dept. Physics, UBC, Vancouver, Canada

Fatty acids labelled specifically with $^2H$ or $^{13}C$ were incorporated biosynthetically at high levels into the membrane lipids of *A. laidlawii*. The NMR spectra of the cell membranes yield quadrupole splittings or spin-lattice relaxation times ($T_1$) which measure molecular order and molecular motion, respectively. The liquid crystal to gel transition of the membrane lipids is manifest in both. In the liquid crystalline state the profile of order versus labelled position of palmitic acid shows constant values for the first 10-12 carbons, with a rapid linear decrease towards the terminal methyl group. At temperatures throughout the phase transition at least two types of spectrum are observed, indicative of the coexistence of two phases in slow (<25,000 $sec^{-1}$) exchange. The $^{13}C$ $T_1$ values are essentially constant over a large portion of the fatty acyl chains, becoming much longer only for the last three or four carbon atoms.

**M-PM-B9** SPIN PROBE STUDIES OF ACHOLEPLASMA LAIDLAWII MEMBRANE STRUCTURE. K. W. Butler, K. G. Johnson* and I. C. P. Smith, Biological Sciences Division, National Research Council, Ottawa, Canada K1A OR6

Membranes containing a high percentage of a particular fatty acid can be prepared by growing *Acholeplasma laidlawii* on a medium enriched with the chosen fatty acid. The ordering of stearic acid spin probes was essentially the same in membranes of *A. laidlawii* grown on media enriched with a number of different specifically deuterated palmitic acids. Spin probe partition experiments yielded data in agreement with published D.S.C. results. In favourable circumstances, spin probes in two environments could be observed in membranes in the temperature range of the gel to liquid crystal transition. The addition of cholesterol to the growth medium stiffened the membranes, increasing molecular order. Lipids in membranes enriched with oleic acid were less ordered than membranes enriched with palmitic acid at temperatures below the growth temperature.

**M-PM-B10** THE CHARACTERIZATION OF LATERAL MOTION IN MEMBRANES. Barton A. Smith and Harden M. McConnell, Chemistry Department, Stanford University, Stanford, CA 94305.

We have carried out preliminary studies of lateral molecular motion in model membranes and living cell membranes by observing fluorescence redistribution after pattern photobleaching (FRAPP). This technique is similar to the earlier FRAP[1] (fluorescence recovery after photobleaching) method, except that instead of bleaching the membrane in a small spot, the membrane is bleached in an extended periodic pattern (such as parallel stripes). Subsequent diffusion or other lateral motions can be observed visually and recorded photographically in a fluorescence microscope. Advantages of the FRAPP method include simplicity of observation and recording, ease of determination of the characteristic diffusion distance, detection of non-diffusive motions, study of mobile cells and liposomes not fixed to microscope stage, and measurement of very low diffusion coefficients ($<10^{-12}$ $cm^2$/sec). The FRAPP method has been used to measure lateral diffusion in multilayers and liposomes in the low temperature phases and to study the lateral motion of fluorescent concanavalin A bound to EL-4 tumor cells.

1) Wu et al., Biochemistry 16, 3937 (1977).

**M-PM-B11** A SPIN LABELED STEARIC ACID AS A RESPIRATORY INHIBITOR IN E. COLI. A. G. McAfee and C. Ho, Dept. of Life Sciences, Univ. of Pittsburgh, Pittsburgh, PA. 15260

Spin labeled stearic acid, 2-(14-carboxytetradecyl)-2-ethyl-4,4-dimethyl-3-oxazolidinyloxy, acts as a respiratory inhibitor upon addition of substrate to E. coli membranes. Respiration-dependent reduction of this spin label has been characterized in terms of substrate efficiency, effects of respiratory inhibitors, temperature, structure of the spin label, and concentrations of both spin label and membrane. Genetic aberrations of respiratory carriers attenuate reduction. Reduction is also decreased by purified D-lactate dehydrogenase or in guanidine hydrochloride extracts of membranes. Certain physiological effects are exhibited with this spin label structure. D-Lactate oxidase is inhibited by 50% with 15 nmoles $mg^{-1}$. Other oxidases are less sensitive. The steady state turnover of cytochrome $b_1$ is retarded, and its reduced level decreased. This inhibition is dependent on both spin label and substrate concentrations. Effects of metal chelators and other inhibitors place this spin label, an artificial electron acceptor, on the reductase side of cytochrome $b_1$ and the oxidase side of nonheme iron. (Supported by research grants from NSF and NIH.)

**M-PM-B12** ELECTRON DIFFRACTION STUDIES OF ERYTHROCYTE MEMBRANE AND ITS LIPID EXTRACT. S. W. Hui and C. M. Strozewski*, Roswell Park Memorial Institute, Buffalo, N. Y. 14263

The organization of lipid molecules in human erythrocyte membrane were studied by electron diffraction in controlled environment. The recrystalization of cholesterol and phospholipids was found to be a result of dehydration. The diffraction patterns from hydrated bilayers of total lipid extracts were similar to those from whole ghost membranes, indicating their common lipid origin. The lipids in fresh, fully hydrated membrane remain in the fluid state at physiological temperatures. The highest (onset) temperatures at which diffraction from solid domains of lipids is detected vary with the treatments of the membranes. The detectable onset temperature of both fresh membrane and its total lipid extract is about -3°±3°, and increase with phospholipase $A_2$ treatment and with storage time. These findings will be correlated with results from other measurements.

**M-PM-B13** MELTING OF DIPALMATOYL LECITHIN IN THE PRESENCE OF fd B-PROTEIN AS STUDIED BY LASER RAMAN SPECTROSCOPY. A. K. Dunker[1], R. W. Williams[1], B. P. Gaber[2], and W. Peticolas[2]. Biochem./Biophys. Prog., Wash. St. Univ.[1], Pullman, WA, and Dept. of Chem., U. of Ore.[2], Eugene, OR

Laser Raman spectroscopy offers the potential to monitor simultaneously the protein and lipid components of a lipid protein complex during phase transitions because both proteins and lipids exhibit conformationally sensitive peaks. Equal weights of dipalmatoyl lecithin and the B-protein from the filamentous phage fd were combined by sonication. The protein exhibited no detactable conformational change between 4° and 50°. In the presence of protein the melting temperature of the lipid was lowered by about 20° and broadened by about 15° as compared to lipid alone. At 15° the protein-associated lipids exhibit an s-trans of 0.63 which is comparable to that of vesicles of 26° and dispersions at 35°, and exhibited an s-lateral of 0.25 which falls between the s-lateral values of vesicles and dispersions at 30°C. So far as we know, such large perturbations of lipid structure by protein have not been previously reported.

**M-PM-B14** CALCIUM AND TETRACAINE INDUCE CLOSE-STACKING OF MYELIN MEMBRANES BY FLOCCULATION OF THE LIPID BILAYERS. V. Melchior,* C. Benitez,* and D.L.D. Caspar (Intr. by David J. DeRosier), Rosenstiel Basic Medical Sciences Research Center, Brandeis University, Waltham, Mass.02154

Calcium and the local anesthetic tetracaine act upon the myelin sheath of intact excised CNS and PNS nerves to induce close-packing of the membrane multilayers and extensive aggregation of membrane particles. Both reagents act in an all-or-none fashion. The critical concentration is ∿10 mM for calcium and ∿3 mM for tetracaine. Rate differences probably reflect differences in sheath permeability to the two reagents. Particle-depleted, close-packed domains have a reduced repeat period of 124-128 Å compared with the normal periods of ∿180 Å for peripheral nerve and ∿158 Å for central nerve, but their bilayer profiles determined from x-ray diffraction analysis remain very similar. Some residual external protein remains with the phase. The particle-aggregating effects of calcium and tetracaine correlate closely with their flocculating action on purified total myelin lipids suspended in PBS or normal Ringers. Membrane particle segregation appears to result from an in situ lipid "flocculation" that laterally displaces protein from the closely stacked lipid layers.

**M-PM-B15** ACTION OF PHOSPHOLIPASE $A_2$ ON GASTRIC PLASMA MEMBRANE VESICLES. G. Saccomani, H. Chang*, H.L. Spitzer, G. Sachs. Laboratory of Membrane Biology, University of Alabama in Birmingham, Birmingham, Alabama 35294

When 50% of the phospholipids are removed from $Mg^{++}$-ATPase (6.6μmoles Pi/mg/hr), $K^+$-ATPase (84.2μmoles) and $K^+$-pNPPase (58.3μmoles) containing gastric vesicles by phospholipase $A_2$ digestion in the presence of defatted BSA under isotonic conditions, $Mg^{++}$-ATPase activity increased 3 times, $K^+$-ATPase activity was inhibited by 70% and $K^+$-pNPPase was unaffected. $H^+$ transport activity was rapidly reduced by an induction of an $H^+$ leak prior to significant ATPase inhibition. Addition of PE or PC restored ∿85% and PS ∿ 66% of the $K^+$-ATPase activity, but little reconstitution of transport activity was observed. Treatment of lyophilized vesicles under the same conditions increased $Mg^{++}$-ATPase activity 1.3 times inhibited $K^+$-ATPase by 76% and $K^+$-pNPPase by 37%. PE, PC and PS restored 64, 47 and 44% of the ATPase activity respectively but did not reactivate $K^+$-pNPPase. Thus, asymmetry of the phospholipids plays a role in determining the relative activities of $Mg^{++}$, $Mg^{++}$ + $K^+$-ATPase and $K^+$-pNPPase in gastric plasma membranes as well as maintaining $H^+$ impermeability. (NIH, NSF support)

**M-PM-B16** ENVELOPED VIRUS GLYCOPROTEIN SPIKE LENGTH MEASURED IN SITU USING QUASI ELASTIC LIGHT SCATTERING AND A RESISTIVE-PULSE TECHNIQUE. B. Feuer, E. Uzgiris, R. DeBlois, D. Cluxton*, and J. Lenard. CMDNJ-Rutgers Med. Sch., Piscataway, N.J. 08854 and G.E., Schenectady, N.Y.

Vesicular Stomatitis virus (VSV) and Sindbis virus have glycoprotein spikes that extend from the lipid bilayer. Intact and protease treated spikeless virion have been measured in aqueous medium by two nondestructive techniques: laser light scattering (LLS) and Nanopar resistive-pulse (RP). Spherical Sindbis has a spike length of 70 Å ± 20 by comparison of LLS size which includes the hydrated exterior with the nonconductive volume measured by RP. This analysis agrees with a LLS Stokes diameter of 735 Å ± 40 for intact particles as compared with 625 and 595 Å for either intact or spikeless virion respectively by RP. A hydrodynamic Stokes diameter of 1425 Å ± 40 has been calculated for the bullet shaped VSV based on its diffusion coefficient. The spike length from LLS of intact and spikeless particles is 215 Å ± 20 and a radius increase of 170 Å ± 20 occurs when purified VSV glycoprotein is added to uniform polystyrene beads. These measurements show that enveloped RNA viruses have appreciably different spike lengths.

PROTEIN STRUCTURE

**M-PM-C1** MULTIPHASIC FOLDING KINETICS AND FOLDING PATTERN OF GLOBULAR PROTEINS. M. I. Kanehisa* and T. Y. Tsong, Department of Physiological Chemistry, The Johns Hopkins University School of Medicine, Baltimore, Maryland 21205

The kinetics of the protein folding and unfolding processes show the multiphasic relaxation. This is usually interpreted as the existence of stable intermediates and/or different unfolded forms, although the nature of such species is not fully understood. Regarding the fact that a protein is a relatively small system, we present a new picture of the multiphasic kinetics based on the concept of the fluctuation and the distribution of native and denatured states. The fast relaxation during unfolding can be visualized as the redistribution of the native state within its free energy valley, followed by slow passing over the free energy barrier to the denatured state. For refolding, because of the broad distribution of the denatured state and because of the movement of the barrier, apparently two denatured forms, fast and slow refolding species, are observed. This picture is also consistent with the microcalorimetric measurements. The origin of the distribution is well related to the general folding pattern where the locally ordered structures are first formed on the amino acid chain which then associate into the native form. (Supported by NSF Grant PCM 75-08690.)

**M-PM-C2** ESTIMATIONS OF INTRASEGMENT ENERGIES IN PROTEIN SECONDARY STRUCTURES. R.L. Jernigan, and S.C. Szu, Lab. of Theor., Biol., DCBD, NCI, NIH, Bethesda, MD 20014

Methods for predicting protein secondary structures are usually based on compilations of statistics derived from crystallographic studies. In principle, such conformational probabilities are averaged to remove long range effects. Here we have specifically investigated long range electrostatic interaction energies in proteins of known structure. The side chain atoms are taken to be at fixed positions relative to the backbone, as determined by their average positions in 6 proteins. Atomic charges are assigned, for ionized groups, from pK values and, for atoms in polar bonds, from small molecule dipole moments. Energies of all possible helix and ß-strand segments are calculated. We have investigated several methods of selecting the most favorable combination of these secondary conformations. This has included development of a very efficient algorithm to determine the lowest total molecular energy, based on the sum of contributing secondary structure energies. We observe significant stabilization of many secondary structures through intrasegment electrostatic interactions.

**M-PM-C3** THE PERSISTENCE OF LOCAL STRUCTURE DURING PROTEIN FOLDING. George D. Rose, University of Delaware, Department of Chemistry, Newark, Delaware 19711.

The protein conformation problem has been historically viewed as an inordinately complex thermodynamic minimization problem on a function of many variables. However, recent findings of the author show that the polypeptide chain is partitioned into separable modules by linearly local sequences of amino acids, and that this decomposition is conserved in the end product of the folding process. Thus, there exists a level of structure intermediate between individual amino acid residues and native protein monomers, and it is likely that the folding problem is much simpler than had previously been suspected.

**M-PM-C4** APPLICATION OF FLUORESCENCE SPECTROSCOPY TO THE STUDY OF PROTEINS AT INTERFACES. F.C. Maenpa* and A.G. Walton, Intr. by S.P. Rao, Department of Macromolecular Science, Case Western Reserve University, Cleveland, Ohio 44106

Fluorescence spectroscopy has been evaluated as a potential means of identifying subtle structural changes which may occur when proteins are adsorbed on surfaces. In this particular work the substrates are polypeptides which, since they are optically active and resemble proteins by other spectroscopic methods, are not easily studied by other more conventional methods. It is found that in the presence of particulate matter, the fluorescence intensity of bovine serum albumin is reduced by three separate processes. The first is the scattering and radiation absorption of the suspension, which may be easily corrected for. Adsorption of the protein on the surface causes essentially complete fluorescence quenching, however protein also accumulates in a "methoric layer" around the particles and undergoes at least partial fluorescence quenching. This fluorescence is recovered when the particles plus adsorbed layer are removed by centrifugation.

**M-PM-C5** LASER RAMAN STUDIES ON THE fd B-PROTEIN. R. W. Williams[1], A. K. Dunker[1], B. P. Gaber[2], and W. Peticolas[2] Biochem./Biophys. Prog., Wash. St. U.[1], Pullman, WA and Dept. of Chem., U. of Ore.[2], Eugene, OR

The B-protein from the filamentous phage fd has been investigated by CD. In the phage the protein exists in the a-state, which has a high α-helix content; when isolated from the phage at high concentrations, the B-protein exists in the c-state, which has a high β-sheet content (Williams and Dunker, J. Biol. Chem. 252, 6253, 1977). We have employed laser Raman spectroscopy to reinvestigate the fd B-protein in the a- and c-states, using the methods described by Lippert, et al., JACS, 98, 7075, 1977. This method gives estimates of 62% α-helix, 14% β-sheet, and 24% random coil for the protein in the a-state. The helix estimate is in good agreement with that obtained from our CD spectra. In contrast, the method of Lippert, et al. gives estimates of -63% α-helix, 145% β-sheet and 18% random coil for the protein in the c-state. The large negative value for the α-helix estimate suggests caution when applying the method of Lippert, et al. to structures with a high β-sheet content. Alternative approaches to the estimation of protein structure by Raman spectroscopy will be discussed.

**M-PM-C6** COLLAGEN FIBRIL FORMATION: EVIDENCE FOR A TEMPERATURE INDEPENDENT IRREVERSIBLE STEP. R.A. Gelman, B. R. Williams* and K.A. Piez*, National Institute of Dental Research, NIH, Bethesda, MD 20014

Fibril formation was initiated by diluting a cold acid solution of monomer, derived from rat tail tendon, with a NaCl-TES-phosphate buffer, pH 7.3, and raising the temperature; the process was monitored by turbidity. An apparent critical concentration of 0-7 μg/ml was obtained. This small value, and an apparent first-order dependence on protein concentration, suggests that assembly may not occur via a reversible nucleation-growth mechanism. This was confirmed by the finding that once the reaction is initiated by heating at 26°C for 10 min. the temperature could be decreased to 4° for up to ∿50 minutes without affecting the overall reaction $t_{1/2}$ (approximately 110 minutes). The intermediate species formed during the period at 4° was stable for several hours. Thus, there appears to be an early irreversible step, probably a conformational change, followed by a temperature-independent assembly to an intermediate aggregate. The final step is a temperature-dependent assembly of the intermediate, which is detected by turbidity measurements.

**M-PM-C7** HIGH RESOLUTION $^{13}C$ NMR STUDIES OF LABELED COLLAGEN FIBRILS. Lynn W. Jelinski*, D. A. Torchia, NIH, Bethesda, MD 20014

High power proton decoupled $^{13}C$ NMR has been used to elucidate the intermolecular interactions in collagen fibrils. Highly purified samples of native tropocollagen containing the following $^{13}C$ enriched amino acids: glycine [1-$^{13}C$], glycine [2-$^{13}C$], alanine [1-$^{13}C$], alanine [3-$^{13}C$], lysine [6-$^{13}C$], methionine [methyl-$^{13}C$], have been prepared from chick calvaria culture. Lineshapes, $T_1$ values, and nuclear Overhauser enhancements have been used to characterize the mobility of the labeled sites in solution and in reconstituted fibrils. These parameters show that the collagen helix in solution is characterized by overall correlation times of ca. $10^{-7}$ and $10^{-3}$ s, whereas the side chain moieties exhibit rapid internal motions ($\tau_i < 10^{-9}$ s). In the fibril the side chain reorientation remains rapid, suggesting that the intermolecular forces that maintain the azimuthal orientation of the molecules in the fibril are not highly cooperative. This conclusion is confirmed by the similar glycyl $C^{\alpha}$ linewidths and $T_1$ values obtained in solution and in the fibril.

**M-PM-C8** AN ELECTROSTATIC MODEL FOR COLLAGEN FIBRILS: THE INTERACTION OF RECONSTITUTED COLLAGEN FIBRILS WITH $H_2PO_4^{-1}$ AND $HPO_4^{-2}$. Shu-Tung Li* and Elton P. Katz* (SPON: B. Rubin). Department of Oral Biology and Institute of Materials Science, University of Connecticut, Farmington, Conn. 06032

Interactions between collagen and phosphate and calcium ions are the basis for a number of steps in the mineralization of bone and dentine. We report here studies of the interaction of purified, reconstituted collagen fibrils with $H_2PO_4^{-1}$ and $HPO_4^{-2}$ at neutral pH by experimental approaches and through the application of an electrostatic model proposed for hydrated collagen fibrils (Li and Katz, Biopolymers, 15, 1439(1976)). The results of these studies indicate that the interaction between collagen fibrils and phosphate ions are governed by long-range electrostatic coulombic forces with no evidence of ion-pair formation between phosphate ions and the specific side chains of collagen. These studies also indicate that within the intrafibrillar solution there is a slight shift of monovalent phosphate ions towards higher charged species. The implications of these findings with regard to the mechanism of collagen mineralization will be discussed. Supported by NIH grant DE-02953 and the Univ. of Connecticut research foundation.

**M-PM-C9** $^{13}C$ NMR STUDIES OF MOLECULAR MOTION OF AORTIC ELASTIN. W.W.Fleming, C.E.Sullivan, D.A.Torchia, NIH, Bethesda, MD 20014 -- The molecular motions of insoluble elastin have been investigated by the use of double resonance $^{13}C$ NMR on samples labeled with $^{13}C$-enriched amino acids. Purified elastin was isolated from embryonic chick aorta cultured in media containing the labeled amino acid. The narrow carbonyl linewidths in the scalar and dipolar proton-decoupled spectra of elastin enriched in Ala(1-$^{13}C$) and Val(1-$^{13}C$) show that molecular motions produce almost complete averaging of the carbonyl chemical shift anisotropy and $^1H$-$^{13}C$ dipolar interactions. However, the ability of the carbonyl carbons to cross-polarize shows that the rapid segmental motions suggested by these results do not produce an isotropic average of the dipolar interactions. The alanyl carbonyl carbon has a greater linewidth and cross-polarizes more effectively than the valyl carbonyl carbon. These observations suggest that the backbone motions of the alanyl residues are more restricted than that of the valyl residues. We therefore conclude that the lysyl-derived cross-link regions in which alanyl residues are concentrated are less mobile than the extensible regions which are rich in valyl residues.

**M-PM-C10** $^{113}Cd$ NMR AS A PROBE OF THE ACTIVE SITE OF METALLOENZYMES. I.M. Armitage,* A.J.M. Schoot Uiterkamp,* J.F. Chlebowski,* and J.E. Coleman* (Introduced by V.T. Marchesi) Yale University, New Haven, Connecticut 06510

Substitution of $^{113}Cd(II)$ for the active site Zn(II) ion(s) in a variety of metalloenzymes has provided an extremely sensitive NMR probe to the dynamics and structure of the enzyme active site. Interpretation of the $^{113}Cd$ NMR results as they relate to the mechanism of action of the various enzymes and the proposed role of the metal ion will be presented as will be models accounting for the modulation in chemical shift, relaxation and coupling.
(Supported by Grants AM 09070-13 and AM 18778-02 from the NIH and Grant PCM 76-82231 from the NSF).

**M-PM-C11** THEORETICAL INVESTIGATION OF HYPERFINE INTERACTIONS IN DEOXYCOBALTGLOBIN. S. Mishra, J.C. Chang, T.P. Das, SUNY, Albany, N. Y. 12222

Using the self-consistent charge extended Hückel procedure, we have investigated the electronic wave-functions and unpaired spin distributions in deoxycobaltglobin. Our results explain the experimental result(Yonetani,Yamamoto and Iizuko 5. Biol.Chem. 249, 2168 (1974) and Chien and Dickinson Proc. Nat. Acad. Sci. 69, 2783 (1972)) only the $^{14}N$ hyperfine interaction associated with the nitrogen atom ($N_\varepsilon$) ligand and the imidazole is observed experimentally, since the $^{14}N$ nuclei of the porphyrins and the other nitrogen of the imidazole have spin densities and order of magnitude smaller than on $^{14}N_\varepsilon$, the calculated hyperfine constant for the latter being about 55% of experiment. Possible sources for bridging the difference with experiment will be discussed. Our results for the $^{59}Co$ hyperfine interaction provide an explanation of the strongly anisotropic experimental hyperfine field in this compound in contrast to those in high spin systems. However, to explain the experimental result quantitatively, a significantly larger 4s component in the unpaired electron wave-function than we find, and that in high spin compounds, seems to be required. Grant NIH HL 15196.

**M-PM-C12** CONFORMATIONAL DEPENDENCE OF POSITRON ANNIHILATION IN BIOLOGICAL MACROMOLECULES. E. D. Handel,*‡ Y-C. Jean and H. J. Ache, Department of Chemistry, Virginia Polytechnic Institute and State University, Blacksburg, VA 24061.

The annihilation of positrons has been shown to be sensitive to certain physical parameters of biological macromolecular systems such as micelles, lipid bilayer systems and aqueous protein solutions. These studies have been extended by employing probe molecules, which show a strong interaction with the positron, within the macromolecular system under investigation. Chemical modification of tryosine residues in proteins by reaction with tetranitromethane results in a highly sensitive probe specifically localized with the protein structure. Conformational changes induced in the protein molecule result in changes in the local environment of the modified tyrosine residue. These changes are reflected in the annihilation characteristics of the positron. Conformational perturbations induced by temperature, pH and chemical environment of protein and micellar systems investigated by the positron annihilation technique will be reported.

‡ NIH Fellow (1 F32 GM06344-01).

**M-PM-C13** LIMITS ON THE WEIGHT AVERAGE TO NUMBER AVERAGE MOLECULAR WEIGHT RATIO. B. V. Bronk, Clemson University, Clemson, SC 29631

The value of the ratio $R=M_w/M_n$ is a useful parameter measuring the heterogeneity of a collection of macromolecules such as DNA since for homogeneity $R \equiv 1$ but when random breakage occurs $R \to 2$. I have proved a theorem for molecular weight distributions which can be characterized by a normalized continuous density function, f(w), which gives the relative number of molecules with molecular weight near w. The following is a special case of the theorem. Suppose e(w) is a normalized exponential function with the same mean as f(w) and f(w) "crosses" e(w) exactly twice. Then R(for f) is greater than (or less than) two if $f(w) > e(w)$ (or $f(w) < e(w)$) for large w (ie w greater than the largest crossing point). Examples are examined to show why $R < 2$ for many of the smooth functions actually encountered.

**M-PM-C14** COMPUTER METHOD FOR QUANTITATION OF PROTEINS ON TWO-DIMENSIONAL GELS. J. Bossinger*, M. J. Miller*, P. Vo*, C. Herring*, N. H. Xuong, and E. P. Geiduschek, UCSD, La Jolla, 92093.

Complex protein mixtures can be resolved by the two-dimensional gel electrophoretic and autoradiographic method developed by O'Farrell (J.B.C. 250:4007-4021 (1975). We have developed a computer method for quantitating radioactivity among the separated proteins.

The film is scanned by a high speed drum scanner which records the optical density of 200 μm by 200 μm squares. This data is analyzed in the following steps: (1) Each data point is averaged by a weighted consideration of the surrounding points. (2) The background density of the film is determined. (3) Spots are detected, by searching for density contours at a selected threshold value. (4) The total radioactivity of each spot is calculated including the area surrounding the spot and correcting for local background variations. (5) Incompletely resolved spots can be split.

The results of two different gels can be compared by matching by hand at least 3 spots on both gels. The coordinates of one film are then transformed to match those of the second film. The positions of other spots can then be matched automatically by computer.

## NERVES AND AXONS I

**M-PM-D1** SODIUM PERMEABILITY OF NERVE MEMBRANE. D. Landowne and V. Scruggs, Univ. of Miami, Fla. 33152

With standard techniques of voltage clamping and internal perfusion of squid axons we find the early peak current at 0 mV is proportional to the difference in sodium concentrations of the two sides. This permeability, P, is about 0.01 mA $mM^{-1}cm^{-2}$ or $10^{-4}$ cm/sec. For positive potentials the current is proportional to V and this conductance, $g = aNa_o + bNa_i$. a and b are 1 and $2.8 \times 10^{-4} \Omega^{-1} mM^{-1} cm^{-2}$ or 1 and $2.9 \times 10^{-6}$ cm/mV sec. Thus, defining $c_m = (aNa_o + bNa_i)/(a+b)$ and noting that $P/(a+b) = kT/e$, the sodium current for positive potentials is well described by

$$I = p(-\Delta Na + c_m eV/kT).$$

For negative potentials a gating factor is needed. The assymmetry, a/b, is about what would be predicted from the known assymmetry of surface charges at the two membrane:aqueous interfaces.

If all the area is available for sodium fluxes these findings suggest a high concentration and low mobility of sodium in the membrane or about 1 ion/phospholipid crossing the membrane in 1 msec.

**M-PM-D2** FRACTION OF SODIUM CHANNELS OPEN AT PEAK CONDUCTANCE. F. J. Sigworth* (intr. by C. F. Stevens), Department of Physiology, Yale School of Medicine, New Haven Connecticut 06510

To relate toxin binding data to electrophysiological measurements the fraction ($p_o$) of the Na channels open at the time of maximum conductance has in the past been calculated from theories of channel gating. I report an experimental estimate of $p_o$ based on the calculation of the variance among members of an ensemble of current records (Nature 270 p.265), with the assumption of a homogeneous population of independently gated channels having one nonzero conductance level. Rana pipiens nodes of Ranvier were voltage clamped at 3° with internal $Cs^+$ and external $TEA^+$ to block K current. From a holding potential of -75 mV depolarizations to -5 mV were preceded by 30 ms prepulses to -105 mV; the resulting current records were filtered at 5 kHz. Under these conditions $p_o$=0.49 ±.04 (SEM; n=5). This value is similar to the value 0.62 predicted by the Hodgkin-Huxley formalism using Hille's (Biophys Physiol Excit Mbns, W. Adelman ed., 1971, p.242) rate constants scaled to 3°, and is also consistent with other theories of gating.

**M-PM-D3** SODIUM TAIL CURRENTS IN MYXICOLA. L. Goldman, and R. Hahin*, Dept. of Physiology, School of Medicine, Univ. of Maryland, Baltimore, Maryland 21201.

The time course of the decay of the $I_{Na}$ on resetting the membrane potential to various levels, ranging from -10 to -130 mV, following test steps in potential was studied. The effects of different prepulse amplitudes and durations on these Na tail currents were also studied. For post pulse potentials of -35 mV and below, these currents may be attributed nearly entirely to the shut down of the activation process, inactivation being little involved. Three distinct relaxations may be detected in the tail currents. The slower two are well defined exponentials with time constants of about 1 msec and 100 μsec in the hyperpolarizing potential range. The fastest relaxation is only poorly resolved, but has a time constant in the vicinity of 30 to 35 μsec. Different initial conditions could alter the relative weighting factors on the various exponential terms, but did not affect any of the individual time constants. The activation of the sodium conductance cannot be attributed to any number of independent and identical two-state subunits with first order transitions. (Supported by USPHS Grant NS-07734).

**M-PM-D4** SELECTIVE BLOCK OF OFF GATING CURRENT. C.M. Armstrong and J.Z. Yeh. Univ. Pennsylvania, Philadelphia, Pa. and Northwestern University, Chicago, Ill.

The quaternary ammonium compound pancuronium (PC) is known from $I_{Na}$ studies to block activated Na pores, and to prevent closing of the activation and inactivation gates of blocked pores. We studied the effect of 1mM PC on gating current in squid axons perfused with Cs and bathed in Na free medium +TTX. To further simplify, inactivation was destroyed by pronase. ON gating current is unchanged by PC. The fast component of OFF gating current is eliminated when most pores are blocked by PC. PC seems to prop open activation gates and immobilize gating charge till PC leaves the pores. In the presence of TTX PC apparently leaves the pores slowly. Results in axons with intact inactivation are similar. The fast, inactivation resistant component of OFF gating current is eliminated by PC, which shows this component is associated with Na pores and may result from a process that closes them so they do not conduct during recovery from inactivation. In contrast $I_{Na}$ is easily measurable during recovery from PC block, because PC prevents this closing process, as is evident from its effect on OFF gating current.

**M-PM-D5** REMOVAL OF TTX SENSITIVITY IN MUSCLE FIBERS BY TRIMETHYLOXONIUM ION: TWO ACID GROUPS AT THE SODIUM CHANNEL. B. C. Spalding, Dept. of Physiology and Biophysics, University of Washington, Seattle, Washington 98195

Voltage clamped frog skeletal muscle fibers treated with 50 mM $(CH_3)_3O^+$ (TMO), a carboxyl modifying reagent, show a population of sodium channels insensitive to TTX and STX (only 46±3% block by 1 μM TTX, 34±5% block by 100 nM STX). Total Na current is also reduced by 66±3%. TMO treatment in the presence of TTX produces no TTX resistance, suggesting competition for a common site. TMO-modified channels can be blocked by 0.5 mM lidocaine, and have normal ionic selectivity (Na substitutes with mV reduction in reversal potential, control in parentheses): hydroxylammonium, 27±8(25±12); ammonium, 38±7(48±1); guanidinium, 47±2(41±4); aminoguanidinium, 74±7(72±4); methyl- and tetramethylammonium remain impermeant. Low pH continues to block modified channels, however pH 5.0 produces 54±2% block at +38 mV in modified channels compared with control block of 68±1%, suggesting the $pK_a$ of a titratable group has been lowered. The TMO-modifiable acid group at the TTX receptor is evidently near but not identical to an acid group at the selectivity filter. (Supported by USPHS grants NS 08174, GM 00260, GM 07270)

**M-PM-D6** ENHANCEMENT OF SODIUM CHANNEL INACTIVATION BY OCTANOL AND DECANOL. R.P. Swenson*, G.S. Oxford and T. Narahashi. Dept. of Physiology & Pharmacology, Duke Univ. Medical Center, Durham, NC 27710 and Dept. of Physiology University of North Carolina, Chapel Hill, NC 27514.

The anesthetic effects of octanol and decanol were examined in intact crayfish axons and perfused squid axons under voltage clamp. Previous work (Armstrong and Binstock, J. Gen. Physiol. 48:265, 1964) revealed that a series of alcohols suppressed both $I_{Na}$ and $I_K$. Similarly, we found that either alcohol (1mM) reversibly decreased peak $g_{Na}$ by ∿44%. Octanol reversibly shifted the steady-state Na inactivation curve ∿5 mv in the hyperpolarizing direction, while decanol produced only marginal effects. At 1mM neither alcohol exhibited a consistent effect on Na activation. In squid axons perfused with 275mN CsF both alcohols eliminated the residual steady-state $I_{Na}$ at the end of depolarizing steps, but had much less effect on peak $I_{Na}$. The ratio $(\Delta I_{ss}/\Delta I_{peak})$ = 5.48. Following removal of inactivation by pronase perfusion $\Delta I_{ss}/\Delta I_{peak}$ declined to 1.09, suggesting that this effect is not an 'ionic' block as seen with pancuronium (Yeh and Narahashi, J. Gen. Physiol. 69:293, 1977). Rather the alcohols seem to enhance the ability of Na channel inactivation gates to close. (Supported by A.E. Sloan Fnd. and NIH NS14144).

**M-PM-D7** PHENYTOIN DEPRESSES SODIUM CURRENTS IN FROG SKELETAL MUSCLE. T. M. Dwyer, Dept. of Physiology and Biophysics, U. of Washington, Seattle, Wa. 98195.

Phenytoin (20-200 μM) depresses $I_{Na}$ in voltage clamped frog skeletal muscle by >50% without affecting time to peak or half time of decay. At a holding potential of -90 mV, the inactivation curve is shifted in the hyperpolarizing direction and is less steeply voltage dependent. Depression is completely relieved by a long hyperpolarizing prepulse and the inactivation curve returns to normal. Depression is enhanced (to >99%) by a conditioning depolarization and continues to increase even as pulses are lengthened beyond 8 msec, suggesting that phenytoin can block both open and inactivated channels. Long depolarizing pulses repeated at low frequency produce greater depression than short pulses at high frequency (same average membrane potential) although steady-state depression is reached more slowly. The rate of recovery at -170 mV (0.69-0.82 $sec^{-1}$) is twice that at -138 mV. The rate of onset at -10 mV (0.18-0.81 $sec^{-1}$) is twice that at -42 mV. Pentobarbital at higher concentrations (0.2-2 mM) has similar actions. Both compounds have pharmacological actions and chemical structures similar to N-ethylmaleimide. (Grants # NS08174 and NS05082.)

**M-PM-D8** ACONITINE ALTERS SELECTIVITY AND KINETICS OF FROG MUSCLE SODIUM CHANNELS. D.T. Campbell, Department of Physiology, Yale Medical School, New Haven, CT 06510.

Sodium currents in frog muscle are studied under voltage clamp conditions. After treatment with 0.15 mM aconitine the following observations are made:

1) inward sodium channel currents are measured when all external sodium is replaced by the normally impermeant ions $Cs^+$ or methylammonium

2) relative sodium channel permeabilities to $Li^+$, $K^+$ and $NH_4^+$ are increased three to four fold

3) the voltage threshold for turning on sodium currents is shifted 40-50 mV in the hyperpolarized direction

4) the peak current-voltage relation has two peaks in $Na^+$ and $Li^+$ solutions, one in $K^+$, $Cs^+$ and $NH_4^+$ solutions.

The results are consistent with the idea that aconitine treatment leaves two populations of sodium channels: one with both selectivity and kinetics dramatically altered, the other with possibly altered selectivity and almost normal kinetics. These results are similar to results in frog nerve (Mozhayeva,et al. 1977. BBA 466: 461-473) except that the kinetically altered nerve channels no longer inactivate whereas the muscle channels do.

(Supported by PHS grants NS07474 and NS05747.)

**M-PM-D9** BLOCKAGE OF RESTING SODIUM CHANNELS BY 5,5-DIPHENYLHYDANTOIN. Paul De Weer, J. Gavin Perry and Leslie McKinney. Washington University School of Medicine, St. Louis, MO 63110.

The anti-epileptic 5,5-diphenylhydantoin (DPH) has been claimed to stimulate the sodium pump or to interfere with its inhibition by digitalis. We have tested this hypothesis on the squid giant axon, and found no evidence for it. It has been shown that DPH blocks the early conductance of voltage-clamped squid axon (Lipicky et al., P.N.A.S. 69: 1758; 1972). We have tested whether DPH blocks resting sodium channels, as well as those opened by veratridine. DPH and tetrodotoxin (TTX) reversibly hyperpolarize squid giant axon, even in the presence of ouabain, but not in the absence of external sodium. DPH does not affect potassium permeability. Membrane depolarization caused by veratridine is reversed by TTX as well as by DPH. In addition, the extra passive sodium influx into frog sartorius muscle, following veratridine, is inhibited by both TTX and DPH. A number of the drug's effects can be ascribed to blockage of sodium channels, e.g.: reduced cell excitability; inhibition of endocrine secretions; and reversal of digitalis poisoning.

**M-PM-D10** SODIUM INACTIVATION MODULATES LOCAL ANESTHETIC BLOCK OF SODIUM CHANNELS IN SQUID AXONS. J. Z. Yeh and C. H. Wu, Northwestern University, Chicago, IL 60611.

The dynamics of blocking action of Na channels by benzocaine, procaine, QX-314, QX-572, and 9-aminoacridine (9-AA) was studied in voltage-clamped squid axons. These drugs were applied internally at the concentration of 0.1 to 1 mM to axons with or without intact Na inactivation. Na inactivation gate was destroyed by using pronase, N-bromoacetamide, or deoxycholate. In axons with intact Na inactivation, all compounds except benzocaine exhibited frequency- and voltage-dependent inhibition of Na current. Upon removal of Na inactivation these characteristics of block were affected to variable degrees depending on the drugs applied. The frequency dependence was lost or became dramatically diminished with procaine, QX-314, and 9-AA, but was retained with QX-572. The voltage dependence disappeared or was altered with procaine, QX-314, and QX-572, but remained intact with 9-AA. The blocking action of benzocaine was not changed by removal of Na inactivation. These results support the notion that Na inactivation modulates the blocking action on the channels by local anesthetics. Supported by NIH grant NS 14144.

**M-PM-D11** REMOVAL OF SODIUM INACTIVATION BY HIGH pH AND TYROSINE SPECIFIC REAGENTS, Brodwick, M. S., and Eaton, D. C., Dept. of Physiology and Biophysics, University of Texas Medical Branch, Galveston, Tx. 77550.

Internal alkalinzation causes 1) a reversible decrease in the steady state inactivation 2) a reversible decrease in maximum inward current $\bar{g}Na$, and 3) a reversible increase in leakage conductance in squid axon. Reversibility was less successful for pH above 10.2. The effects on $\bar{g}Na$ precede the effects on inactivation. The pK for the inactivation effects lies between 9.7 and 10.2 and thus approximately coincides with the pK of the phenolic OH of tyrosine. Similar effects were observed following treatment with tetranitromethane or iodination with lactoperoxidase. These latter reagents react preferentially with the phenolic group of tyrosine. We conclude that an intact tyrosine residue is essential for the proper function of sodium inactivation and may act to stabilize the charged plug in the model as suggested by Rudy and Rojas (J. Physiol. 262, 501-531, 1976) and Armstrong and Bezanilla, J. Gen. Physiol. 70: 567-590, 1977).

Supported by NIH grant NS-11963.

**M-PM-D12** EFFECT OF PROTEIN CROSS-LINKING REAGENTS ON MEMBRANE CURRENTS OF SQUID AXON. R. Horn, M. S. Brodwick and D. C. Eaton, Dept. Physiology & Biophysics, Univ. of Texas Medical Branch, Galveston, Texas 77550.

Protein cross-linking reagents prolong action potentials in crayfish nerve (J. Cell. Physiol. 74:77, 1969; ibid 74:91). We have studied the actions of glutaraldehyde (GLU), formaldehyde and tannic acid on Na and K currents in internally-perfused and voltage-clamped squid axon. All 3 reagents (1) reduced the peak inward Na current, (2) partially or completely abolished Na inactivation and (3) reduced K currents. These effects were irreversible and accompanied by a negligible effect on leakage. GLU was effective when applied on either side of the membrane. After treatment with GLU, the K current did not behave according to the 4th power kinetics described by Hodgkin & Huxley. 40 ms after a depolarizing voltage step the magnitude of K current continued to increase with time instead of saturating at a constant value. GLU apparently decreases the rate of the movement of K gating molecules in response to a depolarized step of membrane potential. This effect may be due to (1) changes in the charge density on the gating molecules and/or (2) a restriction in the mobility of the K gating molecules.

**M-PM-D13** MODIFICATION OF SLOW SODIUM INACTIVATION IN BRAYFISH AXONS BY PROTEOLYTIC ENZYMES. J.G. Starkus and P. Shrager, Dept. of Physiology, Univ. of Rochester Medical Center, Rochester, N.Y. 14642.

Internally perfused crayfish giant axons held at low membrane potentials exhibit an inactivation of sodium channels that has slow kinetics. Sodium conductance can be increased by hyperpolarization or decreased by further depolarization, with time constants on the order of 150 msec to 7 sec. Internal perfusion with low concentrations (.02 mg/ml) of trypsin irreversibly shifts steady state slow inactivation in a depolarizing direction, removing all slow inactivation at the resting potential. Sodium currents are otherwise normal Heating the enzyme to 100° C for 10 min., or addition of soybean trypsin inhibitor, eliminates the effect. N-ethylmaleimide(NEM), a sulfhydryl blocking reagent has been shown to (1) induce slow inactivation, an effect opposite to that of trypsin, (2) modify fast inactivation and (3) block a fraction of the sodium conductance. If a fiber has been previously treated internally with trypsin, NEM has only effects (2) and (3) above. Slow inactivation remains absent. On the other hand, if an axon is exposed first to NEM, trypsin remains capable of removing slow inactivation. Supported by grants 5-RO1-NS10500 and 5-KO4-NS00133 from NIH.

**M-PM-D14** UV IRRADIATION MODIFIES SAXITOXIN BINDING SITES
J. Weigele* and R. Barchi, U. of P. Phila., PA 19104.

$^3$H-STX binds to a single class of high affinity sites on rat synaptosomes. The $K_d$ is 2nM with 2-4 pmoles of ligand maximally bound per mg protein. Using a rapid filtration method validated by correlation with parallel equilibrium dialysis measurements, we find that these binding sites are sensitive to UV light. During irradiation, sites irreversibly disappear with 1st order kinetics. The $T_{1/2}$ is 5 min with 3μwatts/mm$^2$ 280 nm irradiation incident on a 1cm path-length cuvette. The $K_d$ of the remaining sites is unaltered. The $T_{1/2}$ is temperature independent, with a $Q_{10}$ of 1.0 from 5°C to 30°C. The action spectrum has a peak with maximum sensitivity near 280 nm. Presence of STX during irradiation has little or no effect on the deletion rate. $^{22}Na^+$ loaded synaptosomes have an efflux rate enhanced by 0.1 mM veratridine. The veratridine effect is blocked by $10^{-6}$M TTX. Preliminary experiments show a qualitative correlation between the UV deletion of $^3$H-STX binding sites and loss of veratridine stimulated, TTX inhibited $^{22}Na^+$ flux. We suggest that a major event in the deleterious effect of UV light on nerve excitability involves modification of the Na channel ion selectivity filter.

**M-PM-D15** INHIBITION AND ENHANCEMENT OF PHOTOCHEMICAL MODIFICATION OF LOBSTER AXON MEMBRANES SENSITIZED BY DYES OR OPTICAL PROBES.
D.P. Valenzeno and J.P. Pooler Emory University, Atlanta, Georgia

Sodium channels in lobster axons were photochemically modified by illumination for several seconds after treatment for several minutes with 5 μM Eosin Y or 1 μM merocyanine 540 (M540). Modification was inhibited >90% or enhanced >30% by various functional group reagents or agents which interact with singlet molecular oxygen ($^1O_2$). For most agents little or no pharmacological effects were seen in this time span. The best inhibitors (TNBS,NEM) are those expected to react preferentially with SH groups or which quench $^1O_2$(azide). The best enhancer was a $D_2O$ solvent which increases $^1O_2$ lifetime. TNBS inhibition developed rapidly (<30s) with a half maximal effect at 0.5 μM, but decayed slowly (75% inhibition after 4 min rinse) implying TNBS binding. $K^+$ channel modification was also inhibited by TNBS. TNBS (5mM) inhibited >90% of the modification induced by the potential sensitive optical probe M540. These results implicate the involvement of SH, or possibly $NH_2$, groups in photochemical modification, probably via $^1O_2$ as an intermediate. They further suggest that the damage associated with the use of optical probes can be substantially reduced by protective agents.

**M-PM-D16** EFFECTS OF LASER IRRADIATION ON THE ELECTRICAL ACTIVITY OF UNSTAINED NEURONS IN TISSUE CULTURE.
J.E. Olson*, W. Schimmerling and C.A. Tobias, Berkeley, Calif.

Focused laser radiation was used to produce functional changes in neurons from neonatal rat cerebellum in tissue culture. The observed endpoints were the mean firing rate obtained from time interval distributions of spontaneous activity and the threshold for stimulation with an extracellular current pulse. Pulses of laser light in the range 425-700 nm were focused to ≈ 4 μm upon an area of cytoplasm. The irradiation resulted in a sharp decrease of the mean firing rate and a concurrent increase of the stimulation threshold as a function of laser energy. The effect depends on the cell polarization; laser pulses coincident with an action potential (AP) did not show a statistically significant dependence upon laser energy, whereas a sharp threshold was seen with pulses delayed by 6 msec. with respect to an AP. The threshold energy was fould to be wavelength dependent. Possible interpretations in terms of cellular mechanisms will be discussed.

**M-PM-D17** FURTHER EXPERIMENTS ON THE INCORPORATION OF THE SODIUM CHANNEL OF LOBSTER NERVE INTO SOYBEAN LIPOSOMES.
R. Villegas, G.M. Villegas*, and F.V. Barnola*. Centro de Biofísica y Bioquímica, IVIC, Caracas 101, Venezuela.

Recovery of the response to veratridine, grayanotoxin and tetrodotoxin of lobster nerve membrane vesicles stored frozen in sucrose solution was observed after reconstitution by the freeze-thaw-sonication procedure. For reconstitution, frozen membrane (0.5-1.0 mg protein/ml) and liposomes (20-40 mg of soybean phospholipids or a mixture of purified phospholipids) in a phosphate solution (150 mM NaPi, 150 mM KPi, pH 7.5) were used. The recovery was interpreted as due to the incorporation of Na channels in to the liposomes. To obtain further evidence, the relationship between drug response and the protein incorporated into the liposomes was measured. When 40 mg/ml of soybean phospholipids were used for reconstitution, the amount of membrane protein remaining on top of a 12% sucrose solution, after 1 h centrifugation at 76400 x g, was about 50% and the Na channel function was recovered. When only membrane treated by the freeze-thaw-sonication procedure was used, just 15% of the protein remained on top of the sucrose solution and no Na channel function was observed. (CONICIT, Grant No. 31-26.S1-0702).

## MUSCLE PROTEINS II

**M-PM-E1** ROTATIONAL MOTION OF MUSCLE CROSSBRIDGES DURING CONTRACTION IN SPIN-LABELED MYOFIBRILS.
David D. Thomas#, John C. Seidel, and John Gergely, Department of Muscle Research, Boston Biomedical Research Institute, Department of Neurology, Massachusetts General Hospital; and Departments of Neurology and Biological Chemistry, Harvard Medical School. #Present address: Department of Structural Biology, Stanford Medical School, Stanford, CA 94305.

Most current models of the molecular mechanism of muscle contraction propose that force is generated by the ATP-driven rotation of crossbridges (containing the head, or S-1, region of myosin) connecting thick and thin filaments. In order to test this proposal, we have selectively spin-labeled crossbridges in intact, calcium sensitive myofibrils, and performed saturation transfer EPR experiments to detect rotational motion of the crossbridges. In the absence of ATP (rigor), the crossbridges are immobile on the millisecond time scale, but during ATP hydrolysis the spectra indicate rotational motion in the submillisecond time range, both in the presence of 0.1 mM $CaCl_2$ (contraction) and in the presence of 1mM EGTA (relaxation). We have not yet determined (a) the angular range of this rotation, nor (b) the fraction of crossbridges that are attached to actin during ATP hydrolysis.

**M-PM-E2** PHOSPHORYLATION OF MYOSIN LIGHT CHAIN DURING THE CONTRACTION-RELAXATION CYCLE OF FROG MUSCLE. M. Bárány, K. Bárány, J.M. Gillis*, and M.J. Kushmerick, Univ. Ill. Med. Ctr., Chicago, 60612, Univ. Cath., Louvain, Belgium and Harvard Med. Sch., Boston, 02115.

Phosphorylation of the 18,000-dalton light chain of myosin during a single tetanus of frog and rabbit muscle were reported (K. Bárány and M. Bárány, JBCh. 252, 4752, 1977; J.T. Stull and C.W. High, BBRC 77, 1078, 1977). We have found that the phosphorylation was nearly maximal in frog muscles which were frozen in the ascending phase of tetanus as compared to that in muscles frozen during tetanus. Furthermore, the phosphorylation was also complete in semitendinosus muscles which were stimulated at 140% rest length and did not produce tension. These data indicate that stimulation and not contraction per se is necessary for the light chain phosphorylation. Dephosphorylation of the light chain did not correlate with the relaxation of muscle from tetanus. In vitro experiments with frog myofibrils showed a dephosphorylation of myosin light chain in the presence of millimolar concentrations of EGTA. It appears that in vivo the $Ca^{2+}$ has to be reaccumulated by the SR before dephosphorylation of the light chain. (Supported by NS-12172 from NIH and MDA).

**M-PM-E3** INTERACTION BETWEEN TROPONIN-INHIBITORY SUBUNIT (Tn-I) AND TROPOMYOSIN-BINDING SUBUNIT (Tn-T). J. Horwitz, B. Bullard*, and D.A. Mercola, Jules Stein Eye Institute, UCLA School of Medicine, Los Angeles CA 90024, and Department of Zoology, Oxford, England OX1 3PS.

It is known that Tn-C, the calcium-binding subunit of troponin, interacts with Tn-T and Tn-I. However, direct binding of Tn-I to Tn-T has been excluded. We have followed the interaction between Tn-T and Tn-I by monitoring the near UV circular dichroism (CD) spectra of these subunits and by gel filtration chromatography on Sephacryl S-200. Tn-I exhibits a weak, negative-sloping, structureless CD band between 300 and 260 nm. Tn-I exhibits two positive bands, one at 290 nm and the other at 263 nm. Upon addition of Tn-I to Tn-T, the CD spectrum changes drastically, giving rise to a single, relatively strong, negative CD band centered around 280 nm. This new CD band is most intense when the ratio of Tn-T to Tn-I is 1:1. Gel chromatography of the Tn-T—Tn-I mixture shows that a stable complex has been formed. Addition of Tn-C to the Tn-T—Tn-I complex results in a CD spectrum indistinguishable from that of native troponin. The reconstituted troponin possesses all the physicochemical properties of native troponin.

Supported in part by NIH grants EY331, EY1622, and EY 58.

**M-PM-E4** TENSION DEVELOPMENT IN RABBIT ILEUM SMOOTH MUSCLE SKINNED BY STAPHYLOCOCCAL α-TOXIN: ACTIVATION BY $Ca^{2+}$ AND $Sr^{2+}$, IRREVERSIBLE ACTIVATION IN PRESENCE OF ATPγS. P. Cassidy, P.E. Hoar, W.G.L. Kerrick, Dept. of Physiology & Biophysics, Univ. of Wash., Seattle, WA 98195

Rabbit ileum smooth muscle strips may be functionally skinned by exposure to a bacterial exotoxin, staphylococcal α-toxin. After skinning, the preparation can repeatedly undergo $Ca^{2+}$-dependent tension development and relaxation in the presence of ATP. The finding that $Ca^{2+}$ and $Sr^{2+}$ activate tension identically with increasing concentrations of divalent cation in skinned ileum smooth muscle is similar to previous results with rabbit slow twitch skeletal and cardiac fibers but not fast twitch muscle fibers. The ATP analog, ATPγS, induces a $Ca^{2+}$-dependent but irreversible tension development in skinned rabbit ileum. ATPγS does not support tension development in fast twitch fibers, but does support reversible Ca-dependent tension development in slow twitch skeletal and cardiac muscle fibers. These results will be discussed in relation to the possible role of myosin light chain kinase and phosphatase in the $Ca^{2+}$-dependent control of smooth muscle contraction. (Supported by PHS HL 07090, Muscular Dystrophy Assn., American Heart Assn.)

**M-PM-E5** RELATIONSHIP BETWEEN $Ca^{2+}$ ACTIVATION AND PHOSPHORYLATION OF THE 18,000 DALTON MYOSIN LIGHT CHAIN IN SKINNED SKELETAL AND SMOOTH MUSCLE FIBERS. P.E. Hoar, P.S. Cassidy, W.G.L. Kerrick, Dept. Physiology & Biophysics, University of Washington, Seattle, WA 98195

Comparisons were made between the $Ca^{2+}$ and $Sr^{2+}$ activated tension and the degree of endogenous phosphorylation in skinned fibers from both rabbit skeletal muscle and chicken gizzard. The only significant change in pattern of protein phosphorylation observed with varying $Ca^{2+}$ or $Sr^{2+}$ concentration in either muscle type occurred in the 18,000-19,000 dalton myosin light chain. Incorporation of phosphate into the myosin light chains in skinned fibers occurs over the same $Ca^{2+}$ and $Sr^{2+}$ concentration ranges as those required for activation of tension. $Ca^{2+}$ and $Sr^{2+}$ activation of rabbit skeletal muscle light chain kinase correlated well with the activation of rabbit fast twitch, but not slow twitch fibers. It is concluded that phosphorylation of myosin light chains may be a necessary requirement for the $Ca^{2+}$ activation of both skeletal and smooth muscle. (Supported by PHS HL 05527 and HL 07090, The Muscular Dystrophy Association and The American Heart Association.)

**M-PM-E6** THE PROTEOLYSIS OF α-PARAMYOSIN DURING EXTRACTION FROM MERCENARIA MERCENARIA. B. D. Gaylinn, W. H. Johnson. Biology Department, Rensselaer Polytechnic Institute, Troy, N.Y. 12181.

It has been reported by Stafford and Yphantis (Biochem. Biophys. Res. Comm. 49: 848, 1972) that paramyosin isolated from the adductor muscles of Mercenaria mercenaria could contain three distinct forms designated α, β, and γ. The β and γ paramyosins appeared to be degradation products while α paramyosin was thought to be the native form. We have evidence that this degradation is due to the action of bacteria carried over into the extraction step of the isolation procedure. This proteolysis can be slowed by the use of antibiotics or completely prevented with the reducing agent 0.5 mM dithiothreitol as well as with 0.01 M EDTA or by extraction under acid conditions. As the native protein is thought to be in the reduced state, dithiothreitol can serve a dual purpose in the extraction step, thus avoiding the loss in yield caused by EDTA. We have isolated several strains of bacteria from washed minced muscle brie and believe that these organisms, identified as Vibrio and Pseudomonas types exist within the adductor muscle tissue.

**M-PM-E7** KINETICS OF MYOSIN FLUORESCENCE CHANGES. K.A. Johnson*, K.M. Trybus*, and E. W. Taylor, University of Chicago, Chicago, Illinois 60637

The kinetics of the increase in protein fluorescence on the binding of ATP to subfragment-1 (SF-1) have been reinvestigated. The concentration dependence of the rate deviated from a hyperbola and at high ATP a third of the signal amplitude was lost. At 5° the fluorescence transient was biphasic. These results indicate that the fluorescence change occurs in two steps. Analysis by chemical-quench flow methods indicated that the first increase (12%) was correlated with the tight binding of ATP and the second increase (24%) occurred at the same rate as ATP hydrolysis. These results are consistent with the Bagshaw-Trentham mechanism: $M+ATP \overset{1}{\rightleftharpoons} MATP \overset{2}{\rightarrow} MATP^* \overset{3}{\rightleftharpoons} MPr^{**}$ with the important difference that the maximum rate measures the hydrolysis step ($k_2 > 1000\ s^{-1}$, $k_3 = 125\ s^{-1}$ at 20°, pH 7, 0.1 M KCl). Also, there is a 10-12% fluorescence enhancement upon the association of SF-1 with actin. Acto SF-1 dissociates to form MATP* with no net change in fluorescence emission. Biphasic signals and loss of signal amplitude suggest that ADP binding may also be a three step reaction. (Supported by NIH HL 20592 and Muscular Dystrophy Association.)

**M-PM-E8** EVIDENCE FOR PROTON RELEASE IN THE RATE-LIMITING STEP OF THE MYOSIN ATPASE. J.Kevin Culley and Paul Dreizen State Univ. New York Downstate Med. Ctr.,Brooklyn, N.Y.

Effects of pressure on myosin ATPase provide information on the activation volume, $\Delta V^{\ddagger}$, for rate-limiting step(s) of steady-state ATP hydrolysis. At 25°C, pH 7.8, 0.5 M KCl, myosin ATPase has $\Delta V^{\ddagger}$ of -33 cc/mol for both $Ca^{++}$ and $Mg^{++}$ activation. The rate-limiting step involves isomerization of $M^{**}$. ADP·$P_i$, but there is ambiguity whether release of $P_i$ and/or $H^+$ follows or occurs with isomerization. It is uncertain whether $\Delta V^{\ddagger}$ refers to conformational changes and/or product release. We have explored this question by study of pressure effects on myosin ATPase at pH 6.4 to pH 8.0. The data indicate $\Delta V^{\ddagger}$ of -20 cc/mol at pH 6.9. The difference of -13 cc/mol between pH 6.9 and pH 8.0 would indicate participation of $H^+$ release in a rate limiting step. The simplest explanation is that $H^+$ release leads to a $\Delta V^{\ddagger}$ of -15 cc/mol when $P_i$ is ionized at pH 7.8,but this volume component is absent at pH at or below the $P_i$ pK. A more complex pattern is obtained at pH 8 at 5°C, where several rate-constants are known to be slow, and pressure effects suggest a large positive $\Delta V^{\ddagger}$ due to isomerization of M*.ADP. The pH dependence of $\Delta V^{\ddagger}$ at 5°C appears to be consistent with this interpretation.

**M-PM-E9** REVERSIBLE DISSOCIATION OF BOTH REGULATORY LIGHT CHAINS FROM SCALLOP. P. D. Chantler* and A. G. Szent-Györgyi. Department of Biology, Brandeis University, Waltham, Massachusetts 02154.

EDTA treatment at 0° removes 1 mole regulatory light chain per myosin molecule from myofibrils. (Szent-Gyorgyi A. G. et. al. (1973) J. M. B. 74, 179-203). At 30° a similar treatment removes both regulatory light chains completely from Placopecten magellanicus (>90%) and extensively (>75%) from Aequipecten irradians. Myofibrils free of regulatory light chains fully retain their $K^+$-EDTA and $Ca^{++}$-activated ATPase (10mM $CaCl_2$). Their actin activated ATPase has no calcium sensitivity and the activity in the presence of 0.1 mM $CaCl_2$ is reduced by about 60%. Regulatory light chains readily rebind in stoichiometric amounts and restore the actin activated ATPase and the calcium sensitivity. Calcium binding is proportional to light chain content. Regulatory light chains of Mercenaria mercenaria, Spisula solidissima and Loligo paelei can fully substitute for scallop light chains.

This work was supported by a British-American Heart Association Exchange Fellowship and by grants from Public Health Service (AM-15963) and the Muscular Dystrophy Association.

**M-PM-E10** ENZYMATIC AND NON-ENZYMATIC FRAGMENTATION OF CANINE CARDIAC MYOSIN IN SDS SOLUTIONS. R.F.Siemankowski and P.Dreizen. State Univ. of New York, Downstate Medical Center, Brooklyn, New York.

Canine cardiac myosin undergoes fragmentation of heavy chains (HC) to intermediates of 70,000-180,000 mol.wt.in the presence of 1% SDS. For example, after 18 h at 22°C, 15% of HC from normal hearts and 30% of HC from hypertrophied hearts (aortic banding) are degraded. HC degradation is stochastic, with 1st order rate constants of $1.7 \times 10^{-2} s^{-1}$ at 96°C, and $1.7 \times 10^{-4} s^{-1}$ at 22°C. Prior treatment at 96°C does not affect kinetics of degradation during subsequent incubation at 22°C. Proteolysis in the presence of SDS at 96°C would appear to be non-enzymatic in origin. However, there is evidence that contaminant protease(s) may contribute to proteolysis at 22°C, since rate of HC degradation is augmented on addition of crude myofibrils to purified myosin, as isolated from Triton-washed extracts. The seeding experiments indicate different proteolytic rates in myosin preparations from normal and hypertrophic hearts, suggesting possible differences in HC as isolated from these tissues. The light chains are resistant to proteolytic degradation under all above conditions, implying some specificity towards HC.

**M-PM-E11** DISTRIBUTION OF MYOSIN ISOENZYMES IN CHICKEN PECTORALIS MUSCLE. L. Silberstein* and S. Lowey, Rosenstiel Center, Brandeis University, Waltham, MA 02154.

Vertebrate skeletal muscle myosin contains two types of alkali light chains (A1 and A2) that differ only in their N-terminal sequences. Antisera against both light chains have been extensively adsorbed to eliminate cross-reacting antibodies. Immunoadsorbents prepared by coupling antibodies specific for A1 (anti-Δ1) or for A2 (anti-Δ2) to Sepharose are capable of fractionating myosin into two equal populations of light chain isoenzymes. These results confirm the earlier observation that myosin consists largely of homodimers (Holt and Lowey, *Biochemistry*, 1977, 16:4398). Myofibrils were prepared from chicken breast muscle and reacted with fluorescein-coupled anti-Δ1 or anti-Δ2. All fibrils showed bright fluorescence with either antibody preparation. Electron microscopy of negatively stained native filaments that had been reacted with either rabbit anti-Δ1 or anti-Δ2, followed by goat anti-rabbit IgG, showed that all myosin filaments contain both light chains. In conclusion, the two light chain isoenzymes can exist within a single myofibril, and even within a single myofilament. Supported by grants from NIH, NSF and the Muscular Dystrophy, Association, Inc.

**M-PM-E12** THE ORIGIN OF THE PRESTEADY STATE $H^+$ RELEASE AND THE DIFFERENCE SPECTRAL CHANGE DURING THE INTERACTION OF ATP WITH MYOSIN SUBFRAGMENT-ONE. S.P. Chock* (Intr. by R.P. Schwarz). NIH, Bethesda, MD 20014

The two key events which occur during the transient phase of ATP hydrolysis by myosin are the irreversible binding of ATP and the hydrolysis of ATP in the initial Pi burst. Accompanying these events are 1) a fast enhancement of fluorescence, 2) a fast release of $H^+$, and 3) a fast difference spectral change (ΔO.D.). We have previously shown that the fluorescence enhancement is mainly due to the hydrolysis of ATP rather than to the binding of ATP. In this study, the kinetics of all the presteady state changes are monitored. The results show that like the fluorescence enhancement, the rates for the $H^+$ release and the ΔO.D. level off at high ATP concentration while the rate of the irreversible ATP binding becomes too fast to measure. Furthermore, under all conditions tested, the rates of the fluorescence enhancement, the ΔO.D., and the $H^+$ release are all equal to the rate of the initial Pi burst. This suggests that, like the fluorescence enhancement, most of the $H^+$ release and the ΔO.D. change arise from the initial Pi burst rather than from the binding of ATP.

**M-PM-E13** IDENTITY OF MYOSIN ACTIVE SITES. S.P. Chock* and E. Eisenberg (Intr. by T.L. Hill), NIH, Bethesda MD 20014

We have reinvestigated whether the two myosin heads are identical with respect to ATP binding and hydrolysis. By measuring the flourescence enhancement caused by the binding of MgATP, we determined the stoichiometry of ATP binding to myosin, heavy meromyosin (HMM), and subfragment-1 (S-1). By measuring $\gamma^{32}$P-ATP hydrolysis with and without a cold ATP chase in a 3-syringe quenched flow apparatus, we determined the amount of irreversible ATP binding and the magnitude of the initial ATP hydrolysis (initial Pi burst). Our results show that under a wide variety of experimental conditions: 1) the stoichiometry of ATP binding ranges from 0.8 to 1 ATP per myosin head for myosin, HMM, and S-1. 2) 80-100% of this ATP binding is irreversible. 3) 75-90% of the irreversibly bound ATP is hydrolyzed in the initial Pi burst. 4) the first order rate constant for the rate limiting step in ATP hydrolysis by HMM is equal to the steady state HMM ATPase rate only if the latter is calculated on the basis of two active sites per HMM. Based on these results we conclude that the two active sites of myosin are identical with respect to ATP binding and hydrolysis.

**M-PM-E14** IDENTIFICATION OF THE TRYPTIC AND CHYMOTRYPTIC CLEAVAGE SITES BETWEEN THE MYOSIN HEADS AND ROD. Rennè Chen Lu and Jan Sosinski*, Dept. of Muscle Research, Boston Biomedical Research Institute and Dept. of Neurology, Harvard Medical School, Boston, MA 02114.

The $M_r$ of the polypeptide chain of the rod portion of heavy meromyosin obtained by tryptic digests (T-S-2) was estimated as 37k (Balint et al., JBC 250,6168,1975) while that of chymotryptic S-2 (C-S-2) as 59k (Weeds and Pope, JMB 111,129,1977). The present studies show the following amino terminal sequence for T-S-2: Lys-Ala-Glu-Thr-Glu-Lys-Glu-Met-Ala-Asn. The amino terminus of C-S-2 begins with Val-Lys and is followed by the N-terminal sequence found in T-S-2. Thus the tryptic and chymotryptic cleavage sites in the myosin neck region are only two residues apart indicating that T-S-2 is the amino-terminal moiety of C-S-2. The sequences shown above are rich in charged residues, suggesting that the separation of the polypeptide chains forming the coiled-coil rod of myosin begins in the N-terminal portion of S-2. (Supported by grants from NIH (HL-5949,AG00262, SO1 RR 05711) and the Muscular Dystrophy Associations of America, Inc.)

**M-PM-F2** QUANTITATION OF CALCIUM UPTAKE BY SARCOPLASMIC RETICULUM USING CHLOROTETRACYCLINE. M.S. Millman*, A.H. Caswell*, and D.H. Haynes, Dept. Pharm, Univ. of Miami, FL.

A model has been formulated to explain the fluorescence (Fl) changes which occur during active Ca uptake by isolated sarcoplasmic reticulum (SR) in the presence of the Fl chelate, chlorotetracycline (CTC). The model considers the contributions to the total Fl by aqueous and membrane bound CTC and Ca-CTC, and is based on the equilibria: CTC (free)+Ca(free)$\rightleftharpoons$Ca-CTC(free) ($K_o$=0.12 $mM^{-1}$); CTC(free)+SR$\rightleftharpoons$CTC(bound) ($K_1$=0.24 ml/mg SR); and Ca-CTC(free)+SR$\rightleftharpoons$Ca-CTC(bound) or CTC(free)+Ca-SR$\rightleftharpoons$Ca-CTC(bound) (half-saturation about 1-2 mg/ml). The model allows characterization of the system in the passive mode in which the final free [Ca] is known. The Fl enhancement is a hyperbolic function of [Ca] and the $K_d^{app}$ (Ca-CTC) is found to vary with [SR]. The limiting values are 8.7 mM Ca in the absence of SR and about 1 mM Ca when extrapolated to infinite [SR]. Slow phases of Ca influx are seen with $t_{\frac{1}{2}}$= 1-2 min (probe response time <3sec) which is similar to that reported by ANS. The method is applied to active transport in which CTC, in conjunction with $^{45}Ca$, is shown to provide a continuous and quantitative measure of bound and free [Ca]. Supported by NIH 1-PO HL16117 and HL07188-2

**M-PM-F3** RESPONSE OF ARSENAZO III TO pH CHANGES. K. Ogan and E.R. Simons, Perkin-Elmer Corp., Norwalk, Ct. and Boston Univ. Sch. of Medicine, Boston, Ma.

There is increasing use of arsenazo III as an indicator of intracellular calcium ion concentration. We have found this dye to be much more sensitive to changes in $H^+$ concentrations than to changes in $Ca^{++}$ concentrations; hence, intracellular measurements must be interpreted carefully. The differential spectrum resulting from changes in the $Ca^{++}$ concentration has peaks at 604 nm and 654 nm and an isosbestic point at about 572 nm, while the spectrum resulting from pH changes (in the absence of $Ca^{++}$) shows only a single peak at 604 nm and an isosbestic point near 583 nm. This work was supported in part by NIH grants HL 16375 and HL 15335.

## SARCOPLASMIC RETICULUM

**M-PM-F1** THE EFFECT OF MODIFICATION OF PHOSPHATIDYLETHANOLAMINE ON $CA^{2+}$ TRANSPORT IN SARCOPLASMIC RETICULUM. Cecilia Hidalgo and Sandra Tong*, Dept. of Muscle Research, Boston Biomedical Res. Inst., Boston, MA.

Labeling of the free amino groups of sarcoplasmic reticulum (SR) with a water-soluble, non-penetrating complex of fluorescamine with cycloheptaamylose (CFC) in the presence of ATP results in a marked inhibition of $Ca^{2+}$ uptake without affecting the $Ca^{2+}$-ATPase activity. Fast labeling, which parallels the time course of inhibition of $Ca^{2+}$ uptake, takes place into about 80% of the phosphatidylethanolamine (PE) present in SR; a slower label incorporation was also observed into the $Ca^{2+}$-ATPase. Addition of the fluorescent PE derivative extracted from CFC-labelled SR to unlabeled vesicles results in inhibition of $Ca^{2+}$ uptake without apparent changes in the $Ca^{2+}$-ATPase activity. Similar results were observed with other PE derivatives containing amino groups modified with fluorescamine or trinitrobenzenesulfonate. These data suggest that the free amino group of PE is essential for the coupling of the hydrolysis of ATP to the translocation of $Ca^{2+}$. (Supported by grants from NIH (AM16922), MDAA and AHA).

**M-PM-F4** FUNCTIONAL LOCATION OF $Mg^{2+}$ AND $K^+$ IONS WITH THE SKELETAL SARCOPLASMIC RETICULUM. V.C.K. Chiu* and D.H. Haynes, Dept. of Pharm. Univ. of Miami, Miami, Florida.

A method using 1-anilino-8-naphthalene sulfonate($ANS^-$) as a calcium indicator has been described(Cir.Res.Supp. III 56,97,1977). Fluorescent signals arising from $ANS^-$ binding to the inside and outside surfaces of the ATPase-rich sarcoplasmic reticulum(SR)membrane were distinguished on their rates of appearance in a rapid mixing experiment($t_{\frac{1}{2}}$=8sec and $t_{\frac{1}{2}}$<3msec respectively). Changes in the amplitude of the slow process can be used to measure the internal $Ca^{2+}$ concentration. With the addition of valinomycin as a catalyst, this slow process can be speeded up($t_{\frac{1}{2}}$=20msec)and is capable of monitoring $Ca^{2+}$ transport kinetics. The rate of passive $Ca^{2+}$ influx(10mM)is slow($t_{\frac{1}{2}}$ ca. 120 sec). In a series of stopped flow mixing experiments to measure active $Ca^{2+}$ transport in the mixing configuration(SR,valinomycin,$ANS^-$,$Ca^{2+}$,$Mg^{2+}$,$\pm K^+$) vs ($ANS^-$,$Ca^{2+}$,$Mg^{2+}$,ATP,$\pm K^+$)the $t_{\frac{1}{2}}$ values are 10 sec and 2 sec in the absence and presence of 5mM $K^+$ respectively. When either $K^+$ or $Mg^{2+}$ is mixed with no pre-equilibration the $t_{\frac{1}{2}}$ is 6sec. The results indicate that both $K^+$ and $Mg^{2+}$ are required inside the SR for maximal rates of $Ca^{2+}$ transport. (Supported by NIH 1-PO-HL16117 and Florida Heart Association.)

**M-PM-F5** MEMBRANE PHOSPHORYLATION OF THE 36,000 AND 64,000 DALTON PROTEINS OF THE HEAVY SARCOPLASMIC RETICULUM VESICLES. Kevin P. Campbell & Adil E. Shamoo., Univ. of Rochester, Sch. of Med. & Dent., Rochester,N.Y.14642

Heavy sarcoplasmic reticulum vesicles(HSR) were phosphorylated at 25° for 10 min. in 5 mM $MgCl_2$, 1 mM EGTA, 10 mM HEPES (pH 7.4) and 10 μM [$\gamma$-$^{32}$P] ATP . $^{32}$P-phosphoproteins were determined by SDS-gel electrophoresis and autoradiography. In the absence of EGTA the two proteins of molecular weight 36,000 and 64,000 were slightly phosphorylated but when 1 mM EGTA was present the phosphorylation of these two proteins increased several fold. The phosphorylation is not increased by c-AMP and is hydroxylamine resistant. The addition of 10 mM EDTA, 1mM $ZnCl_2$, or 1% KDOC caused the complete inhibition of HSR phosphorylation. KCl(200mM) increases the phosphorylation of the 64,000 dalton protein and NEM(1mM) increases the phosphorylation of the 36,000 dalton protein. Caffiene (5mM) decreases the phosphorylation of both proteins by 50%. We are currently studying the effects of phosphorylation on calcium permeablity of the HSR and hope to be able to correlate changes in calcium permeablity with changes in protein phosphorylation.

Supported by US DOE Cont. and assigned RPT# UR-3490-1290

**M-PM-F6** TWO CLASSES OF HIGH AFFINITY CALCIUM BINDING SITES IN $Ca^{++}$-$Mg^{++}$-ATPase OF SR. Terrence L. Scott and Adil E. Shamoo, (Intr. by I. Feldman), University of Rochester School of Med. & Dent., Rochester, N.Y. 14642.

Passive $Ca^{++}$ binding to the $Ca^{++}$ + $Mg^{++}$-ATPase of sarcoplasmic reticulum (SR) has been studied by the flow dialysis technique. Tryptic digestion of the enzyme in intact SR vesicles has previously been shown to uncouple $Ca^{++}$ transport from ATP hydrolysis by cleavage of an essential bond in the 55K dalton fragment. This cleavage disrupts $Ca^{++}$ uptake but leaves ATPase activity unimpaired. $Ca^{++}$ binding to the ATPase enzyme is altered specifically by the digestion of the 55K dalton peptide. Digestion induces a transition of one class of high affinity ($K_d$ = 5 μM) sites to sites of reduced affinity ($K_d$ = 20 μM) with conservation of the total number of sites. This change in affinity without destruction of sites is similar to the effect of low (0-4°) temperature on $Ca^{++}$ binding to the ATPase. The combined effects of tryptic digestion and reduced temperature on $Ca^{++}$ binding, $Ca^{++}$ transport and ATP hydrolysis will be presented and the implications for the molecular mechanism of the ATPase enzyme will be discussed.

Supported by U.S. DOE Contract and Assigned Report No. UR 3490-1294.

**M-PM-F7** ISOLATION OF CNBr FRAGMENTS OF THE $Ca^{2+}$ + $Mg^{2+}$ DEPENDENT ATPase OF SARCOPLASMIC RECTICULUM. A. Klip,*D.H. MacLennan,*and A.E. Shamoo (Intr. by P. A. Knauf). C.H. Best Inst., Univ. of Toronto, Toronto, Ont. M5G 1L6, and Dept. of Rad. Biol. and Biophys., Univ. of Rochester, Rochester, N.Y. 14642.

Experiments have been carried out to localize $Ca^{2+}$ ionophoric activity within a short primary sequence of the ($Ca^{2+}$ + $Mg^{2+}$)ATPase of sarcoplasmic reticulum. Amino acid sequences show that the alignment of large tryptic fragments of this enzyme is: Ac-N-20,000-30,000-45,000-COOH. Following CNBr cleavage of the 20,000 dalton fragment, which contains ionophoric activity, two large polypeptides, $C_2$ and $C_3$, were isolated by gel filtration and hydroxyl apatite chromatography. Both $C_2$ (>8,000 daltons) and $C_3$(7,950 daltons) are free of methionine residues. $C_3$ is located at the COOH terminal end of the 20,000 dalton fragment, and its amino acid sequence is known. Ionophoric properties of these fragments will be discussed.

**M-PM-F8** EFFECTS OF IONOPHORES ON CALCIUM PERMEABILITY OF SARCOPLASMIC RETICULUM. C.F. Louis*, G. Fudyma*, P. Nash-Adler*, M. Shigekawa* and A. M. Katz. Univ. Conn. Health Center, Farmington, CT 06032 (Intro. by F.Bronner)

Ca uptake by rabbit sarcoplasmic reticulum (SR) vesicles (6 μg/ml), measured in 120 mM KCl, 5 mM MgATP, 50 mM phosphate, 40 mM histidine buffer (pH 6.8), PK/PEP regenerating system, and various concentrations of $^{45}CaCl_2$ at 25°C, was modified by the monovalent cation ionophores Nigericin, Valinomycin or Gramicidin (G). Inclusion of ionophore from the start of the reaction did not affect initial Ca uptake rate, but cessation of Ca uptake was delayed causing initial peak Ca "capacity" to more than double. Addition of ionophore during the spontaneous transient Ca release phase seen after the initial peak of Ca content (Katz et al., Circ. 56, III-87, 1977) led immediately to renewed Ca uptake, G having the most pronounced effect. The uncoupler CCCP had little effect, indicating that proton movement through the membrane did not cause the ionophore effects. Monovalent cation entry into SR vesicles may explain these effects, which are due in part to reduced Ca efflux. (Supported by HL-22135, HL-21812, Conn. Heart Assoc. #11-2020778 and MDA).

**M-PM-F9** DISTINCTION OF THIOLS INVOLVED IN THE SPECIFIC REACTION STEPS OF THE PURIFIED $CA^{2+}$ ATPASE OF SARCOPLASMIC RETICULUM. S. Yamada* and N. Ikemoto, Dept. Muscle Research, Boston Biomedical Research Institute; and Dept. Neurology, Harvard Medical School, Boston, MA 02114.

The extent and mode of inhibition of the purified ATPase of sarcoplasmic reticulum by incorporation of [$^{14}$C]MalNEt are strongly dependent upon [$Ca^{2+}$] during the incorporation, although the net incorporation is virtually [$Ca^{2+}$]-independent. The blockage of the most reactive thiol ($SH_1$) has no effect on ATPase activity. Blockage of a second thiol ($SH_2$) prevents decomposition of the phosphorylated intermediate (EP). Further blockage of one or more kinetically indistinguishable thiol(s) ($SH_3$) inhibits the EP formation. The rate of $MalNEt_{2+}$ incorporation into $SH_2$ increases in parallel with $Ca^{2+}$ binding to the α sites ($K = 3 \times 10^6 M^{-1}$), but that into the $SH_1$ and $SH_3$ is [$Ca^{2+}$]-independent. The results suggest that the activation of ATPase by $Ca^{2+}$ binding to the α sites is mediated by a conformational change which may be taking place in the vicinity of $SH_2$. (Supported by grants from NIH(AM16922), NSF(PCMN84124), the Amer. Heart Assoc. and MDAA)

**M-PM-F10** QUANTITATIVE MODELS FOR THE RESPONSE OF POTENTIAL-SENSITIVE PROBE MOLECULES. M.C.Foster and J.Yguerabide, Dept. of Biology, UCSD, La Jolla, Ca. 92093

We have examined several proposed models for the potential-dependent changes in fluorescence intensity observed for some charged carbocyanine dyes in cell and vesicle suspensions and have derived expressions which allow us to determine quantitatively the ability of each model to predict the experimental observations. The models assume that the probe is soluble in the membrane and in the aqueous solution and that the equilibrium distribution of the probe across the membrane follows the Nernst equation. For consistency with the observed response of some charged carbocyanine dyes it is necessary to assume that the fluorescence efficiency of these probes is much higher in the aqueous solution than in the membrane. The expressions may also be used to study the response of other charged lipid-soluble molecules to a change in transmembrane potential and to optimize the magnitude of the response. The predictions of the models are sensitive to the partition of the probe into the membrane, to the surface charge of the membrane, and to the concentrations of lipid and probe in the suspension.

Supported by NEI 5 K07 EY00027-03 and NSF PCM75-191054.

**M-PM-F11** PROPERTIES OF EXCITABLE MEMBRANE SITES AS REVEALED BY USE OF CHEMICAL STIMULANTS AND REAL-TIME SPECTRUM ANALYZER. I. Tasaki, Bethesda, Maryland 20014

Electrophysiological properties of membrane sites (ionic channels) were examined by using a Nicolet 440A spectrum analyzer in combination with the following chemical stimulants: sea water with reduced calcium, veratridine, scorpion venoms, aminopyridine derivatives, glutaraldyhyde, etc. When one of these stiulants was applied to a squid giant axon, electric responses of 1-30 μV in amplitude repeating spontaneously at frequencies around 150 Hz could be observed with an intracellular recording electrode. These responses were found to be sensitive to temperature changes, as well as to TTX and TEA; it was shown that they represent repetitive activation of a small number of membrane sites by the stimulants. These miniature responses could be evoked without being accompanied by a change in the membrane potential. The effects of electric current, KCl, etc. on these responses were examined. [A part of this work has been published in the Japan. J. Physiol. 27(5): 1977.]

**M-PM-F12** TETRODOTOXIN INDUCED PROTEIN RELEASE FROM THE AXON INTERIOR. S. Terakawa* and H. Pant. (Intr. by T. Yoshioka), Bethesda, Maryland 20014

Using internally perfused squid giant axons, we measured the amount of protein released into perfusate by the method of covalent labeling with [I-125] Bolton-Hunter reagent. External application of tetrodotoxin (TTX) caused significant increase in the protein release from the axon interior into the perfusate. In the presence of TTX the action potential was suppressed completely. Upon removal of TTX from the external solution the rate of protein release returned to the original level and action potentials reappeared. Internal application of TTX had no effect either on the protein release or on the excitability. Saxitoxin, when applied externally, showed similar effects on the rate of protein release and on the axon excitability as did TTX. The molecular weight distribution of the protein released showed a major peak at 12,000 daltons and minor peaks at 45,000 and 68,000 daltons. This finding strongly suggests that membrane macromolecules which have TTX binding sites on their external surface can alter the state of the thin protein layer which is undercoating the internal surface of the membrane.

**M-PM-F13** ELECTRICAL PROPERTIES OF MEMBRANE SYSTEMS: POTENTIAL AND IONIC DIPOLES OF THE WATER SURFACE. Giuseppe Colacicco*. (Intr. by M.I. Cohen). Albert Einstein College of Medicine, Bronx, N.Y. 10461.

An obstacle to the molecular interpretation of membrane and surface potentials is a lack of knowledge of the role played by interfacial water. Using radioactive air (R) and saturated Ag/AgCl electrodes, I determined each term in the equation

$$Vo = V(R/air) + V(Air/water) + V(Ag/AgCl)$$

In the given system, with V(R/air)=120 mV and V(Ag/AgCl) =-220 mV, Vo was -400 to -600 mV, depending on the cleanliness of the water surface. For Vo=-400 mV, the electrical potential of the air/water interface was determined for the first time as V(air/water)=-300 mV. This corresponds to an excess of $3.4 \times 10^{13}$ ($\mp$) dipoles/cm$^2$, namely one ($\mp$) ionic dipole of water for every 100 water molecules at the surface, as opposed to one ionized water molecule in 555 million in bulk. This unique ionization of interfacial water institutes a new dimension in the interpretation of membrane potentials and other membrane functions. The positive surface potential of nonionic lipids means ($\pm$) water and not lipid dipoles. (NIH Grant from the Heart, Lung and Blood Institute).

**M-PM-F14** LINEAR ELECTRICAL PROPERTIES OF THE LENS OF THE EYE. R.T. Mathias, J. Rae*, and R.S. Eisenberg, Dept. of Physiology, Rush Medical College, Chicago, Il. 60612 and Dept. of Ophthalmology, Univ. of Texas Med. Branch, Galveston, Texas 77550.

The impedance of the lens of the frog eye has been measured using microelectrodes for intracellular recording and passing of current. A stochastic current was applied near the center of the lens. The potential just under the surface was recorded and both signals were digitized. Power spectra and cross power spectra of the input current and output voltage were computed, averaged, and used to estimate the transfer function (impedance) over the frequency range 0-200 Hz.

The transfer function closely fits an electrical model of the lens with parameters in reasonable agreement with the structure of the preparation and the expected properties of the membranes and intra- and extracellular spaces. The inner membranes contribute importantly to the electrical properties, although the d.c. length constant of about 0.7 mm ensures a significant radial variation of potential even at d.c.

**M-PM-F15** ELECTRICAL PROPERTIES OF A SPHERICAL SYNCITIUM. R.S. Eisenberg, V. Barcilon*, and R.T. Mathias, Dept. of Physiology, Rush Medical College, Chicago, Il. 60612.

The lens of the eye and some tissue culture preparations of cardiac muscle are spherical syncitia in which individual cells are electrically coupled. Such syncitia enclose a pervading extracellular space and so have several pathways by which current can flow from the cytoplasm to the surrounding bathing solution. An electrical model--a pair of coupled partial differential equations with boundary conditions--has been constructed from first principles to describe 1) the flow of current through the cytoplasm, across the inner membranes and through the pervading extracellular space and 2) the flow of current through the cytoplasm and across the outer membrane into the bathing solution. Anisotropic properties and general morphometric parameters have been included.

The solution to the equations has been found using perturbation theory. The result is pleasingly simple, directly analagous to the traditional models of the t-system of skeletal muscle; the results agree with experimental data taken over a wide frequency range from the lens of the eye.

POSTER SESSIONS

HEMOGLOBIN II

**M-POS-A1** QUANTITATION OF THE ALLOSTERIC EQUILIBRIA OF CARP Hb. R.R. Pennelly* and R.W. Noble. Veterans Administration Hospital and Departments of Medicine and Biochemistry, SUNYAB, Buffalo, New York 14215.

IHP induced UV difference spectra of various liganded derivatives of carp hemoglobin have been measured as a function of pH. In these spectra, the difference in the induced absorbance change at 287 and 293 nm is proportional to the change in the R-T equilibrium. At low pH these values were maximal, about 2% of the total absorption, and constant with respect to pH. A smooth, S-shaped curve extends toward higher pH where the values approach zero. A pK for this transition defining R=T in the presence of IHP can be assigned. For the low spin $CN^-$ and $N_3^-$ ligands this pK is 6.7 while high spin $H_2O$ and $SCN^-$ yield a pK of 7.1. Experiments with ferrous forms of carp hemoglobin gave a pK for the low spin CO derivative that was identical to that of the low spin ferric forms while the pK of the deoxygenated hemoglobin was 8.5. Thus the change in the conformational equilibrium that accompanies the conversion from the low spin CO derivative to the high spin unliganded or deoxy form is only partially duplicated by a spin state change alone.

Supported by VA Research Funds and USPHS Grant HL-12524

**M-POS-A2** MOLECULAR AND FUNCTIONAL PROPERTIES OF Hb C HARLEM. K.Adachi*, T.R.Kinney*, E.Schwartz* and T.Asakura, Children's Hospital of Phila. Univ.of Pa. Phila.Pa.19104

The molecular stability of Hb C Harlem ($C_H$) which has double mutations, β 6(Glu→Val) and β 73(Asp→Asn), was studied by using the mechanical shaking method and heat stability test. By the shaking method, the oxy-, carboxy- and met-forms of Hb $C_H$ denatured at a rate 2.6-2.7 times faster than the corresponding forms of Hb S. The deoxy-form of Hb $C_H$ denatured 17 times faster than that of Hb S. The difference in the stability of Hb $C_H$ from that of Hb S must be attributed to the additional amino acid substitution at the β 73. The heat stability test demonstrated that the oxy-, met- and carboxy-forms of Hb $C_H$ were less heat stable than corresponding forms of Hb A and Hb S. The deoxy- and carboxy-forms of these hemoglobins were more heat stable than their oxy- and met-forms. These results suggest that denaturation by shaking is related to protein conformation while the rate limiting step by heat denaturation is the formation of methemoglobin. The oxygen affinity and Bohr effect of Hb $C_H$ with and without organic phosphates were similar to those of Hb A and Hb S. The effect of two mutation sites on the structure and function of Hb $C_H$ will be discussed.

**M-POS-A3** ON THE CONCENTRATION DEPENDENCE OF THE DIFFUSION COEFFICIENT OF HEMOGLOBIN. A. P. Minton* and P. D. Ross, NIAMDD, National Institutes of Health, Bethesda, Md. 20014

The concentration dependence of the frictional coefficient for diffusion of hemoglobin in solution has been extracted from the results of classical self-diffusion experiments after correction for the effects of thermodynamic non-ideality. We find that this dependence may be represented over the concentration range 0-35 g/dl by a one parameter semiempirical expression previously used to describe the concentration dependence of the frictional coefficient for sedimentation. The observed diffusion constant of hemoglobin, D, at any protein concentration, c(g/dl), is given by

$$D = D_o (1 - 0.0144\, c)^{\alpha} (1 + \partial \ln \gamma / \partial \ln c)$$

where $D_o$ is the value of the diffusion constant at infinite dilution, $\gamma$ is the activity coefficient of the hemoglobin and $\alpha$ is a semempirical parameter whose value is close to 7. The applicability of this equation is consistent with the view that, under conditions of moderate ionic strength and pH near the isoelectric point, the hemoglobin solution behaves thermodynamically and hydrodynamically as a suspension of non-interacting quasi-spherical particles.

**M-POS-A4** TEMPERATURE INDUCED DIFFERENCE SPECTRA OF OXYHEMOGLOBIN A AND ITS SUBUNITS. M. L. Adams and T. M. Schuster (Intr. by Gerson Kegeles), Biological Sciences Group, University of Connecticut, Storrs, 06268.

The temperature difference spectrum of oxyhemoglobin tetramer has a characteristic shape similar to that produced by organic phosphates. Qualitatively similar difference spectra have been obtained for the isolated αSH and βSH chains. The $\Delta\varepsilon/\Delta T$ is constant over the 5-25°C range for all three hemeproteins. The temperature differences occur in the submicrosecond time range as shown by temperature jump methods. In order to inquire into the relative contribution of each chain to the difference spectrum, we have redetermined the extinctions of the oxy-tetramer and αSH and βSH chains using an iron phenanthroline method and highly purified, met-free samples. At 5°C in 0.10M HEPES, 1mM EDTA, pH 7.0, the λmax, ε mM-1, $cm^{-1}$, and $\Delta\varepsilon/°C$ for each are:

HbO2: 576nm, 15.0, -0.025; 540nm, 13.9, -0.012
α : 575nm, 15.3, -0.036; 539nm, 14.0, -0.015
β : 577nm, 14.7, -0.016; 541nm, 13.9, -0.014

The relative contribution of each chain type to these difference spectra will be discussed. Supported by grants HL 17494 (NIH) and PCM 76-20041 (NSF).

**M-POS-A5** PH DEPENDENCE OF THE CONFORMATIONAL EQUILIBRIUM OF NITROSYL HEMOGLOBIN WITH IHP. D. Bartnicki, Dept. of Biology, Wayne State Univ., Detroit, Michigan 48202

The binding of inositol hexaphosphate (IHP) to nitrosyl hemoglobin has been shown by several investigators to shift the conformation of HbNO from the Relaxed to the Tense state. An ESR marker for the "T" state of HbNO has been suggested, and consists of an asymetric hyperfine resonance centered at g=2.067. Using a normalized peak height parameter of the low field hyperfine resonance, I have determined the R-T composition of HbNO-IHP solutions between pH 6.0 and 8.0 held at constant ionic strength. Samples for ESR were prepared by introducing a known mixture of HbCO and IHP with a small amount of Hb-reductase (Diaphorase) to a quartz flat cell. HbNO was formed by replacement of the liganded CO by NO gas, and spectra obtained within 15 min. at room temperature. From the spectral titration data with IHP a conformational phase diagram was constructed. The region of maximum "T" state composition occurred for HbNO samples below pH 6.5 containing at least an equvalent molar ratio of IHP. However, above pH 7.9 no "T" state conformation could be detected. The pK for the R-T transition was found to be 7.3. This work was supported by the B-Haley Award (Biology, WSU).

**M-POS-A6** MECHANISM OF NUCLEAR RELAXATION BY HUMAN MET-HEMOGLOBIN. R.K. Gupta and J.L. Benovic* (Intr. by J. Glusker), Inst. for Cancer Research, Phila., PA 19111

The enhancement of water tritium relaxation ($1/T_1$) by the heme-iron of aquomethemoglobin (MHb) is exchange-limited as indicated by its temperature dependence. A comparison of the paramagnetic effects of MHb on $1/T_1$ of $^3H$ and $^1H$ in water reveals a primary isotope effect of ~2 ($\kappa_H/\kappa_T$) on the dissociation rate of protons from the heme-iron re-establishing the exchange of protons and not the exchange of entire water molecules to be the chemical mechanism of MHb relaxivity. The paramagnetic effect of $80\pm20\ s^{-1}\ M^{-1}$ on water deuterons reveals a distance of $\leq 2.6$ Å for 2 exchanging deuterons establishing their origin in the innersphere of heme-iron. Consistent with this, cooperativity in the pH titrations of relaxivity with $n=3.0\pm0.1$ and $2.0\pm0.1$ is observed with IHP and 2,3-DPG, resp. Relaxivity titrations with azide reveal that the two heme-irons per tetramer having higher affinity for azide relax water protons 4- and 2-fold more efficiently compared to others with and without IHP, resp. All 4 hemes of MHbF, however, contribute equally to the $1/T_1$ of water protons. ($^3H$ NMR was done at SUNY, Stonybrook; Supported by NIH grant AM19454 and RCDA AM00231.)

**M-POS-A7** LASER INDUCED PHOTOLYSIS AS A PROBE OF SICKLE CELL HEMOGLOBIN GELATION. F.A. Ferrone, J. Hofrichter*, and W.A. Eaton, Laboratory of Chemical Physics, National Institutes of Health, Bethesda, Md. 20014

In order to study the gelation of sickle cell hemoglobin (Hb S) in samples partially saturated with carbon monoxide (CO), we have used an argon ion laser as a photolysis source in conjunction with a polarization-modulated microspectrophotometer. Both the photolytic and heating effect of the laser may be used to induce rapid gelation. We can thus study the kinetics of gelation as well as the composition of the resulting polymers. Linear dichroism measurements on spontaneously-oriented polymers formed in the presence of CO have shown almost no bound CO. The small linear dichroism signal from polymerized COHb S can be separated from the large deoxy-Hb S signal using modulated photolysis with phase-sensitive detection. Comparison of the polymer and monomer signals calibrates the fractional saturation of the polymer. The kinetics of CO binding to both the polymer and monomer can also be measured in this experiment.

**M-POS-A8** ORGANIC PHOSPHATE EFFECTS UPON SICKLE HEMOGLOBIN AGGREGATION. M.E. Johnson, University of Illinois Medical Center, 833 S Wood, Chicago, IL 60612, T. Lionel* & L. Dalton* Vanderbilt University, Nashville, TN 37232.

The motion of sickle Hemoglobin (HbS) and normal adult hemoglobin (HbA) have been compared by spin label methods. In the absence of organic phosphate, HbACO and HbSCO exhibit nearly identical behavior. In the presence of inositol hexaphosphate (IHP), however, HbSCO exhibits a motional restriction (as compared to HbACO) with a temperature and concentration dependence which indicates that IHP induces weak HbSCO aggregation. Upon deoxygenation HbS exhibits much stronger aggregation. Thus saturation transfer ESR methods, which are sensitive to very slow molecular motion, were used to study the effects of organic phosphate. In the absence of organic phosphate deoxy HbS exhibits a rather slow aggregation rate. Upon addition of 2,3-diphosphoglycerate (DPG), the aggregation rate increases substantially; substitution of IHP for DPG produces a further significant increase in the aggregation rate. These effects suggest that the red cell phosphate level may be important in determining clinical severity in sickle cell anemia. (Supported by the Research Corporation, NIH and NSF.)

**M-POS-A9** ORDERED ARRAYS OF HEMOGLOBIN S FIBERS. Crepeau, R.H.* Garrell, R. L.* and Edelstein, S.J.* Cornell Univ., Ithaca, N.Y. 14853

Ordered arrays of fibers have been prepared from concentrated solutions of hemoglobin S in which gelation is prevented by stirring. Electron microscopy on negatively stained samples of the arrays reveals that the fibers possess the same general structure found in single fibers from sickled cells or gelled hemolysates. Observations on embedded and positively stained arrays sectioned perpendicular to the fiber axes reveal either a square lattice 20nm on a side or a hexagonal cross-sectional lattice. Computer-based image reconstruction techniques have been applied to the micrographs with two goals in mind: (1) extending the level of resolution beyond the 3nm available with single fibers by using negatively stained (or unstained) arrays so as to determine the structure of the individual fibers in greater detail, and (2) describing the inter-fiber packing arrangements which are likely to be of significance in sickling of cells, as similar (but generally much smaller) square and hexagonal lattices can be detected in fiber bundles in sectioned, sickled cells. Initial findings on both aspects of the project will be described. Supported by NSF grant BMS 74-00012.

**M-POS-A10** EFFECT OF DIMETHYL ADIPIMIDATE (DMA) ON RED BLOOD CELL (RBC) DEFORMABILITY AND HEMOGLOBIN (Hb)-S GELATION. R. Pennathur-Das, W. M. Lande,* W. C. Mentzer,* B. H. Lubin,* Bruce Lyon Mem. Res. Lab., Children's Hosp., Oakland, CA; Dept. Ped., Univ. Calif., San Francisco.

Human RBC with normal (AA), sickle trait (AS) and sickle (SS) Hb were treated with DMA. Optimal binding to AA RBC occurs at pH-8.4, while cell deformability is impaired as measured by filtration through 3 μm filters and by ektacytometer which generates laser diffraction patterns of deforming RBC. In contrast, AA and AS RBC treated with DMA at pH-7.4 retain normal deformability. Hence AS and SS RBC were treated at pH-7.4 to assess the antisickling effect of DMA. The increased $K^+$ loss observed with hypoxic ouabain incubated SS RBC is decreased by DMA to that of AA RBC. The solubility of deoxyHb measured by the sedimentation method increases linearly with increasing DMA concentrations. Thus, treatment of SS RBC with DMA causes no change in deformability, decreases $K^+$ leak from hypoxic cells and inhibits gelation of deoxyHb.

NEUROBIOLOGY I

**M-POS-A11** CRITICAL NUCLEUS SIZE IN SICKLE HEMOGLOBIN GELATION. M.J. Behe,* and S.W. Englander. Department of Biochemistry and Biophysics, University of Pennsylvania, Philadelphia, Pennsylvania 19104

Sickle hemoglobin (HbS) gelation proceeds through a rate limiting nucleation step. The size of the critical nucleus may be related to the order of the reaction with respect to HbS activity. HbS activity is substantially different from concentration at the high protein concentrations required for gelation. Equilibrium and kinetic experiments were designed to evaluate relative activity coefficients as a function of concentration. When this effect is specifically accounted for, the nucleation reaction is seen to be 10th order with respect to the number concentration of HbS. The closeness of the reaction order to the number of strands in models of the HbS microtubule may indicate a nucleus size close to one turn of the HbS microtubule.

**M-POS-A12** THE ORIGIN OF A SLOW COMPONENT IN THE ALKALINE DENATURATION OF HUMAN HEMOGLOBIN. D. R. Wilson* and A. H. Burr. Simon Fraser University, Burnaby, B. C. V5A 1S6

The kinetics for alkaline denaturation of 50μM oxyHb (oxyhemoglobin A) in 25 mM sodium phosphate and 0.10 M NaCl at pH 11.7 are resolved into 2 first-order components with half-times of 1.4 and 46 min. Denaturation was assayed as the amount of protein insoluble at pH 6.8. The slower component is spectrally similiar to metHb (methemoglobin) and is insoluble in 24% ammonium sulfate at neutral pH (native oxyHb, metHb and fetal hemoglobin are soluble under these conditions). The slow component formed amounts to 12% of the original protein when oxyHb is used as the starting material, 52% when metHb is used under the same conditions, and <1% when deoxyhemoglobin is used in the presence of 10-fold excess dithionite. The rate constant for denaturation of the slow component is the same $(2.5 \pm 0.8) \times 10^{-4}\ s^{-1}$, whether the starting material is metHb or oxyHb. The slow component formed with oxyHb solutions cannot be from metHb present before the reaction, because the solutions initially contain <1% metHb. It appears that 1) metHb is a precursor of the slow component, and 2) some metHb arrises rapidly in the oxyHb solution after the pH is raised to 11.7.

**M-POS-B1** SPONTANEOUS AND EVOKED TRANSMITTER RELEASE SHARE SOME COMMON MECHANISMS. J.E. Zengel & K.L. Magleby Univ. of Miami Sch. of Med., Miami, Fla. 33152

End-plate potentials (epp's) and miniature end-plate potentials (mepp's) were recorded intracellularly from the frog sartorius muscle (0.4 mM $Ca^{++}$, 5 mM $Mg^{++}$). The nerve was stimulated with conditioning trains of 10 to 200 impulses at 20/sec. The mepp frequency increased during the train, then decayed back to the control frequency following the train. The decay of mepp frequency could be described by 4 exponentials with time constants similar to those that describe facilitation (two components), augmentation, and potentiation of evoked release. Replacing the $Ca^{++}$ in the bathing solution with 0.8 mM $Sr^{++}$ led to a greater increase in mepp frequency during the time of the second component of facilitation. Adding 0.2 mM $Ba^{++}$ to the bathing solution led to a greater increase in mepp frequency during the time of augmentation. These effects of $Sr^{++}$ and $Ba^{++}$ are similar to the effects of these ions on evoked release (Zengel & Magleby, Science 197,67). These results support the idea that spontaneous and evoked release share some common mechanisms. (Supported by USPHS grants NS 10277 and NS 07044.)

**M-POS-B2** A NEW METHOD FOR OLIGODENDROCYTE ISOLATION. S. Szuchet, B. G. W. Arnason,* and P. E. Polak,* Dept. of Neurology, Univ. of Chicago, Chicago, Illinois 60637

Oligodendrocytes synthesize myelin. Published methods for oligo isolation yield fragile cells which at best survive 2-3 days in culture. Oligo subpopulations differing in size, density and metabolic activity are recognized in situ but have not been isolated. Our method was developed to isolate intact viable cells and fractionate oligo subpopulations. Ovine white matter (W.M.) is incubated in 0.1% trypsin at 37°C (3.5 min/g W.M.), disrupted by passage through a series of screens (350 μm down to 30 μm pore size) and the suspension in 0.9 M sucrose centrifuged at 770 g for 10 min to remove myelin. The cell pellet resuspended in 3-4 ml of 0.9 M sucrose is applied to a linear sucrose gradient (1.0 to 1.2 M) and centrifuged at 277 g for 40 min. Three bands separate. Band I ($d_1$=1.1329 g/ml) contains red blood cells plus "astrocytes"; cells in both Bands II ($d_2$=1.1415 g/ml) and III ($d_3$=1.1485 g/ml) fit ultrastructural and chemical criteria for oligos suggesting that 2 subpopulations have been separated. Cells in both bands are morphologically intact and remain metabolically active in culture for 3 weeks.

**M-POS-B3** MECHANOSENSORY RESPONSES IN THE CUNEATE-GRACILE REGION OF CHICKENS. P. F. Hitchcock*, S. T. Sakai*, and J. I. Johnson, Biophysics, Psychology and Zoology Depts. and Neuroscience Program, Michigan State University, East Lansing, Michigan, 48824.

In the cuneate-gracile nuclear region of the brain stem of chickens, using glass-insulated tungsten microelectrodes, we recorded neural unit and unit cluster responses to mechanical stimulation of body surfaces in penetrations regularly spaced 0.2 mm apart. The subjects were Straight Leghorn chickens, 10 to 30 days old, anesthetized with Dial-urethane. Mechanosensory responses were most frequently evoked by movements of feathers or delicate perturbations of the skin; even those produced by movements of air currents were effective. Most of the sensory projections were from the wing (40%) and hindlimb (40%); those from the trunk (20%) were from the neck, breast and tail. Hindlimb projections were near the midline, those from wing were more lateral, and most lateral in the spinal trigeminal region were projections from face. Thus this avian system shows a well-developed functional organization similar to that seen in reptiles and mammals. (Supported by NIH research grant NS 05982 and NIMH fellowship MH 05390.)

**M-POS-B4** CHOLINERGIC AGONIST-INDUCED AFFINITY ALTERATIONS IN CNS α-BUNGAROTOXIN BINDING SITES. Ronald J. Lukasiewicz and Edward L. Bennett*, Lab. Chemical Biodynamics, Univ. Calif., Berkeley, CA 94720

High affinity, specific α-Bungarotoxin (α-Bgt) binding sites on membrane fractions derived from rat brain display unique sensitivity to cholinergic ligand. When agonist is preincubated with membranes prior to exposure to α-Bgt, the concentration at which 50% of α-Bgt binding is blocked ($IC_{50}^{pre}$) is lower than that for the coincubation condition ($IC_{50}^{co}$). The ratio of $IC_{50}^{co}$ to $IC_{50}^{pre}$ (θ) is 40 for acetylcholine (AcCh) and decreases in the rank order AcCh >AcSCh>decamethonium > butyrlSCh≈$Me_3\phi NH$ ≈ carbachol >nicotine >hexamethonium = 2.0, θ being ca. 1.0 for lobeline and antagonists d-tubocurarine and gallamine. Preincubation periods of less than one minute are sufficient to produce the conditioning effect, which is rapidly and fully reversible on dilution of agonist. For pretreatment at high concentrations of agonist, α-Bgt binding inhibition takes on non-competitive character. A given concentration of agonist is less effective toward blocking toxin binding at low toxin concentrations than at saturation. The nature of these results suggests that the entity under study is an AcCh receptor and that these agonist-induced affinity changes may represent a biochemical equivalent of desensitization phenomena. (Supported by DBER of DOE & NINCDS)

**M-POS-B5** DECAY OF BULLFROG SYMPATHETIC GANGLION FAST EXCITATORY POSTSYNAPTIC CURRENT IS VOLTAGE INSENSITIVE. A. MacDermott*, V.E. Dionne, and R.L. Parsons*, Dept. Physiology & Biophysics, U. Vermont, Burlington, VT 05401

Fast EPSC's were recorded under voltage clamp from the IX and X sympathetic chain ganglia of Rana catesbiana. Measurements were made on directly visualized cells maintained in a HEPES buffered Ringer's solution (mM: NaCl 117, KCl 2.5, $CaCl_2$ 1.8, HEPES 1.0; pH 7.3, 13-16°C). A two microelectrode voltage clamp system was used to hold membrane voltage from -90 to +20mV. The fast EPSC peaks in a few msec then decays exponentially. Commonly, the peak I-V relation is linear with reversal potential between -10 and 0 mV. In any cell the decay time constant does not change significantly as a function of voltage. Preliminary data indicate that the decay time constant has a $Q_{10}$ near 2. In contrast to the amphibian muscle EPC, the fast EPSC at this vertebral CNS synapse is slower and voltage insensitive. The lack of voltage sensitivity may indicate different molecular properties of the synaptic activation mechanism, since diffusion limited decay is unlikely with a $Q_{10}$ of 2. Supported by NIH grants NS-12306 and NS-13581.

**M-POS-B6** STUDIES OF THE SURFACE CHARGE AND AGGREGATION OF SYNAPTIC VESICLES AND PRE-SYNAPTIC MEMBRANES BY ELECTROPHORETIC LIGHT SCATTERING. D. P. Siegel and B. R. Ware, Department of Chemistry, Harvard University, Cambridge, Massachusetts 02138.

The mechanism of vesicular secretion in synapses and certain endocrine glands is generally believed to involve the fusion of the secretory vesicles with the plasma membranes of the secretory cells, followed by exocytotic release of the vesicle contents. The stimulus for the initiation of secretion is an influx of calcium ions, whose role may include a lowering of the electrostatic repulsion between the vesicles and their target membranes by reduction of the membrane surface charge. We are investigating this question using the technique of electrophoretic light scattering (ELS), in which the Doppler shifts of laser light scattered from particles which are migrating in an electric field are measured to determine the electrophoretic distributions and sizes of the particles in the sample. The initial series of experiments includes the effects of various preparation techniques and washing procedures on the surface charge, aggregation, and surface reactions of the synaptic vesicles and pre-synaptic membrane vesicles.

**M-POS-B7** UNCOUPLING OF EARTHWORM AXON SEPTAL MEMBRANES WITH DNP AND CYANIDE. P. Brink*, and M. M. Dewey, SUNY at Stony Brook, Stony Brook, New York 11794.

Freeze fracture has been used to show that the septa contain nexal particles which are found predominantly on the PF face with pits on the EF face. An estimate of the number of nexal particles/$\mu^2$ has been made from the freeze fracture studies. Septal membrane area was calculated with an automated planimeter and the number of particles and pits were counted. The average for 15 septa was 250 particles/$\mu^2$. Flux data were calculated assuming that the only conducting parts of the septal membrane were the nexal particles. The effects of dinitrophenol and cyanide on the flux of fluorescein across the septa of the median axon were investigated. Short exposure (1-2 hrs) of the nerve cord to DNP (100 uM) and cyanide (1 mM) caused no change in fluorescein flux across the septa. Nerve cords serving as controls were incubated in saline for equivalent time periods. The flux of fluorescein across the septa averaged $1x10^{-10}$ moles/$cm^2$·sec assuming 250 particles/$\mu^2$ (5% of the septum). Longer exposure (16 hrs) of nerve cords to these metabolic uncouplers caused a decrease in the fluorescein flux across the septa (reduced to about 5% to 15%).

**M-POS-B8** BLOCKAGE OF THE $Ca^{2+}$INDUCED $K^+$ CURRENT BY TEA IN MOLLUSCAN BURSTING PACEMAKER NEURONS. A. Hermann* and A.L.F. Gorman, (Intr. by W. Lehman), Dept. of Physiology, Boston U. Sch. of Med., Boston, MA 02118.

$Ca^{2+}$-ions iontophoretically injected into the soma of Aplysia R15 neuron under voltage-clamp conditions induce a $K^+$ - outward current ($I_{K(Ca)}$). Extracellular TEA blocks $I_{K(Ca)}$ in the voltage range around the membrane resting potential (-50mV); the blockage is incomplete, however, with more depolarized holding potentials. In contrast, intracellular TEA does not block $I_{K(Ca)}$. Both extra- and intracellular TEA block the voltage dependent potassium current ($I_{K(V)}$). Extracellular TEA changes the regular bursting activity of the cell to irregularly occuring spikes with prolonged depolarized plateaus. In zero $Ca^{2+}$-TEA solution the spikes were further prolonged. Our results suggest that $I_{K(Ca)}$, which is essential for a bursting activity is completely blocked by extracellular TEA at negative potentials but only partially blocked at more positive potentials. Therefore, during a prolonged action potential the resulting $Ca^{2+}$ accumulation in the cell activates part of $I_{K(Ca)}$ to repolarize the membrane. Supported by NS 11429.

**M-POS-B9** STRUCTURE AND STOICHIOMETRY OF ISOLATED TORPEDO ELECTRIC ORGAN SYNAPTIC VESICLES. H.Breer*, G.H.C.Dowe*, S.J.Morris, K.Ohsawa*, H.Stadler* and V.P. Whittaker* Max Planck Institute for Biophysical Chemistry, D-3400 Göttingen, BRD.

Vesicles prepared either by zonal gradient centrifugation or bucket gradients followed by CPG10-3000 chromatography contain 6-8 nmol Acetylcholine (ACh) and 1.2-1.6 nmol ATP per µg protein and $17x10^4$ ACh molecules per vesicle. The membrane contains a $K^+$,$Na^+$-inhibited,$Mg^{2+}$, $Ca^{2+}$-ATPase. Vesicles are good osmometers at osmotic pressures higher than 800 mOsm but leak ACh and ATP when hypotonically stressed. The membrane density of osmotically-lysed vesicles drops in an all-or-none fashion upon prolonged dialysis. These measurements and others are consistent with a 90-100 nm sphere enveloped by a 4-5 nm lipid-rich membrane. ACh and ATP are in true solutions in osmotic equilibrium with the suspension medium and are easily released. The particles also contain a small amount of dense glycosaminoglycan material which requires vigorous treatment for removal.

**M-POS-B10** AGONIST-TRIGGERED ENDPLATE CHANNEL OPENING. P. R. Adams,* & B. Sakmann* (Intr. by L.Sordahl) U.T.M.B., Galveston, TX 77550 & M.P.I. für biophys. Chemie, Göttingen, G.F.R.

An external microelectrode was used to record focal membrane noise from voltage-clamped frog endplates during bath perfusion of ACh or carbachol, at 12° and -80 mV. The dependence of the variance/mean current ratio and the correlation function time constant on agonist concentration was consistent with a 3 step model for receptor activation: $A+R \rightleftharpoons AR \rightleftharpoons A_2R \rightleftharpoons A_2R^*$. Sequential independent binding of 2 agonist molecules (K=30 µM for ACh, 300 µM for Carb) is followed by a single rate-limiting isomerization (forward rates: 2.2 & 1.6 $ms^{-1}$, backward rates 0.3 & 1.0 $ms^{-1}$ for ACh and Carb respectively). These kinetic constants successfully predict the independently measured absolute amplitudes of equilibrium currents for small ACh or Carb concentrations, as well as the observed time constants and relative relaxation amplitudes in voltage jump experiments. If it is assumed that all of the quantal ACh packet ends up on doubly liganded receptors (i.e., no wastage), the kinetic constants for ACh predict an m.e.p.c. of the correct amplitude. We estimate that in our experiments high enough concentrations of ACh or carbachol can open about 90% and 60% respectively of the available channels.

**M-POS-B11** PRECONJUGATION BEHAVIOR OF THE CILIATE STENTOR POLYMORPHUS. Victor K.H. Chen and David Grandy, Dept. of Biology, Case Western Reserve University, Cleveland, Ohio 44106

Pairs of Stentor polymorphus display coordinated movements and contacts up to 13 hours before conjugation. A bulge develops in the frontal field of the cells. The membranelles beat in metachrony while the body cilia are motionless during most of the following displays. The basic movements, as follows, are repeated in varying orders. 1)Pair of cells perpendicular to each other come in close contact and move back and forth along their own longitudinal axes. 2)One cell spirals around the other and continually maintaining close contact. 3)The membranelle bands and/or bulges touch while the cells are in the same orientation. 4)With cells parallel, the frontal fields move toward each other.5)The bulges adhere; the anterior ends of the cells move towards and away from each other repeatedly. 6)Cells fuse at the bulge and swim as one. 7)Before fusion, cells may lose contact and later continue display with a third cell.

**M-POS-B12** A $Ca^{++}$- $K^+$ ACTION POTENTIAL IN A HYPERPOLARIZING PHOTORECEPTOR. M. Carter Cornwall and A.L.F. Gorman Boston Univ. Sch. of Med., Boston, Mass. 02118.

The off response of hyperpolarizing photoreceptor cells of the scallop retina is associated with an action potential with a peak amplitude of -30 mV. This response is elicited in darkness when $Na^+_o$ is removed and the membrane is hyperpolarized. Current steps which depolarize the membrane to threshold induce a $Ca^{++}$- $K^+$ dependent depolarizing response followed by a slower repolarization and a hyperpolarizing after potential. Repolarization and peak amplitude of the after potential are also a function of $Ca^{++}_o$. When $Ca^{++}_o$ was changed from 9 to 50 mM, rate of repolarization changed from -.06v/sec. to -.49 v/sec. and the peak of the after potential decreased by 12 mV. $Ba^{++}$ and $Sr^{++}$ can serve as charge carriers during the depolarization phase, but these slow repolarization. TEA (50 mM) increases the rate of rise and maximum amplitude of the early depolarization phase while slowing the rate of repolarization. Our results suggest that an increase in $Ca^{++}_o$ during the depolarizing phase of the action potential activates an increase in $K^+$ permeability which assists in membrane repolarization. Supported by EY01157.

**M-POS-B13** ARSENAZO III FORMS A 2:1 COMPLEX WITH Ca UNDER PHYSIOLOGICAL CONDITIONS. M.V. Thomas* and A.L.F. Gorman, (Intr. by B. Kaminer), Dept. of Physiology, Boston U. School of Medicine, Boston, Ma. 02118.

The stoichiometry of the interaction between $Ca^{2+}$ and arsenazo III has been investigated both in the Aplysia R15 neuron and under comparable in vitro conditions. The absorbance change in vitro is linear with [Ca], but for a constant change in free [Ca] (defined by EGTA buffering) it increases with $[dye]^2$, which can be explained if the Ca-arsenazo complex contains one $Ca^{2+}$ ion and two arsenazo molecules. Such a complex is stereochemically and theoretically feasible. This behavior occurs both with impure and 98% pure dye, and is also observed in the R15 neuron. When $Ca^{2+}$ entry into R15 was induced by a constant amplitude depolarizing pulse, the absorbance change was again found to vary very closely with $[dye]^2$ and a similar relation was observed for the absorbance change during a burst of action potentials. The implications of a 2:1 complex with regard to dye calibration, its selectivity against other ions and possible buffering of internal $Ca^{2+}$ by the dye will be discussed. Supported by NS11429.

**M-POS-B14** OPTICAL STUDIES OF ISOLATED RAT ADRENAL CHROMAFFIN CELLS. D. Englert. Dept. of Biological Sciences, SUNY, Albany, New York 12222

Many isolated adrenal chromaffin cells, when examined with Nomarski differential interference contrast, were seen to have microvilli or microspikes on their surfaces. Perfusion with solutions expected to cause large secretory responses increased the number and length of the microspikes. They formed in the presence of 50 ug/ml cytochalasin B (CB). The microspikes presumably are a consequence of the incorporation of secretory granule membranes into the plasma membrane.

When time lapse movies of these cells were analyzed, optically resolvable particles were occasionally seen to make saltatory movements in the cytoplasm.

Intensity fluctuations of laser light scattered from these cells were studied using a specially modified microscope. The scaled intensity autocorrelation had decay times of seconds and had the greatest amplitude and rate of decay at large scattering angles. Low temperatures and 50 ug/ml CB significantly decreased the amplitude and rate of decay of the autocorrelation. The intensity fluctuations may arise at least in part from active particle movements in the cytoplasm.

Supported by USPHS Research Grant NS07681

**M-POS-B15** CONDUCTANCE CHANGES ASSOCIATED WITH A SOMAN-PRODUCED BIPHASIC DEPOLARIZATION IN ELECTROPHORUS ELECTROPLAX. D. Farquharson*, (Intr. by K. Kusano) Biology Dept., IIT, Chicago, Illinois 60616

Some aspects of organophosphate neurotoxicity appear not to be directly related to the well-documented inhibition of acetylcholinesterase displayed by many of these compounds. At the neuromuscular junction some aspects of organophosphorus toxicity can be attributed to changes in acetylcholine receptor function. Using intracellular recording techniques and a voltage clamp I have found that the organophosphate, Soman, has two effects on membrane conductance both of which apparently result from an interaction with the acetylcholine receptor and both of which cause a depolarization. The initial effect is a decrease in conductance, apparently to $K^+$. A later effect is an increase in conductance similar to that produced by carbamylcholine. The decrease-increase conductance sequence corresponds to a slow-rapid depolarization sequence caused by Soman. These results suggest that some of the $K^+$ leak conductance is intimately related to acetylcholine receptor function. Soman's multiple effects may result from its ability to react covalently with its binding site. (NS09090)

## MUSCLE PHYSIOLOGY I

**M-POS-B16** PARTICLE SEGREGATION IN COMPACTED MYELIN. C.Benitez,* D.L.D. Caspar, D.A. Kirschner,* and V.M. Melchior*, The Rosenstiel Basic Medical Sciences Research Center, Brandeis University, Waltham, MA 02154

Lowered water activity, increased calcium ion concentration, and the local anaesthetic tetracaine, all lead, in myelin, to the co-existence of a compacted membrane lattice with a native or expanded period lattice. Compaction is always accompanied by particle segregation out of the plane of the compacted membrane as seen by freeze fracture microscopy. Co-operativity of particle movement is demonstrated by the extensive contracted domains marked by a boundary which is staggered from layer to layer in a very exact step-wise fashion. When the resulting particle-free faces are compared to the fracture faces from purified myelin, similar appearances are obtained with such treatments as DMSO or acetone. Glutaraldehyde can be used to fix the periodicity of the particle-rich domains. Separation of the smooth membranes is not stabilized, however, and they are free to swell apart in hypotonic solutions. Tetracaine and calcium appear to alter the normal membrane contacts, allowing separations to occur at the cytoplasmic boundary when they would normally occur at the external boundary.

**M-POS-B17** PATTERN DETECTION IN SPIKE TRAINS. J. Dayhoff and G. L. Gerstein, Dept. of Physiology, Univ. of Pa., Philadelphia, Pa. 19104.

Many neurons are known to fire spontaneously in the absence of controlled sensory stimuli. It is not known whether spike trains from such neurons contain detectable patterns which could be used for information transfer. We describe a new mathematical test for searching such data for temporal patterns that occur more frequently than expected on a random model. In the random model, each interspike interval is independent of all previous intervals. The patterns detected consist of several particular sequential interspike intervals, forming a specific "word". The calculation does not require a priori specification of a template word. Sensitivity of the new calculation has been tested on simulated spike trains with known pattern characteristics.

Supported by NIH grants GM07229, RR-15, and 2 R01 NS 05606-12.

**M-POS-C1** LIPOSOMES:VEHICLES FOR INTRODUCING A NON-PENETRATING SUBSTANCE INTO MUSCLE FIBERS. J. Leung and S. Putnam, CVRI Univ. Calif., San Francisco, Ca. 94143.

We made positively charged unilamellar liposomes which encapsulated the fluorescent dye 1,-5IAEDANS with dipalmitylphosphatidylcholine (100μM), stearylamine (10μM), and various amount of palmityllysophosphatidylcholine (0-10μM) as described by Batzri and Korn (BBA 289:1015, 1973). Bundles of 20-40 fibers dissected from the semitendinosus muscles of the frog Rana pipiens bathed in a suspension of these fluorescent liposomes for 3-18 h were able to give propagated twitches. The maximal twitch tension decreased with time and the rate of decrease depended on the amount of palmityllysophosphatidylcholine. SDS-polyacrylamide gel electrophoresis of these bundles showed that the proteins of the thin filament were labeled by the fluorescent dye. In contrast bundles bathed in Ringer solution containing 1mM free dye for 4-8 h showed no fluorescence in the gels. Higher free dye concentrations caused irreversible contracture. We conclude that these liposomes may be useful as vehicles for introducing other non-penetrating or toxic substances into muscle fibers without loss of excitability. (Supported by the National Heart, Lung, and Blood Institute HL 16683).

**M-POS-C2** ENERGY BALANCE IN THE INITIAL TETANUS COMPARED TO TETANI IN A METABOLIC STEADY STATE. R.J. Paul[1] & D.R. Wilkie*, University College London, WC1E 6BT England.

The discrepancy between the enthalpy production and that calculated from the known chemical reactions for the initial isometric tetanus was compared to that measured for tetani under steady state metabolic conditions. Frog sartorius muscle tetanized for 3s every 256s attains in 25 min at 0°C a steady state in which the rate of $O_2$ consumption ($\dot{J}O_2$), initial heat ($\dot{Q}_I$), recovery heat ($\dot{Q}_R$) and tension-time integral ($\int Pdt$) are the same for each subsequent tetanus. The phosphagen breakdown ($\Delta\sim P$) during contraction can be measured as the difference in content between one muscle of a sartorius pair stimulated n times and the other stimulated (n-1) times [n=1, or ≥ 9].

| Isometric Tetanus | | $\int Pdt$ N·s/cm$^{+2}$ | $\Delta\sim P$ μmol/g | $\dot{Q}_I$ mJ/g | $\dot{Q}_R$ mJ/g | $\dot{J}O_2$ μmol/(min·g) |
|---|---|---|---|---|---|---|
| 1st | 3s | 85.3 | 1.3 | 115 | | |
| 9th | 3s | 75.5 | 1.1 | 94 | 93 | .092 |

These results indicate: 1) the discrepancy is proportionally the same in the 1st & 9th tetanus; 2) oxidation of glucose can account for the total enthalpy production; 3) $\dot{J}O_2$ is greater than that calculated from $\Delta\sim P$ during contraction using theoretical stoichiometry.

[1]British-American Heart Association Fellow.

**M-POS-C3** LENGTH-TENSION RELATION OF LIMULUS MUSCLE. B. Walcott and M. M. Dewey. Department of Anatomical Sciences, SUNY, Stony Brook, New York 11794.

In Limulus telson muscle, the A-band length varies linearly with the sarcomere length and at sarcomeres below 7.0 μm, the A-band decrease is due to shortening of the thick filaments themselves. We have determined the length-tension relation for this muscle and compared it to that previously published for frog muscle where A-band is relatively constant in length. In our experiments small (< 0.5 mm diameter) bundles of fibers were clamped in a chamber by their origin and insertion. A laser diffraction image was recorded at the end of a 2 s. tetanic plateau simultaneously with the tension. The length of the bundles was adjusted with a micromanipulator. The sarcomere length within a bundle was uniform within 0.5 um from end to end during tension development. The plateau of peak tension ($P_o$=4-5 Kg/cm$^2$) extended from sarcomere length of 6.5 to 7.5 μm and 50% or more of the maximal tension was developed between sarcomere lengths of 3.5-11.0 μm, the normal in vivo length range. Passive tension was insignificant below sarcomere length of 10.0 μm. This is a much greater length-tension range than has been reported for frog muscle. Supported by NIH AM 18750.

**M-POS-C4** CONTRACTILE PROPERTIES OF RELAXATION OF SINGLE MAMMALIAN CARDIAC CELLS. N. De Clerck*, V. Claes* and D. Brutsaert*, (Intr.by G. Morrill) Dept.Physiol., University Antwerp, Belgium.

Cardiac preparations(80x15μm) without functional sarcolemma were manually dissected and activated by iontophoretical calcium pulses. Sarcoplasmic reticulum(SR) was eliminated with Brij-58. A transducer system simultaneously allowed control of force and measurement of shortening, velocity of shortening and force. Preload and afterload were set by an electronic stop. Contraction reproducibly depended on the amount of released calcium ions. Sudden load alterations during contraction and relaxation did not alter the time course of relaxation. When the duration of maximally activating calcium pulses was prolonged, a prolonged contraction ensued. In contrast to intact preparations of mammalian cardiac muscle, where relaxation largely depends upon the instantaneous loading conditions, contraction and relaxation of these isolated, SR deprived, cardiac cells are solely determined by activation.

**M-POS-C5** KINETIC AND BIOCHEMICAL SEPARATION OF DELAYED RECTIFIER CURRENTS IN FROG STRIATED MUSCLE. C. Lynch.* University of Rochester, Rochester, N.Y. (Intr. by P. Horowicz).

The delayed rectifier (outward potassium) currents of frog toe muscle fibers(lumbricalis longissimus digiti IV) were studied by voltage clamp techniques in hypertonic Ringer's solution at 5 C. The short length of these fibers(1.0-1.4 mm) permits a two microelectrode voltage clamp over the entire length of the fiber. The delayed rectifier current has two components: (1) a fast one fit by $n^4$ Hodgkin-Huxley kinetics ($\tau$=7.8 msec at 0 mV) previously described in sartorius; (2) a slower one fit by $n^2$ Hodgkin-Huxley kinetics ($\tau$=90 msec at 0 mV). The majority of fibers have a variable mixture of these two currents, while a number of fibers have either all fast or slow types. 1 mM 4-Aminopyridine and 115 mM TEA block >95% of the fast type and ~50% of the slow currents. The slow current kinetics can be converted to a faster form similar to the fast component by decreasing pH, the effect having a pK of 5.8. The slow current can be selectively eliminated by applying 1 mM diethylpyrocarbonate, a histidine reagent.

This work was supported by NIH Grant AM01004-12.

**M-POS-C6** FORCE-VELOCITY RELATIONS IN CARDIAC MUSCLE. D. S. Joseph* and L. L. Huntsman. Center for Bioengineering, University of Washington, Seattle, Wa. 98195

Force-velocity (F-v) relations have been determined in papillary muscle segments using a new technique which infers segment length from muscle cross-sectional area. At constant muscle length, central segments contract auxotonically while end regions stretch. Auxotonic contractions and load clamps imposed at various times in a twitch have been used to obtain F-v data. Control segment length (SL) is defined as 100% at Lmax. The F-v relation for the auxotonic and load clamp twitches appears to be hyberbolic and independent of SL above about 85% SL. The data are also time-independent from just after stimulus to nearly time to peak force and show no mechanical history dependence over this same period. Using the distance of the F-v curve from the origin as a measure of "activation", the results suggest that activation in cardiac muscle reaches an early plateau (<50 ms) which is maintained until late in the rising phase of the twitch. Therefore, the time course of active force is not indicative of the time course of activation, but rather the interaction of muscle F-v characteristics, segment loading, and the intrinsic F-SL relation of the muscle.

**M-POS-C7** INTRACELLULAR POTASSIUM ACTIVITY OF THE CHICK EMBRYONIC HEART DURING DEVELOPMENT. S-S. Sheu* and H.A. Fozzard, M.D., Univ. of Chicago, Chicago, Il. 60637

The electrophysiological properties of embryonic chick heart ventricular muscle change during development. Membrane resting potential ($E_m$) and intracellular K activity ($a_K^i$) were studied at four different stages of development. $E_m$ was measured by conventional microelectrodes(20-60MΩ). Potassium (K) activity was measured by K-selective glass microelectrodes and K-selective liquid ion-exchanger (LIE) microelectrodes. K equilibrium potential ($E_K$) was calculated from the intracellular and extracellular K activities.

| Age(days) | 4 | 7 | 12 | 18 |
|---|---|---|---|---|
| $E_m$(mv) | 65.4±1.1 | 71.9±0.8 | 73.5±0.6 | 75.8±0.6 |
| $a_K^i$(mM K-glass) | 74.2±1.4 | 84.4±1.3 | 90.0±1.1 | 91.2±1.5 |
| $a_K^i$(mM K-LIE) | 71.7±2.6 | 82.8±1.6 | 88.8±1.4 | 91.1±1.1 |
| $E_K$(mV,K-glass) | 74.3 | 77.6 | 79.3 | 79.6 |
| $E_K$(mV,K-LIE) | 73.4 | 77.1 | 78.9 | 79.6 |

$E_m$, $a_K^i$ and $E_K$ increase during development. $E_m$ is close to, but less negative than, $E_K$. The difference decreases as development progresses. (Supported by HL 20592).

**M-POS-C8** Na/K PERMEABILITY RATIO ($P_{Na}/P_K$) IN NORMAL AND DYSTROPHIC MOUSE SKELETAL MUSCLE. L.C. Sellin*& N. Sperelakis. University of Virginia School of Medicine, Charlottesville, Va. 22903.

The resting membrane potential ($E_m$) of the extensor digitorum longus in normal Ringer solution was -63 mV for dystrophic muscle (Re J-129) and -76 mV for the normal muscle. By varying the external K concentration ($[K]_o$), $E_m$ vs log $[K]_o$ curves were generated. Differences in $E_m$ between the normal and dystrophic muscles were observed in the 0.6-5.0 mM $[K]_o$ range. Above 5.0 mM $[K]_o$, the $E_m$ of both muscles decreased in a similar fashion. Extrapolation of the linear portion of the curve (>40 mM $[K]_o$) indicated intracellular K concentrations ($[K]_i$) of 184 mM and 186 mM for the dystrophic and normal muscles, respectively. At low $[K]_o$ (0.1 mM), both normal and the dystrophic muscles became depolarized to about -47 mV. As calculated from the constant-field equation, the $P_{Na}/P_K$ was greater in the dystrophic (≈0.09) than in the normal muscle (≈0.05) between 0.6-5.0 mM $[K]_o$. The data suggest that the difference in $E_m$ between dystrophic and normal muscles is not due to a difference in $[K]_i$, but could be predicted by the difference in $P_{Na}/P_K$ ratio. (Supported by the MDA.)

**M-POS-C9** DISTRIBUTIONS OF 1st ORDER DIFFRACTION LINE PEAKS OBTAINED FROM FROG SKELETAL MUSCLE. W. Halpern
Univ. of Vermont, Physiology, Burlington, VT 05401

A diode array system (W.Halpern, Proc.San Diego Biomed. Symp. Academic Press 16:429-439, 1977)was used to examine the meridional intensity distributions of diffraction lines from different regions of 4 single fibers at 10-20°C. The patterns usually contained many peaks. Peak separations were measured every 1 ms. It is assumed that each peak represents a population of sarcomeres of nearly homogeneous length within a 0.75 mm muscle segment. In each of 13 measurements during rest and plateau of tetanus the separations between 5 or 6 adjacent peaks fell into 2 distinct groups. The mean of the average of 9 groups($2.05<\bar{s}<2.43\mu m$) were 14.9±0.5 and 14.5±0.3(s.e.)nm/half sarcomere at rest and plateau,respectively. Similarly, 4 other groups($2.69<\bar{s}<2.88\mu m$)were 26.1±1.4 and 24.8±0.5. In spite of possible optical problems related to the complex diffracting units within muscles, individual sarcomere populations assume lengths that differ by a distance comparable to the spacing of 1 or 2 myosin heads. (Supported by NIH AM 17163)

**M-POS-C10** THE CHEMICAL ENERGETICS OF FORCE DEVELOPMENT FOLLOWING A QUICK RELEASE IN MAMMALIAN SMOOTH MUSCLE. T.M. Butler*, M.J. Siegman and S.U. Mooers*. Dept. of Physiology, Jefferson Medical College, Phila., PA 19107.

In the rabbit taenia coli at 18°C and 93% $l_o$, the average rate of chemical energy usage (Δ phosphocreatine + Δ ATP when respiration and glycolysis are blocked) is higher during the first 25 sec of an isometric tetanus when force increases than during the next 35 sec when force is nearly constant (0.0083±0.0008 vs. 0.0028±0.0008 mole/mole Ct·sec, n= 15 and 18, respectively. Values are normalized to total creatine, Ct = 2.7 μmole/g). During sustained stimulation (60 Hz, 10 V rms) muscles at 102% $l_o$ were allowed to develop force for 20 sec, quickly released (0.2 $l_o$/sec) to 93% $l_o$ and allowed to redevelop force at this length for 25 sec. The average rate of energy usage during the redevelopment of active force from 0±4% $P_o$ immediately after release to 95±6% $P_o$ at 25 sec was 0.0031±0.0020 mole/mole Ct·sec, n=7. This is less ($P<0.05$) than that required for initial development of force, and suggests that the initial high rate of energy usage is not due to crossbridge cycling associated with force development, but rather with the transition from the resting to the active state. Supported by HL 15835 and HD06074.

**M-POS-C11** PERIODICITY OF THICK FILAMENTS AND LMM FROM INSECT FLIGHT MUSCLE. W. E. Garrett, Jr., and M. K. Reedy, Dept. of Anatomy, Duke University, Durham NC 27710

Thick filaments isolated from the flight muscle of Lethocerus species have been examined by electron microscopy using negative staining. The filaments demonstrate more order than that preserved in thick filaments prepared from other striated muscle types. Like thick filaments from guinea pig taenia coli (J. V Small, 1977), Lethocerus flight thick myofilaments show a strong axial period of 14.5 nm, manifest as rows or ridges of stain-excluding projections from the surface of the thick filament. These projections and the 14.5 nm period can be removed by treatment with papain which cleaves the S-1 moiety from the myosin molecule. Although subunit structure occasionally can be demonstrated within the 14.5 nm period, the surface symmetry of the crossbridges on the thick filament cannot be determined. Papain decapitated filaments retain S-2 segments as a faintly brushy structure in the bridge bearing regions, by contrast with the smoother, thinner bare zone in midfilament. Aggregates of light meromyosin prepared from Lethocerus demonstrate a 14.5 nm period. (NIH and MDAsupport)

**M-POS-C12** CAN SLOW INWARD CURRENT BE ADEQUATELY VOLTAGE-CLAMPED IN CARDIAC PURKINJE FIBERS? R.S. Kass, S. A. Siegelbaum and R. W. Tsien. Department of Physiology, Yale University School of Medicine, New Haven, CT 06510.

Spatial nonuniformity is a serious concern in voltage clamp experiments in cardiac tissue. We have obtained evidence that nonuniformity is not severe enough to distort measurements of slow inward current ($I_{si}$) found in short calf Purkinje fibers. Rapid sodium current was eliminated with 10 μM TTX and a depolarized (~ -50 mV) holding potential. During the flow of $I_{si}$ the following results were found: 1) Longitudinal nonuniformity was small when measured directly as a difference signal between two internal voltage microelectrodes, ΔV. 2) Close agreement was found between ΔV and total applied current ($I_T$), two independent measures of membrane current density ($I_m$). Nonlinear cable theory shows that such agreement checks against deviation from the $I_m$ that would be measured with a longitudinal space clamp. 3) Radial voltage nonuniformity was small in simulations using 200 Å-wide clefts and experimental I/V characteristics. 4) I/V curves and slow response upstrokes are consistent: (maximal inward current) ≅ (measured total capacity) x (measured $\dot{V}_{max}$ of slow response).

**M-POS-C13** ELECTRICAL EVIDENCE FOR WIDE CLEFTS IN VOLTAGE CLAMPED RABBIT PURKINJE FIBERS. PRESENCE OF SLOW INWARD CURRENT. T.J.Colatsky, S.Siegelbaum,* and R.W.Tsien, Department of Physiology, Yale University School of Medicine, New Haven, Connecticut 06510.

Narrow intercellular spaces complicate most cardiac voltage clamp experiments by introducing problems of nonuniformity in both voltage control and ion concentration. Sommer and Johnson (1968) found rabbit Purkinje fibers (PF) had wider clefts (1 μ) than sheep and calf PF (20-40 nm). We have voltage clamped short rabbit PF using two microelectrodes and found the electrical behavior of this preparation to reflect its more favorable geometry: 1) Total capacitance and capacity transient time course were minimally changed by reducing bathing fluid conductivity, while larger changes occured in calf PF. 2) Currents attributable to potassium depletion from clefts were negligible. The rabbit PF showed plateau currents like those in other preparations, including a slow inward current which was blocked by D-600 but not TTX. These data demonstrate the suitability of the rabbit PF for voltage clamp study, and argue against explaining the slow inward current as an artifact of poor voltage control.

**M-POS-C14** MEMBRANE BRIDGES ACROSS THE TRIADIC GAP AFTER TANNIC ACID FIXATION. Somlyo, A.V.,* Pennsylvania Muscle Institute, Philadelphia, PA 19104 (Intr. by A.P. Somlyo)

Frog semitendinosus muscles fixed in glutaraldehyde followed by 4% tannic acid at pH 7.2 and reacted with 1% Fe $Cl_3$ show high contrast and fine delineation of the trilaminar structure of the T-tubule (TT) and terminal cisterna (TC) membranes. The staining density of the junctional gap was suggestive of proteinaceous material. In ultrathin sections, electron lucent periodicities traversing the gap were continuous with the electron lucent central lamina of the trilaminar membranes of both the TT and the TC. In these regions the outer leaflets of the TT or TC membranes appeared to make a sharp right angled turn. Similar sharp turns of divergent membrane leaflets have been observed in tubular myelin (Sanderson and Votter, J.Cell Biol. 74:1027,1977) and during exocytosis (Palade, Science 189:347,1975). These images suggest that the outer membrane leaflets of the TC and TT are continuous, but not their lumina, in agreement with electron probe studies (Somlyo et al., J.Cell Biol. 74:828,1977). The content of the TC appeared well ordered in some views, forming longitudinally oriented rows of granules radiating from the scalloped TC membranes. (Supported by HL 15835 to PMI)

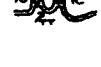

M-POS-C15 KINETIC STUDIES OF THE MYOFIBRILLAR ATPase. C.C. Goodno*, (Introduced by D.E. Goll), Muscle Biology Group, Department of Nutrition and Food Science, University of Arizona, Tucson, Arizona 85721.

We have examined the initial-rate ATPase kinetics of rabbit skeletal myofibrils (in 0.05 M KCl, 4 mM $MgCl_2$, 2 mM Tris·HCl, pH 7.0, 25°, with either 1 mM EGTA or 0.25 mM $CaCl_2$). Under activating conditions (0.25 mM $Ca^{++}$) the ATPase obeys Michaelis-Menten kinetics over the range of 0.03 - 5.0 mM MgATP ($K_m$ = 16 ± 6 μM, $V_{max}$ = 0.4 ± 0.1 $\mu mole \cdot min^{-1} \cdot mg^{-1}$). Under relaxing conditions (1 mM EGTA), however, pronounced substrate inhibition occurs above 0.05 mM MgATP. Since the activated ATPase does not experience substrate inhibition, the net effect of raising the MgATP concentration is to depress the relaxed ATPase relative to the activated ATPase. Thus, calcium sensitivity increases with increasing MgATP concentration, and we find that a physiological level of MgATP (2-5 mM) is required for optimal calcium sensitivity. These results suggest that calcium does not function as a simple activator of the myofibrillar ATPase; rather, it functions as an antagonist of MgATP inhibition. (This study was performed under a Muscular Dystrophy Association postdoctoral fellowship).

M-POS-C16 A KINETIC MODEL FOR MECHANICAL ACTIVATION ALTERATIONS IN SKELETAL MUSCLE FIBERS. S. H. Bryant, Dept. Pharmacology & Cell Biophysics, Univ. of Cincinnati Col. of Medicine, Cincinnati, Ohio 45267

Using the point voltage-clamp method of Adrian et al. (J.Physiol.240:247,1969) the "strength-duration" curves for mechanical activation thresholds were determined in mammalian muscle fibers affected by conditions that influence excitation-contraction coupling. These include myotonia and malignant hyperthermia, and drugs such as dantrolene, anthracene-9-carboxylic acid and a calcium ionophore. In the model, similar to that of Almers and Best (J.Physiol.262:583,1976), the rate of calcium release from the SR is proportional to voltage-dependent charge movement in the T-system and the uptake of calcium is first order. Threshold calcium concentration was constant for each curve. The voltage-dependence of the rate constants for charge movement were of the form given by Chandler et al.(J.Physiol.254:245,1976). Reasonable fits to the data under the various conditions were obtained by digital computer. The model predicts how the release and uptake processes were altered. (Supported by USPHS, NIH Grant NS-03178).

M-POS-C17 REGIONAL SHORTENING DURING ISOMETRIC CONTRACTION IN ARTERIAL SMOOTH MUSCLE. S.P. Driska, D.N. Damon*, and R.A. Murphy, Dept. of Physiology, Univ. of Virginia Sch. of Medicine, Charlottesville, Virginia 22901

Interpretations of mechanical studies of smooth muscle tissues are based on the assumption of uniform cellular responses to stimulation. This assumption was tested by looking for regional shortening during isometric $K^+$ contractures. Regional shortening would not occur if cellular responses were uniform, and was detected by measuring the movement of markers deposited along strips of the pig carotid media of constant cross-section. At 0.7-0.8 $L_o$ ($L_o$ = optimum length for force generation) marker movement was substantial and variable, averaging 265 ± 34 μm (SEM, N=29) or 4.7% of strip length. However, at 1.0-1.05 $L_o$, marker movement was slight, averaging 38 ± 10 μm (N=28), or 0.4% of tissue length. Marker movement in the region of damaged cells near the tissue clips was similar to that in other regions. Thus, tissue injury did not contribute greatly to the 7.2% series elasticity measured in this tissue at $L_o$. We conclude the assumption of uniform cellular contractions in this preparation is only valid at tissue lengths above 0.95 $L_o$ where passive stress is appreciable. Supported by NIH Grants HL 19242 and HL 05180.

M-POS-C18 MASS PER UNIT LENGTH OF SKELETAL MUSCLE THICK FILAMENTS. M. K. Lamvik, Rosenstiel Center, Brandeis University, Waltham, Massachusetts 02154

The number of myosin molecules per repeat in the thick filament of vertebrate skeletal muscle is a quantity that has been measured by several indirect methods. The mass of isolated protein aggregates may be determined directly by quantitative detection of scattered electrons. Rabbit muscle filaments were measured this way* using the scanning transmission electron microscope of A.V. Crewe. The mass per length of myosin was found to be 87 ± 23 kD/nm. Rates of electron-induced mass loss were measured and used for extrapolation to pre-exposure values. Muscle thin filaments and tobacco mosaic virus were used as calibration standards. Critical point drying and freeze drying were used to preserve the shape of the unstained filaments. Parallel controls were done using negative stain and metal shadowing. The result is consistent with three myosin molecules per 14.3 nm unit length.

* M. Lamvik, Ph.D. thesis, University of Chicago, 1976. Supported by ERDA. Further analysis was completed at Brandeis University, supported by USPHS grant #AM17346 and a postdoctoral fellowship from the Muscular Dystrophy Association. (In press, J. Mol. Biol.)

M-POS-C19 MYOSIN SYNTHETIC FILAMENT STRUCTURE WITH AND WITHOUT C-PROTEIN. J.F.Koretz. Dept. of Biology, RPI, Troy, NY 12181.

Artificial filaments, prepared from Sephadex A50-purified rabbit skeletal myosin and dialyzed against a 0.1M solution at pH7, demonstrate both a 14.3nm subunit repeat and a 43nm axial repeat when investigated by optical diffraction of negatively stained electron micrographs. The addition of C-protein to the myosin solution before dialysis in a molar ratio of 1:3-4 -- the approximate molar ratio in the banded region of natural thick filaments -- results in preservation of the 14.3nm subunit repeat, but a change in axial spacing to 114.4nm (8 x 14.3nm). C-protein:myosin ratios either higher or lower than 1:3-4 result in specific types of disorder. Addition of C-protein to already-formed filaments made from column-purified myosin alone causes the axial spacing again to be changed, this time to 143nm (10 x 14.3nm) while subunit spacing is preserved. Models for synthetic filament structure, the location of C-protein along the filament in two of these cases, and a mechanism for transition among the three filament types are proposed, based upon optical diffraction studies and computer simulations.

M-POS-C20 THE CHANGE OF pH WITH TEMPERATURE IN FROG MUSCLE. C.T.Burt, Univ. of Ill. at the Med. Ctr., Dept. Biol. Chem., Chicago, Ill. 60612

Muscle pH was studied as a function of temperature using $^{31}P$ NMR. This method is useful since it uses an internal probe, the chemical shift of the inorganic phosphate ($P_i$). Initial pH's of 7.2 at 28°C and 7.5 at 4°C were found for intact frog muscle. The pH may be shifted by merely raising or lowering the muscle's temperature. In many muscles imidazole groups (carnosine, anserine or histidine in proteins) provide the main buffering capacity. Determination of pH by either NMR or pH electrode show a small change (<0.5 units) for a low phosphate (1mM fructose disphosphate, 1mM $P_i$, 5mM glycerol phosphoryl choline, 5mM ATP, 12mM $MgCl_2$ 20mM phosphocreatine, and 10mM MKCl) test solution over a 24°C temperature range (4 to 28°C). Addition of 10mM carnosine or 10mM carosine+20mM histidine causes a .45pH change for the test solution over the same 24°C range. These results imply a $Q_{10}$ measurement on frog muscle will not simply measure the effect of temperature. (Supported by Chicago Heart).

ENERGY COUPLING I

**M-POS-D1** ACTIVE PROTON TRANSLOCATION IN CHROMAFFIN GRANULES OBSERVED BY 31-P NMR. D. Njus, G.K. Radda,* G.A. Ritchie,* P.J. Seeley,* and P.A. Sehr,* Dept. of Biochemistry, Oxford University, Oxford, Great Britain.

Chromaffin granules, the catecholamine storage vesicles of the adrenal medulla, have an inwardly directed proton-translocating ATPase. This hydrolyzes ATP added to the extragranular solution but cannot hydrolyze the 0.1 M ATP contained within the granules. We have shown that the 31-P NMR resonance frequency of the $\gamma$-$PO_4$ of intragranular ATP shifts upfrequency during proton pumping and provides a qualitative indicator of internal pH (Casey et al., Biochemistry 16, 972, 1977). We have now calibrated this signal to give quantitative pH measurements. In spectra taken at intervals after addition of external ATP, the intragranular pH drops from ~5.5 to ~5.1 (±0.1). The intensities of the signals from external ATP decrease as hydrolysis proceeds and signals from extragranular ADP, AMP, and $PO_4$ increase. Consequently, the information needed to calculate the rates of proton translocation and ATP hydrolysis, the $H^+$/ATP stoichiometry, and the $PO_4$ potential ($G_o$+[ATP]/[ADP][$PO_4$]) may all be obtained from a single sequence of 31-P NMR spectra on a single sample.

**M-POS-D2** ΔpH AND TRANSMEMBRANE POTENTIAL IN CHROMAFFIN GHOSTS. R.G. Johnson, D. Pfister*, A. Scarpa. Dept. Biocnem.-Biophys., Univ. of PA, Phila., PA 19104.

The origin of tne $H^+$ gradient existing in chromaffin vesicles (J. Gen. Physiol. 68:601 1976) was studied using chromaffin ghosts, prepared by osmotic lysis and extensive dialysis of the isolated chromaffin granules. In the absence of ATP, neither a ΔpH nor a Δψ was measured using ghosts. However, when ATP was added to ghosts in KCl buffer, $H^+$ ions were transported inside the vesicles, resulting in a ΔpH of 1 unit acidic inside ($^{14}C$ methylamine distribution) and no Δψ ($^{14}C$ $SCN^-$ distribution). $H^+$ ion gradients were inhibited by FCCP and 30 mM $NH_4Cl$. By contrast, when ATP was added to ghosts in isothionate buffer, a transmembrane potential of 50 mV, positive inside, and negligible ΔpH were measured. This potential was inhibited by FCCP, 50 mM $SCN^-$, but not by ammonia. These results indicate that a $H^+$ translocating ATPase exists in the chromaffin granule capable of the generation of both a Δψ and a ΔpH across the membrane. This study in ghosts devoid of endogenous catecholamines may provide quantitative data on the role of either ΔpH or Δψ in the accumulation of catecholamines into isolated cnromaffin granules. (Supported by AHA 77-675)

**M-POS-D3** MOLECULAR MECHANISMS FOR PROTON TRANSPORT ACROSS MEMBRANES. J. F. Nagle and H. J. Morowitz, CMU Pittsburgh, PA 15213 and Yale U., New Haven, CT 06520.

The last decades of research in bioenergetics have increasingly focused attention on the transport of protons as an intermediate mechanism in energy transduction. In this paper we draw upon studies of proton transport in inorganic systems to suggest likely mechanisms for the conduction of protons through membranes. The fundamental structural element is postulated to be continuous chains of hydrogen bonds formed from the protein side groups and a molecular example is presented. From studies in ice such chains are predicted to have low impedance and can function as proton wires. The attachment of such a wire to a proton injector, such as the Schiff base of a chromophore, yields a simple proton pump. In addition, conformational changes in the protein may be linked to the proton conduction. Allowing this possibility a different proton pump is described which can be reversed into a molecular motor driven by an electrochemical potential across the membrane.

**M-POS-D4** MITOCHONDRIAL $Ca^{2+}$ UPTAKE AT 4°C. R. Charlton and C. Wenner, Roswell Park Mem. Inst., Buffalo NY 14263

In view of reported differences in $Ca^{2+}$ homeostasis between mitochondria derived from liver and Ehrlich ascites tumor cells, it is of interest to examine $^{45}Ca^{2+}$ uptake by these mitochondria at 4°C, where efflux is minimal. The nature of this uptake and its source of energy were determined using respiratory inhibitors and uncouplers of oxidative phosphorylation. $Ca^{2+}$ uptake of 55-75 nmol/mg protein at 10' was observed with both types of mitochondria, which had respiratory control ratios of 2.5 -4.6 and $Ca^{2+}/2e^-$ ratios of 1.85-2.0 at 37°C. In both types of mitochondria $Ca^{2+}$ uptake was found to be completely sensitive to the uncoupler S-13 ($2 \times 10^{-7}$M). Rotenone gave up to an 80% inhibition in the presence of endogenous substrates, considered to be mainly $NAD^+$-linked. Since antimycin A gave only 30% inhibition, it is considered likely that $O_2$ is not the sole electron acceptor at 4°C. ATP has a relatively small role in $Ca^{2+}$ uptake, since 4 μg/ml oligomycin has little or no effect. The ATP translocase does not appear to be involved, since atractyloside has little or no effect. In view of these similarities, it is suggested that the differences between the 2 types of mitochondria in $Ca^{2+}$ homeostasis are not attributable to $Ca^{2+}$ uptake.

**M-POS-D5** ENERGY-LINKED FLUORESCENCE DECREASE OF AMINOACRIDINES ASSOCIATED WITH BEEF HEART SUBMITOCHONDRIAL MEMBRANES. Cheng-Schen Huang and C. P. Lee, Department of Biochemistry, Wayne State Univ.Sch. Med., Detroit, Mi.

9-amino-3-chloro-7-methoxyacridine(A), 9-(3-diethylamino-1-propylamino)-3-chloro-7-methoxyacridine(B) and 9-aminoacridine(C) exhibit an energy-linked fluorescence decrease when associated with beef heart submitochondrial membranes(SMP). The fluorescence polarization(P) of the dyes associated with SMP in energized(E) and nonenergized (NE) states was measured. For B, P was increased by > 2 fold upon energization of SMP (P(NE)=0.07 & P(E)=0.20), as seen with quinacrine(QA). For A & C, P was independent of the membrane state (P(NE)=P(E)=0.01). These data together with those reported previously (Biochim. Biophys. Acta, 459, 241, 1977) indicate that the substitution at the 9-amino group controls the interaction between the dyes and SMP. QA & B probe a region of SMP different from that probed by A & C. The fluorescent dye molecules are located in the membrane phase of energized SMP in the case of QA & B. In the case of A & C, the membrane-bound dye molecules appear to be non-fluorescent and the fluorescent dye molecules are those remaining in the medium in the free form.

**M-POS-D6** THE KINETICS OF THE VOLTAGE-SENSITIVE PROBE OXONOL VI IN SUBMITOCHONDRIAL PARTICLES, Jerry Smith, Univ. of Penna. Med. Sch., Phila., PA 19104

A homologous series of dyes of the oxonol class has been studied in a number of membrane preparations. The energy-linked spectral response of the dyes is a red shift of the absorption spectrum and a decrease in the fluorescence yield. In order to gain insight into the mechanism by which these spectral changes occur, a detailed kinetic study of one of these dyes, oxonol VI, is being carried out using submitochondrial particles. The time course of the dye red shift induced by NADH, ATP and $O_2$ pulses has been followed in a regenerative flow rapid mixing device. The dye response to single pulse of ATP and NADH is biphasic consisting of a second order process and a first order process some six orders of magnitude slower. The response of an anerobic suspension of particles, dye and NADH to an $O_2$ pulse is also second order, but since the $O_2$ is rapidly consumed the slower process is not significantly developed under these conditions. The faster process is consistent with a mechanism in which the spectral red shift is due to an enhanced occupancy of the energized membrane by the probe. The slower process however is of a more obscure nature.
Supported by NIH Grant No. GM 12202.

BIOENERGETICS II

**M-POS-D7** PHOTOVOLTAIC CELL CONSTRUCTED WITH BACTERIORHODOPSIN IN A LIPID IMPREGNATED MILLIPORE FILTER MEMBRANE. P. K. Shieh, R. Mehlhorn, and L. Packer. Membrane Bioenergetics Group, Univ. of California, Berkeley, CA 94720

An improved method of constructing a photovoltaic device from bacteriorhodopsin, lipids and a millipore filter membrane has been developed. Photovoltage and photocurrent are related to the conditions of membrane formation, including composition of the membrane, liposome sonication time, different strains of Halobacterium halobium, weight ratio of lipid to bacteriorhodopsin in the liposomes, and ions in the aqueous phase. The maximum open-circuit photovoltage, short-circuit photocurrent obtainable for a single membrane are: 300-380 mV, 0.4-0.9 ma under saturating light intensity. The stability of this membrane system was also studied. Ninety minutes of continuous illumination cause a complete loss of photoresponse. In the dark the membrane can be stored up to six months. When five membranes were connected in series, a photovoltage of about 1.5 volts was produced. Work is in progress to attempt to couple this system to the performance of electrochemical work, such as the production of hydrogen and oxygen from water.
(Research supported by the Department of Energy.)

**M-POS-D8** RATE DETERMINATION IN VIVO BY NMR MAGNETIZATION TRANSFER. T. R. Brown, K. Ugurbil,* & R. G. Shulman. Bell Laboratories, Murray Hill N.J., 07974.

The in vivo exchange rates between ATP and $P_i$ have been measured in aerobic E. coli cells by high resolution $^{31}P$ NMR experiments using a saturation transfer technique. In the experiment at a NMR frequency of 145.7 MHz the well resolved terminal phosphate resonance of ATP was saturated and the intensity of the internal $P_i$ peak was reduced by ~20%. This led to rates at 25°C of 0.6±0.15 and 10±5 $sec^{-1}$ from $P_i$ to ATP and the reverse respectively. The saturation transfer was not observed after incubation with DCCD, an ATPase inhibitor. The application of this and similar techniques to other in vivo enzyme systems will be discussed.

**M-POS-E1** THE ORIENTATION OF THE NO LIGAND IN MULTILAMELLAR ARRAYS OF THE NO COMPOUND OF REDUCED CYTOCHROME c OXIDASE. C.H. Barlow,* M. Erecinska,* (Intr. by D.F. Wilson) Dept. of Biochem/Biophys,U. of Pa.,Phila,PA.

The orientation of hemes a and $a_3$ with multilamellar cytochrome c oxidase have been determined in oriented "membranous" cytochrome oxidase using EPR and polarized light spectroscopy. The oriented multilayers possess cylindrical symmetry with the unique axis normal to the membrane plane (1). The normal to the planes of both hemes is perpendicular to the normal to the membrane plane(2). The NO compound of reduced cytochrome oxidase was obtained by treating the oriented multilayers with dithionite + $NaNO_2$ in hypertonic sucrose. EPR spectra at -140°C were obtained for each 10° rotation of the membrane normal with respect to the magnetic field direction. The g tensors at 2.09 and 1.98 were oriented perpendicular and parallel to the membrane normal respectively while maximum hyperfine intensity was observed at 45°. These results support a maximum NO bond angle with respect to the heme plane of 135°.
(1) Blasie, J.K. et al, Biophys. J., 17, 63A (1977)
(2) Erecinska, M. et al, B.B.A. (in press) supported by HL - 18708

**M-POS-E2** SWELLING OF HEART MITOCHONDRIA IN CHLORIDE SALTS INDUCED BY TRIPROPYLTIN. D.W. Jung* and G.P. Brierley. Dept. Physiol. Chem., Ohio State U., Columbus.

Tripropyltin (TPT) promotes $Cl^-/OH^-$ exchange across membranes and induces passive swelling of mitochondria in NaCl (Selwyn, 1976, Adv. Chem. 157, 204). This swelling, like that in $Na^+$ acetate, seems best explained by the activity of a $Na^+/H^+$ exchange component in the coupling membrane. The exchanger shows a cation selectivity sequence of $Na^+ >> Li^+ > K^+$, $Rb^+$, $Cs^+$, choline$^+$ = 0, a sharp pH optimum between pH 7.2-7.4, insensitivity to $Mg^{+2}$ and EDTA, and inhibition by $Mn^{+2}$ and valinomycin. In respiring mitochondria, TPT promotes swelling with a cation selectivity of $Na^+$, $Li^+ > K^+$, $Rb^+$, $Cs^+ >$ choline$^+$. Succinate-dependent swelling induced by TPT in LiCl shows high rates from pH 7.2 to 8.3, extreme sensitivity to $Mg^{+2}$ (5μM inhib. 50%), and activation by EDTA. The corresponding reaction in KCl is nearly insensitive to $Mg^{+2}$. Respiration-dependent swelling in acetate and in chloride (with TPT) is consistent with cation uniport in response to an internal negative membrane potential. These and other studies suggest that multiple uniport pathways may be present. Supported by USPHS Grant HL09364.

**M-POS-E3** THE EPR MANIFESTATION OF A MITOCHONDRIAL METALLOPROTEIN. P.R. Rich*, J.S. Leigh, J.C. Salerno*, D.M. Tiede, and W.D. Bonner, Jr., Johnson Res. Foundation and Dept. of Biochem. & Biophys., U. of Pennsylvania, Philadelphia, PA 19104.

Whole mitochondria isolated from wild-type Neurospora crassa cells were treated with sodium nitrite and sodium dithionite to produce nitric oxide in situ. The EPR spectrum of such a sample revealed a rhombic signal with g-values of 4.05, 3.89 and 2.01. No hyperfine structure was detectable. The component was present in at least a 10-fold excess over the ferredoxin-type centers and was released into the supernatant fraction after French pressure cell treatment to disrupt the mitochondria, which indicated a possible matrix or intermembrane-space location. Signals in this region of the spectrum have previously been observed in spin-coupled copper dimer systems and in the iron-containing superoxide dismutase of E. coli. The lack of nuclear hyperfine structure in our signal rules out an involvement of copper and instead a species with iron in a non-heme and non-iron sulfur environment is favored. This notion is supported by studies of a model ferrous-EDTA-NO complex which was found to have a similar, although more axial spectrum.

**M-POS-E4** $^{31}$P NMR STUDY OF MITOCHONDRIA S. Ogawa,* T. R. Brown, H. Rottenberg, & R. G. Shulman, Bell Laboratories, Murray Hill, N.J. 07974

$^{31}$P NMR spectra of intact mitochondria were measured at various energetic states. In the absence of external substrate the $P_i$ concentration gradient and $\Delta pH$ were mutually in equilibrium and consistent with the $H_2PO_4^-/OH^-$ exchange transport scheme. Upon oxygenation, in the presence of substrate, ADP was converted to ATP. The internal $P_i$, ADP and ATP were distinguishable from the corresponding external compounds because of the chemical shift differences due to $\Delta pH$ and the divalent metal ion concentration gradient. Residual adenylate kinase activity could be monitored by changes of external AMP peak.

**M-POS-E5** POTENTIATION OF CALCIUM-INDUCED TRANSITION OF BEEF HEART MITOCHONDRIA BY DIPHENYLHYDANTOIN AND BARBITURATES. H. Komai, D.R. Hunter*, and H.A. Berkoff* Dept. of Surgery and Inst. for Enzyme Research, Univ. of Wisconsin, Madison, WI 53706

Diphenylhydantoin (DPH) at the concentration of 0.5 mM abolished respiratory control of beef heart mitochondria following $Ca^{2+}$ uptake in the presence of Pi. Addition of DPH to the mitochondria that accumulated $Ca^{2+}$ (but not $Sr^{2+}$) resulted in the alkalinization of suspending media, suggesting the efflux of accumulated $Ca^{2+}$. The efflux of $Ca^{2+}$ induced by DPH was confirmed using $^{45}Ca^{2+}$.

A decrease in light scattering characteristic of the $Ca^{2+}$ - specific aggregated to orthodox transition (Hunter D.R. et al. J. Biol. Chem. 251 5069 (1976)) was observed upon addition of DPH to a suspension of mitochondria that accumulated $Ca^{2+}$. Barbiturates such as thiamylal (0.2mM) and Amytal (2mM) showed an effect similar to that of DPH in potentiating the $Ca^{2+}$-induced transition. These results indicate that in addition to the known effect of DPH and barbiturates as inhibitors of respiration, these compounds may influence $Ca^{2+}$ homeostasis of the cells by potentiating the $Ca^{2+}$-induced membrane transition of mitochondria.

**M-POS-E6** IDENTIFICATION OF PHOSPHOCITRATE, A NATURALLY OCCURRING INHIBITOR OF BIOLOGICAL CALCIFICATION. W. Tew*, C. Mahle*, and A. Lehninger. (Intr. by J. L. Gamble). Johns Hopkins Univ. Sch. Med., Baltimore, Maryland 21205

Many living systems contain $Ca^{2+}$ and $P_i$ concentrations in excess of the $K_{sp}$ of hydroxyapatite (HA), yet no crystallization is normally observed. There is ample evidence that biological systems contain factors which regulate calcium phosphate mineralization by stabilizing non-crystalline, amorphous calcium phosphate (ACP) and preventing the crystallization of HA. Using assays which measure the rate and extent of the transformation of ACP to HA and the rate of HA crystal growth, we have found that mitochondria contain phosphocitrate, an extremely potent naturally occurring inhibitor of HA crystal growth. Mitochondria have been shown to contain $Ca^{2+}$ and $P_i$ in amorphous form and have been implicated as sites of initial concentration of ACP for utilization during bone growth. Further studies indicate that pyrophosphate and phosphocitrate may function together in the biological regulation of calcium phosphate mineralization. Supported by NIH (GM05919) and NSF (PCM75-21923).

**M-POS-E7** MAGNESIUM CONTENT AND TRANSPORT OF ISOLATED BOVINE VASCULAR SMOOTH MUSCLE MITOCHONDRIA, B.F. Sloane,* A. Scarpa, and A.P. Somlyo, (Intr. by S. Papa), University of Pennsylvania, Philadelphia, PA. 19104.

Endogenous magnesium content and magnesium transport of isolated bovine main pulmonary artery smooth muscle (vsm) mitochondria were studied. Mitochondria isolated from vsm with an increased incidence of yellow streaks contained approximately three times as much magnesium (178 nmol/mg mitochondria protein) as those isolated from vsm without yellow streaks (67nmol/mg mitochondrial protein). Electron opaque granules were visible in the unstained, unfixed mitochondria and could be shown with electron probe analysis to consist of magnesium, calcium and phosphorus. At concentrations of external $Mg^{2+}$ from 0-6mM, the vsm mitochondria exhibited respiratory substrate-supported release of $Mg^{2+}$ as studied with the metallochromic indicator, Eriochrome Blue, using dual wavelength spectrophotometry. The maximal velocity of energized release (3nmole $Mg^{2+}$/sec/mg mitochondrial protein) was observed at 4mM external $Mg^{2+}$ and the half maximal transport occurred at 0.5mM. (Supported by HL15835 to the Pennsylvania Muscle Institute and NIGMS-GM-00092 to B.F. Sloane.

**M-POS-E8** ISOLATION AND CHARACTERIZATION OF THE BIOLOGICALLY ACTIVE NUCLEOID FROM MITOCHONDRIA: PRESENCE OF A MITOHISTONE. M.Hillar, V. Rangayya*, B.A. Jafar, D. Chambers*, and M. Vitzu*, Texas Southern University, Houston, TX 77004

Mitochondrial nucleoid which was first isolated by T.Kuroiwa from Physarum polycephalum was isolated from rat liver and bovine heart mitochondria by differential centrifugation of mitochondrial lysate in 1 % triton X-100. It does not contain any respiratory chain component, its yield is about 30 µg prot./mg mit. prot. and contains about 3-5 µg DNA/mg prot. It rapidly synthesizes RNA with 3H-CTP at a rate of about 3000 cpm/10 min mg prot. It contains several basic proteins separated on urea-polyacrylamide gel electrophoresis of which one was extracted with 0.2 M sulfosalicylic acid. This protein, mitohistone, occurs in a DNA : protein ratio = 1 : 1 w/w and contains moderate amounts of Lys, His, and Arg.

Supported by a grant from H.I.H. No PR 0806